24th ICSLS 2018

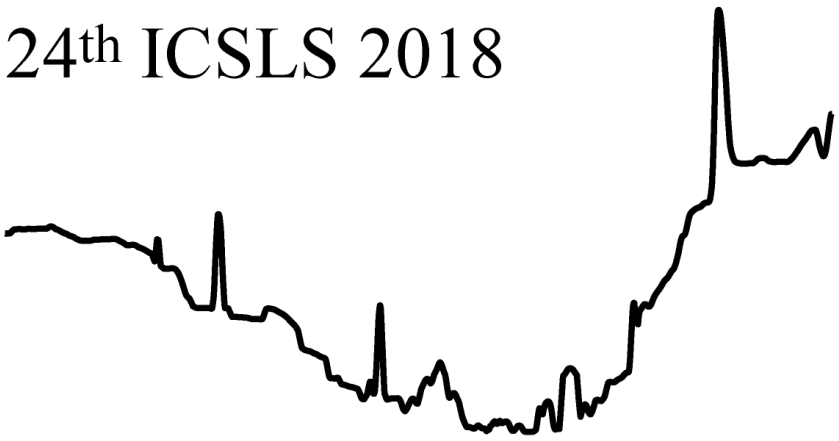

17 – 22 June 2018, Dublin, Ireland

24th International Conference on Spectral Line Shapes

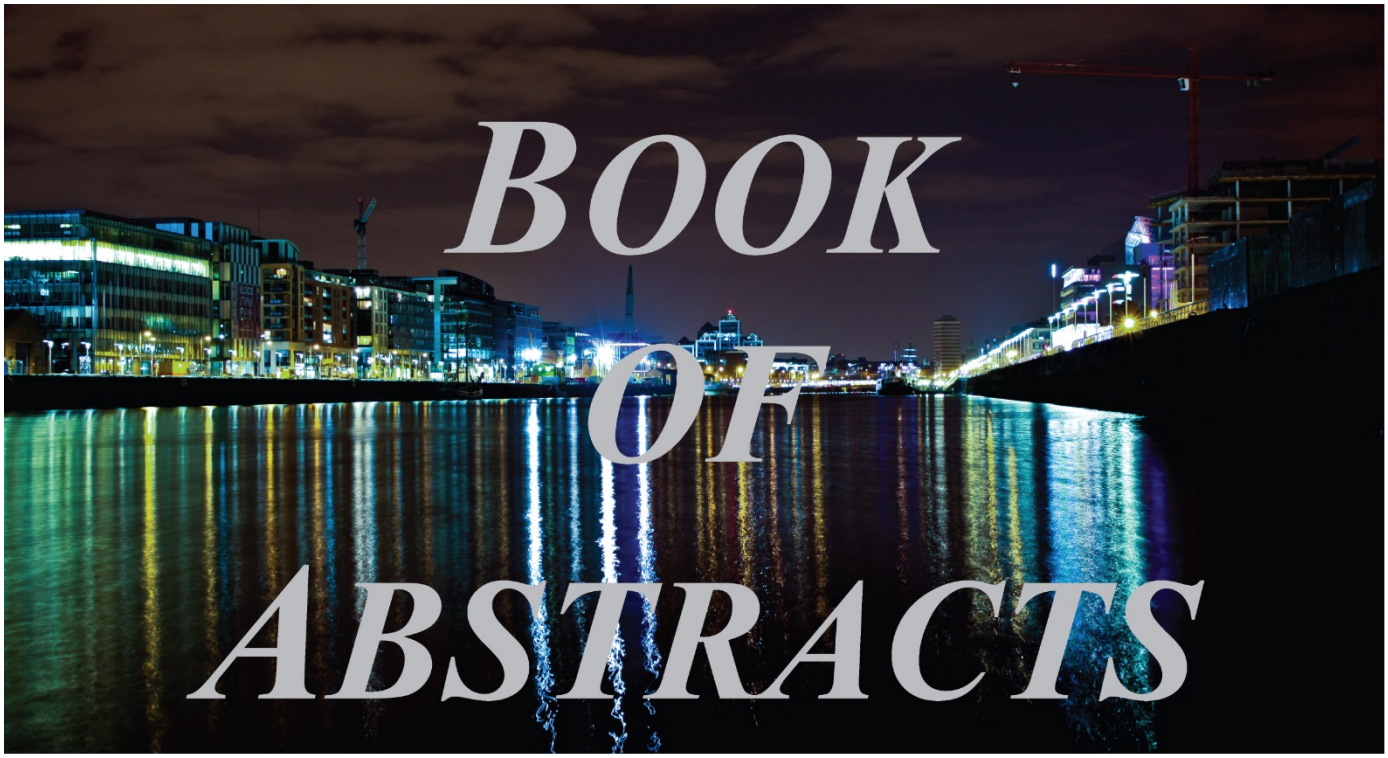

17 – 22 June 2018, Dublin Ireland

CONTENTS

Programme Timetable

Invited Talk	Selected Talk

Time	Sunday June 17th	Monday June 18th	Tuesday June 19th	Wednesday June 20th	Thursday June 21th	Friday June 22th
08:40 - 09:00		OPENING				
09:00 - 09:20		Chris Parigger	Reinhard Kienberger	Richard Russo	Valeriy Astapenko	Kimberly Strong
09:20 - 09:40						
09:40 - 10:00		Mateusz Borkowski	Thomas Pfeifer	Patrick Hayden	Robert Gamache	Katarzyna Bielska
10:00 - 10:20				Mossy Kelly	Tigran Vartanyan	Agata Cygan
10:20 - 10:40		Coffee Break	Coffee Break	Coffee Break	Coffee Break	Coffee Break
10:40 - 11:00		Milan Dimitrijević	Eugene Kennedy	Alain Campargue	Thomas Baumert	Shinichi Namba
11:00 - 11:20						
11:20 - 11:40		Joel Rosato	Emma Sokell	Jeanna Buldyreva	Yan Tan	V. González Fernández
11:40 - 12:00		Gamal Daniel Roston	Nikodem Stolarczyk	Magnus Gustafsson	Adriana Predoi Cross	Michal Slowinski
12:00 - 13:00		Lunch (IPC Business Meeting - Closed)	Lunch	Lunch	Lunch	CLOSE
13:00 - 14:00					13:45 Travel to city	
14:00 - 14:20		Colette McDonagh	Franck Thibault	Shigeru Morita	Guinness Store House Tour	
14:20 - 14:40						
14:40 - 15:00		Jason Greenwood	James Williams	Mohammed Koubiti		
15:00 - 15:20		Coffee Break	Coffee Break	Coffee Break		
15:20 - 15:40		Ali Adawi	Tijs Karman	Nelly Bonifaci		
15:40 - 16:00						
16:00 - 16:20		Calin Hrelescu	Peter van der Burgt	Motoshi Goto		
16:20 - 16:40				U Erozbek Gungor		
16:40 - 17:00		Oliver Martin				
17:00 - 18:00			Poster Session 1	Poster Session 2		
18:00 - 18:40	Welcome Reception and Registration					
18:40 - 19:00						
19:00 - 20:00			Conference Banquet 1838 Club			
20:00 - 21:00						
21:00 - 22:00						

International Programme Committee

Valeriy Astapenko (Russia)

Dionisio Bermejo (Spain)

Roman Ciurylo (Poland)

John Costello (Ireland)

Elisabeth Dalimier (France)

Alexander Devdariani (Russia)

Robert Gamache (USA)

Motoshi Goto (Japan)

Magnus Gustafsson (Sweden)

Carlos Iglesias (USA)

Eugene Oks (USA)

Christian Parigger (USA)

Gillian Peach (UK)

Luka Popovic (Serbia)

Adriana Predoi-Cross (Canada)

Roland Stamm (France)

Kimberly Strong (Canada)

Ha Tran (France)

Local Organising Committee

John Costello (DCU) – Chair

Peter van der Burgt (MU)

Louise Bradley (TCD)

Hugh Byrne (DIT)

Jason Greenwood (QUB)

Paddy Hayden (DCU)

Mossy Kelly (Hull)

Deirdre Kilbane (UCD)

Ernst de Mooij (DCU)

Noel Moore (FB Consulting)

Albert Ruth (UCC)

Matt Shaw (INTEL)

Emma Sokell (UCD)

Irene Ryan (DCU)

Sponsors

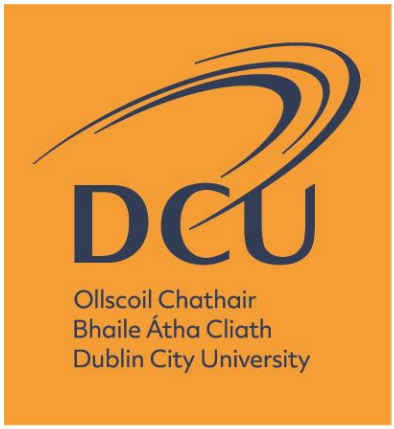
DCU
Ollscoil Chathair
Bhaile Átha Cliath
Dublin City University


EXTATIC


MEET IN
IRELAND


APPLIED SPECTRA
Transforming the way the world does chemistry


COHERENT®


mks
Newport®


PHASETECH
spectroscopy shaping science

Invited Speakers

Ali M. Adawi
(University of Hull, Hull, United Kingdom)

Valeriy Astapenko
(Moscow Institute of Physics and Technology, Dolgoprudnyi, Russia)

Thomas Baumert
(Universitaet Kassel, Kassel, Germany)

Nelly Bonifaci
(Laboratoire G2Elab CNRS & Grenoble University, Grenoble, France)

Mateusz Borkowski
(Nicolaus Copernicus University, Torun, Poland)

Alain Campargue
(Université Grenoble Alpes, CNRS, LIPhy, Grenoble, France)

Milan S. Dimitrijević
(Astronomical Observatory, Belgrade, Serbia)

Colette McDonagh
(Dublin City University, Dublin, Ireland)

Tijs Karman
(Durham University, Durham, United Kingdom)

Eugene Kennedy
(Dublin City University, Dublin, Ireland)

Reinhard Kienberger
(Technische Universität München, Garching, Germany)

Oliver J. F. Martin
(Swiss Federal Institute of Technology Lausanne, Lausanne, Switzerland)

Shigeru Morita
(National Institute for Fusion Science, Gifu, Japan)

Shinichi Namba
(Hiroshima University, Hiroshima, Japan)

Christian G. Parigger
(University of Tennessee, Tennessee, U.S.A.)

Thomas Pfeifer
(Ruprecht-Karls-Universität Heidelberg and Max-Planck-Institut für Kernphysik, Heidelberg, Germany)

Richard Russo
(Lawrence Berkeley National Laboratory and Applied Spectra, California, U.S.A.)

Kimberly Strong
(University of Toronto, Toronto, Canada)

Franck Thibault
(Université de Rennes, Rennes, France)

24th ICSLS 2018
Dublin, Ireland

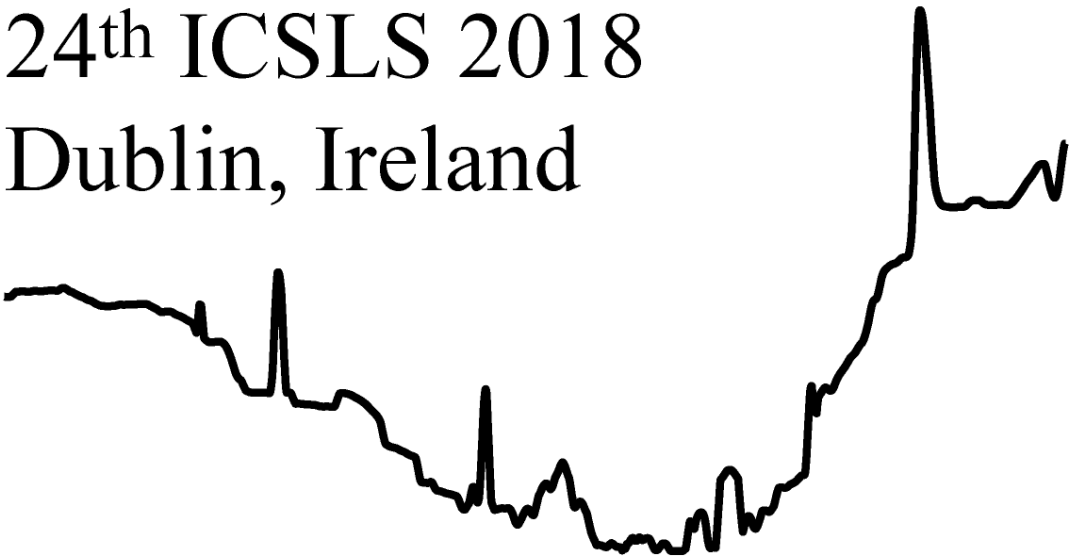

Conference Programme

SUNDAY JUNE 17th, 2018

Location: Foyer of the School of Nursing and Human Sciences, DCU, Glasnevin, Dublin 9.

17:00 – 20:00 ***Welcome Reception and Registration***

MONDAY JUNE 18th, 2018

Location: Lecture theatre HG22 in the School of Nursing and Human Sciences, DCU.

08:40 – 09:00 ***Opening***

09:00 – 10:20 **Monday Oral Session 1**

09:00 – 09:40 Christian G Parigger: *Laboratory Plasma Diagnoses With Applications To Spectra Of White Dwarf Stars* **(Mo.O.1.I1)**

09:40 – 10:20 Mateusz Borkowski: *Optical Clock Transitions in Weakly Bound Molecules* **(Mo.O.1.I2)**

10:20 – 10:40 ***Coffee break***

10:40 – 12:00 **Monday Oral Session 2**

10:40 – 11:20 Milan S. Dimitrijević: *Stark Broadening In Stellar Spectra* **(Mo.O.2.I1)**

11:20 – 11:40 Joel Rosato: *Line Shape Modeling For Magnetic White Dwarf and Tokamak Edge Plasmas: Common Challenges* (**Mo.O.2.C1**)

11:40 – 12:00 Gamal D. Roston: *Effect of Gamma Ray and Signal Line Shapes on the Spectral Performance of Fiber Bragg Grating* **(Mo.O.2.C2)**

12:00 – 14:00 ***Lunch (IPC Business Meeting - Closed Session)***

14:00 – 15:00 **Monday Oral Session 3**

14:00 – 14:40 Colette McDonagh: *Plasmon-enhanced Fluorescence for Improved Bioassay Performance* **(Mo.O.3.I1)**

14:40 – 15:00 Jason B. Greenwood: *Asymmetric Photoelectron Emission From Chiral Molecules Using A High Repetition Rate Laser* **(Mo.O.3.C1)**

15:00 – 15:20 ***Coffee break***

15:20 – 17:00 **Monday Oral Session 4**

15:20 – 16:00 Ali M. Adawi: *Determining Molecular Orientation via Single Molecule SERS in a Plasmonic Nano-gap* **(Mo.O.4.I1)**

16:00 – 16:20 Calin Hrelescu: *Near-perfect absorption in the visible range using metal-dielectric-metal nanostructure plasmonic array* (**Mo.O.4.C1**)

16:20 – 17:00 Olivier J.F. Martin: *Fano Resonances in Plasmonic Systems: Bright Modes, Dark Modes and Critical Coupling* **(Mo.O.4.I2)**

TUESDAY JUNE 19th, 2018

Location: Lecture theatre HG22 in the School of Nursing and Human Sciences, DCU.

09:00 – 10:20 **Tuesday Oral Session 1**

09:00 – 09:40 Reinhard Kienberger: *Free Electron Streaking Reveals Attosecond Dynamics On Surfaces And Layered Systems* **(Tu.O.1.I1)**

09:40 – 10:20 Thomas Pfeifer: *Switching Lorentzian To Fano Line Shapes With Intense Lasers — From Attosecond Electronics To Sub-Ångstrom Nuclear Resonance Metrology* **(Tu.O.1.I2)**

10:20 – 10:40 ***Coffee break***

10:40 – 12:00 **Tuesday Oral Session 2**

10:40 – 11:20 Eugene.T. Kennedy: *Photoionization of Atomic and Molecular Ions* **(Tu.O.2.I1)**

11:20 – 11:40 Emma Sokell: *Investigation of the double photoionization mechanism in benzene* **(Tu.O.2.C1)**

11:40 – 12:00 Nikodem Stolarczyk: *First Comprehensive Dataset Of Beyond-Voigt Line-Shape Parameters From Ab Initio Quantum Scattering Calculations For The HITRAN Database* **(Tu.O.2.C2)**

12:00 – 14:00 ***Lunch***

14:00 – 15:00 **Tuesday Oral Session 3**

14:00 – 14:40 Franck Thibault: *Ab Initio Line Shape Parameters For Speed Dependent Hard Collision Profiles: Applications To Rovibrational Lines Of H_2, D_2, HD In He Or H_2* **(Tu.O.3.I1)**

14:40 – 15:00 James F. Williams: *Spectral Line Shapes and Angular Momentum* **(Tu.O.3.C1)**

15:00 – 15:20 ***Coffee break***

15:20 – 16:20 **Tuesday Oral Session 4**

15:20 – 16:00 Tijs Karman: Collision-Induced Absorption By Oxygen And Nitrogen Molecules **(Tu.O.4.I1)**

16:00 – 16:20 Peter J. M. van der Burgt: *Fragmentation Of Anthracene And Phenanthrene By Low Energy Electron Impact* **(Tu.O.4.C1)**

16:40 – 18:40 **Tuesday Poster Session** **(Tu.P)**

Location: Foyer of the Stokes Building - School of Electronic Engineering, DCU

19:00 – 22:00 **Conference Banquet**

Location: 1838 Club, Albert College, DCU

WEDNESDAY JUNE 20th, 2018

Location: Lecture theatre HG22 in the School of Nursing and Human Sciences, DCU.

09:00 – 10:20 **Wednesday Oral Session 1**

09:00 – 09:40 Richard E. Russo: *Optical Isotopic Analysis with Laser Induced Plasmas* **(We.O.1.I1)**

09:40 – 10:00 Paddy Hayden: *Applications Of Vacuum Ultraviolet Laser Induced Breakdown Spectroscopy (VUV-LIBS) – Analysis Of Pharmaceuticals* **(We.O.1.C1)**

10:00– 10:20 Mossy J. Kelly: *Time Resolved Studies of Optical Emission Spectroscopy from Aluminum Oxide formed by Laser Induced Plasma* **(We.O.1.C2)**

10:20 – 10:40 ***Coffee break***

10:40 – 12:00 **Wednesday Oral Session 2**

10:40 – 11:20 Alain Campargue: *Water Absorption Spectroscopy: From Doppler-Free Saturation Dips To Continuum* **(We.O.2.I1)**

11:20 – 11:40 Jeanna Buldyreva: *Non-Markovian relaxation matrix for two linear colliders in dense gas media* **(We.O.2.C1)**

11:40 – 12:00 Magnus Gustafsson: *Hydrogen Dimers in Giant-planet Infrared Spectra* **(We.O.2.C2)**

12:00 – 14:00 ***Lunch***

14:00 – 15:00 **Wednesday Oral Session 3**

14:00 – 14:40 Shigeru Morita: *Quantitative analysis on tungsten spectra of W^{6+} to W^{45+} ions* **(We.O.3.I1)**

14:40 – 15:00 Mohammed Koubiti: *Line shape modeling for the emission from carbon pellet ablation clouds in presence of a magnetic field* **(We.O.3.C1)**

15:00 – 15:20 ***Coffee break***

15:20 – 16:20 **Wednesday Oral Session 4**

15:20 – 16:00 Nelly Bonifaci: *Spectroscopic Analysis of Corona Discharge Cryoplasma in Helium with Molecular Nitrogen and Hydrogen Addivities* **(We.O.4.I1)**

16:00 – 16:20 Motoshi Goto: *Modeling of Lyman-α Line Polarization in Fusion Plasma due to Anisotropic Electron Collisions* **(We.O.4.C1)**

16:20 – 16:40 Ümmügül Erözbek Güngör: *The Stark Broadening Parameters of The Nitrogen HF RF-CCPs* **(We.O.4.C2)**

16:40 – 18:40 **Wednesday Poster Session** **(We.P)**

Location: Foyer of the Stokes Building - School of Electronic Engineering, DCU

THURSDAY JUNE 21st, 2018

Location: Lecture theatre HG22 in the School of Nursing and Human Sciences, DCU.

09:00 – 10:20 **Thursday Oral Session 1**

09:00 – 09:40 Valeriy A. Astapenko: *Lineshapes In Photoprocesses Induced By Ultra Short Laser Pulses* **(Th.O.1.I1)**

09:40 – 10:00 Robert R. Gamache: *Temperature Dependence of Half-Widths and Line Shifts for Molecular Transitions in The Microwave and Infrared Regions* **(Th.O.1.C1)**

10:00– 10:20 Tigran A. Vartanyan: *Exited Atoms-Surface Collisions and Their Manifestations in the Fluorescence Excitation Line Shapes* **(Th.O.1.C2)**

10:20 – 10:40 ***Coffee break***

10:40 – 12:00 **Thursday Oral Session 2**

10:40 – 11:20 Thomas Baumert: *Multiphoton Ionization of Chiral Molecules* **(Th.O.2.I1)**

11:20 – 11:40 Yan Tan: *Water vapor line-broadening coefficients for molecules in the HITRAN database* **(Th.O.2.C1)**

11:40 – 12:00 Adriana Predoi-Cross: *Temperature dependent spectroscopic study of carbon monoxide in the fundamental band* **(Th.O.2.C2)**

12:00 – 13:00 ***Lunch***

13:00 **Travel to City Centre**

***Meeting Point*:** Outside the School of Nursing and Human Sciences

---

14:20 – 18:00 **Guinness Store House Tour**

Location: St James's Gate, Ushers, Dublin 8

FRIDAY JUNE 22nd, 2018

Location: Lecture theatre HG22 in the School of Nursing and Human Sciences, DCU.

09:00 – 10:20 Friday Oral Session 1

09:00 – 09:40 Kimberly Strong: *The Impact of Line Mixing and Speed Dependence on Retrievals of Atmospheric CO_2 and CH_4 from Ground-Based Solar Absorption Spectra* **(Fr.O.1.I1)**

09:40 – 10:00 Katarzyna Bielsk: *Line Shape Investigation of O_2 B-band Transitions: Simultaneous Observation of the Speed-Dependence and Dicke Narrowing* **(Fr.O.1.C1)**

10:00– 10:20 Agata Cygan: *Advantages of Dispersion over Absorption Measurements in Cavity-Enhanced Spectroscopy* **(Fr.O.1.C2)**

10:20 – 10:40 *Coffee break*

10:40 – 12:00 Friday Oral Session 2

10:40 – 11:20 Shinichi Namba: *Characteristics of High-density Cascade Arc Discharges for an Atmosphere-vacuum Interface* **(Fr.O.2.I1)**

11:20 – 11:40 Verónica González Fernández: *Study of the Influence of the Cathode Material in the Behaviour of a Hollow-Cathode Glow-Discharge in Hydrogen* **(Fr.O.2.C1)**

11:40 – 12:00 Michał Słowiński: *H_2-He Interaction And Its Scattering States Observation With Highly Accurate Cavity-Enhanced Spectroscopy* **(Fr.O.2.C2)**

12:00 Conference Closes

24th ICSLS 2018
Dublin, Ireland

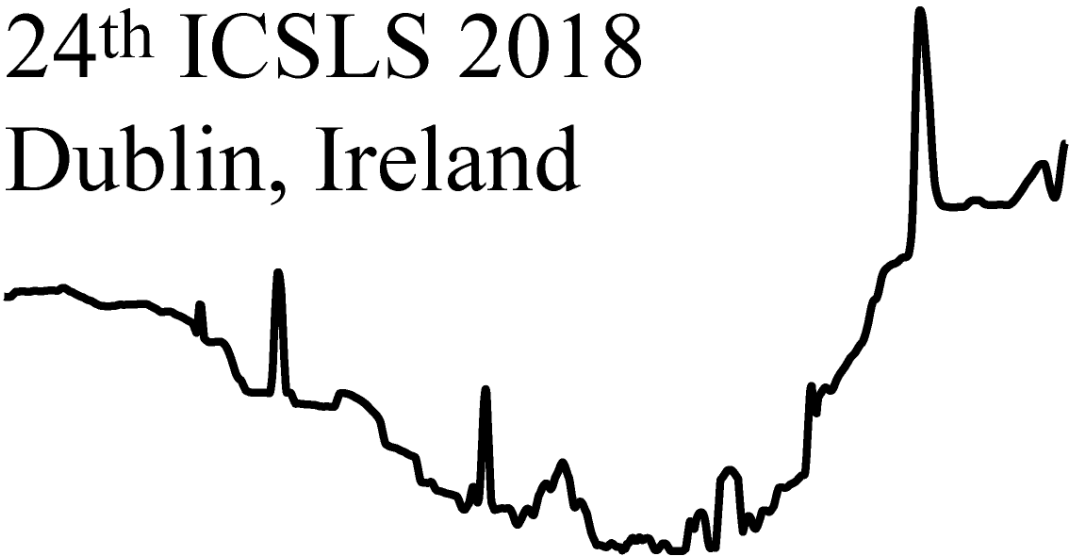

Poster Sessions

TUESDAY JUNE 19th, 2018

16:40 – 18:40 **Tuesday Poster Session** **(Tu.P)**

Location: Foyer of the Stokes Building - School of Electronic Engineering, DCU

Tu.P.1	Anna Dudaryonok, Nina Lavrentieva, Jeanna Buldyreva	*Line-shape Parameters and Their Temperature Dependence for the v_6 Band of CH_3D-N_2*
Tu.P.2	Muhammad Bilal Alli, Daniela Szwarcman, Daniel Salles Chevitarese, Patrick Hayden	*Vacuum Ultraviolet Laser Induced Breakdown Spectroscopy (VUV-LIBS) With Machine Learning For Pharmaceutical Analysis*
Tu.P.3	Hu Lu, Patrick Hayden, Piergiorgio Nicolosi and John Costello	*VUV Photoabsorption Spectra of Pb and Bi Ions Using Dual Laser Plasma Technique*
Tu.P.4	C B Doherty, M Kelly, T Donnelly, J G Lunney, J T Costello	*Ion Energy Distribution from Colliding Laser Plasmas*
Tu.P.5	M. Witkowski, R. Muñoz-Rodriguez, M. Borkowski, P. S. Żuchowski, R. Ciuryło, M. Zawada	*Photoassociation spectroscopy in the RbHg system*
Tu.P.6	A. Nishiyama, F. Thibault, M. Słowiński, M. Zaborowski, N. Stolarczyk, D. Charczun, A. Cygan, S. Wójtewicz, G. Kowzan, P. Masłowski, R. Ciuryło, D. Lisak, P. Wcisło	*Modeling of line and continuum spectral emission of hydrogen for recombining plasma conditions*
Tu.P.7	M. Hammad, E. P. Martin, M. Deseada Gutierrez, P. D. Lakshmijayasimh, G. Jainb, P. Landais, J. Braddell and P. M. Anandarajah	*Compact Gain Switched Optical Frequency Comb Generator for Sensing Applications*
Tu.P.8	O S Alekseeva, A Z Devdariani, M G Lednev, A L Zagrebin	*The Probabilities of the $v'1(^3P_1)$– $v''0^+1(^1S_0)$ Transitions and the Radiative Lifetimes of the $v'1(^3P_1)$ States of the CdAr Molecules*
Tu.P.9	A Z Devdariani, N A Kryukov, M G Lednev, A L Zagrebin, V V Olevskaia	*Determination of Radiation Characteristics of Molecular Transitions. Band $HgXe(A^3O^+)$ – $HgXe(X^1O^+)$*
Tu.P.10	Alaa Abo Zalam, V. A. Srećković, M. S. Dimitrijević, N. N. Bezuglov, and A. N. Klyucharev	*Fluorescence Spectrum Of Rydberg Atomic Hydrogen In The Dynamic Chaos Regime*
Tu.P.11	S. Chandran, A. A. Ruth, E. P. Martin, F. Peters, P. M. Anandarajah	*Gain Switched Frequency Comb lasers for Atmospheric Trace Pollutant Monitoring*
Tu.P.12	Christopher M Helstern, Christian G Parigger	*Radial Distribution Of Cyanide in Laser-Induced Plasma*

Tu.P.13	Wissam Fakhardji, Magnus Gustafsson, M.S.A El-Kader, Anastasios Haskpoulos, George Maroulis	*Contribution of the dimers on the collision induced absorption spectra in a Ar-Kr gas mixture – Benchmark for a new Ar-Kr potential*
Tu.P.14	Robert R. Gamache, Bastien Vispoel	*Vibrational Dependence And Prediction Of Line Shape Parameters For The H_2O-H_2 Collisional System*
Tu.P.15	Jason B. Greenwood, Caoimhe Bond	*Asymmetric Photoelectron Emission From Chiral Molecules Using A High Repetition Rate Laser*
Tu.P.16	Hannachi I., Meireni M., Rosato J., Stamm R., Marandet Y.	*Effect of Wave Collapse on Lyman and Balmer lines*
Tu.P.17	T. M. Petrova, A. M. Solodov, A. A. Solodov, V. M. Deichuli, V. I. Starikov	*Measurements and calculations of H_2-broadening and shift parameters of water vapor transitions in a wide spectral region*
Tu.P.18	M. Meireni, I. Hannachi, J. Rosato, M. Koubiti, Y. Marandet, R. Stamm	*Stark Broadening Analysis of Balmer Lines in Tokamak Edge Plasmas*
Tu.P.19	Václav Nevrlý, Petr Bitala, Vít Klečka, Michal Vašinek, Zdeněk Zelinger, Jan Suchánek, Michal Dostál, Václav Válek	*Analysis of Wavelength Modulation Spectra for Determination of OH Radical Concentration in an Atmospheric Pressure Laminar Premixed Flames*
Tu.P.20	De-Yin Wu, Jingdong Zhang, Zhong-Qun Tian, Jens Ulstrup	*Line Shapes of Raman and Plasmon-Enhanced Raman Spectroscopy for Probing Molecules in Solutions and on Noble Metals of Nanostructures*
Tu.P.21	K. Touati, M.T. Meftah, K. Chinini and S. Douis	*Collisional contribution to line profiles in plasmas in presence of an external magnetic field*
Tu.P.22	Vasily V. Buyadzhi	*Radiative and Collisional Spectroscopy of Multicharged Ions: Advanced Quantum Approach*
Tu.P.23	Valentin B. Ternovsky, Vasily V. Buyadzhi, Anna A. Kuznetsova, Andrey A. Svinarenko, Pavel A. Zaichko	*Spectroscopy of Rydberg atoms in a Black-Body Radiation Field: Relativistic Theory of Excitation and Ionization*
Tu.P.24	Eugeny V. Ternovsky, Alexander V. Glushkov, Anna V Ignatenko, Olga Yu. Khetselius, Valery Mansarliysky	*Computing Collisional Shift and Broadening of Heavy Atom Hyperfine Lines in an Atmosphere of the Buffer Inert Gas*
Tu.P.25	Alexander V. Glushkov, Anna A. Kuznetsova, Anna A Buyadzhi, Alexandra Makarova	*Spectroscopy of Heavy Atoms and Nuclei in a Strong Laser Field: Stark effect, Autoionization and Multiphoton Resonances*
Tu.P.26	Olga Yu. Khetselius, Y. V. Dubrovskaya, L. A. Vitavetskaya, V. B. Ternovsky	*Spectral Parameters for Hyperfine and Electroweak Interaction and Parity Non-conservation Effect in Heavy Atoms and Nuclei*

16:40 – 18:40 **Wednesday Poster Session** **(We.P)**

Location: Foyer of the Stokes Building - School of Electronic Engineering, DCU

We.P.1	N. Nimavat, M. Goto and T. Oishi	*Measurement of Line Emission Polarization for a Study of Anisotropy in the Electron Velocity Distribution Function at LHD*
We.P.2	Nina Lavrentieva, Anna Dudaryonok	*Calculation of SO_2 and NO_2 Linebroadening Induced by Carbon Dioxide*
We.P.3	A Z Devdariani, N A Kryukov, M G Lednev, A L Zagrebin	*Radiative Decay of the Metastable State $Hg(6^3P_2)$ in the Atmosphere of the Ar Atoms*
We.P.4	A Devdariani	*Bound-To-Bound and Bound-To-Continuum Optical Transitions In Negative Quasi-Molecules*
We.P.5	K.N.R. Tejaswi	*Modeling of line and continuum spectral emission of hydrogen for recombining plasma conditions*
We.P.6	Lazaros Varvarezos	*Vacuum-UV Ionization of Kr*
We.P.7	Syedah Sadaf Zehra, Muhammad Bilal Alli, Piergiorgio Nicolosi, John Costello, Paddy Hayden	*LIBS for thin films depth profiling- A comparison of Time Integrated and Time resolved methods*
We.P.8	Tetsutarou Oishi, Shigeru Morita, Yang Liu, Motoshi Goto and the LHD Experiment Group	*Doppler Profile Diagnostics On VUV Spectra For Emission Intensity, Ion Temperature And Flow Velocity Of Impurity Ions In Edge Plasmas Of Large Helical Device*
We.P.9	Roston G D, Mahran O , Ellsaid N and Nagham	*Effect of the macro bending and the signal line shapes on the spectral performance of fiber Bragg grating*
We.P.10	G. Seguineaud and M. Goto	*Spatial Characterization of Plasma Parameters inside Ablation Clouds in LHD*
We.P.11	Michael B Shattan, Christian G Parigger	*Line Selection For Nuclear Debris Analysis In Laser-Induced Plasmas*
We.P.12	Todd A Van Woerkom, Glen P Perram, Christian G Parigger	*Titanium Monoxide Diagnostic Of Pulsed Ablation*
We.P.13	R.R. Sheeba, M. Koubiti, S. Ferri, Y. Marandet, T. Qbaich, J. Rosato, R. Stamm	*Modeling of line and continuum spectral emission of hydrogen for recombining plasma conditions*
We.P.14	M. Konefał, M. Słowiński, M. Zaborowski, D. Lisak, P. Wcisło	*Analytical Extension Of Hard-Collision Model Of Velocity-Changing Collisions In The Hartmann-Tran Profile*
We.P.15	V. A. Srećković, M. S. Dimitrijević, Lj. M. Ignjatović, N. N. Bezuglov and A. N. Klyucharev	*Atom-Rydberg Atom Collisions In Hydrogen Plasmas: Cross Sections And Rate Coefficients*

We.P.16	H. Cybulski, H. Jóźwiak, N. Stolarczyk, P. Wcisło, F. Thibault	*The Ab Initio Calculations Of The Line-Shape Parameters For The CO-N_2 Complex*
We.P.17	Raúl Z. Martínez, Dionisio Bermejo, Franck Thibault, Piotr Wcisło	*Line-Shape Parameters For Pure Rotational Raman Lines Of D_2 In He*
We.P.18	Yan Tan, Shanelle Samuels, I.E. Gordon, R.V. Kochanov, L.S. Rothman	*H_2, He and CO_2 line-broadening coefficients for molecules in the HITRAN database. Part II: H_2CO, HCN, CO_2, H_2S, N_2O*
We.P.19	Gita Revalde, Atis Skudr, Natalja Zorina, Anda Abola	*Studies of Thallium Line Spectra in Thallium – Mercury Discharge*
We.P.20	Natalja Zorina, Gita Revalde, Atis Skudra	*Validity Of Deconvolution Method For Multicomponent Spectral Line Shapes*
We.P.21	Muhammad Hassan Sayyad, Ramshah Ahmad Toor, Syed Afaq Ali Shah, Nazia Nasr, Fatima Ijaz and Munawar Ali Munawar	*Choosing a Functional for Computing Absorption Transition Positions, Intensities and Shapes of Organic Semiconductors with TD-DFT*
We.P.22	Vasily V. Buyadzhi, Eugeny V. Ternovsky, Tatyana B. Tkach, Yuliya G. Chernyakova	*Multi-photon Spectroscopy of Many-electron Atoms and Ions in the Debye Plasmas*
We.P.23	Yuliya V. Dubrovskaya, Olga Yu. Khetselius, Larisa A. Vitavetskaya, Eugeny V. Ternovsky, Inga N. Serga	*Energy and Radiative Parameters and Spectral Line Shape for Hadronic Atomic Systems*
We.P.24	Valentin B. Ternovsky, Dmitry A Mironenko, Alexander V Glushkov, Eugeny V Ternovsky, Andrey A. Svinarenko	*Radiation Transition Probabilities for Heavy Rydberg Atoms within Advanced Relativistic Energy Approach*
We.P.25	Alexander V. Glushkov, Anna V. Ignatenko	*New Spectroscopy of Cooperative Laser Electron-γ-Nuclear Processes in Diatomic and Multiatomic Cryogenic Molecules*
We.P.26	Olga Yu. Khetselius, Alexander V. Glushkov Anna A. Kuznetsova, Vasily V. Buyadzhi	*"Shake-Up" and NEET Effects in Laser Electron-Gamma-Nuclear Spectroscopy of Atoms and Multicharged Ions*

24th ICSLS 2018
Dublin, Ireland

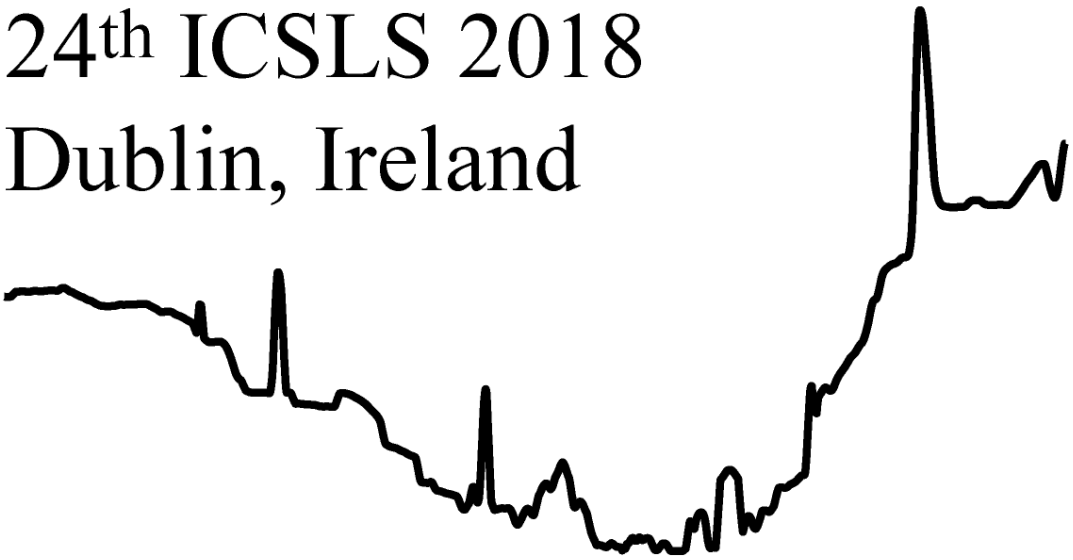

Monday Oral Session 1
Mo.O.1

Laboratory Plasma Diagnoses With Applications To Spectra Of White Dwarf Stars

Christian G Parigger

University of Tennessee, University of Tennessee Space Institute, Center for Laser Applications, 411 B.H. Goethert Parkway, Tullahoma, TN 37355, U.S.A.
e-mail: cparigge@tennessee.edu

This work presents details of time-resolved spectroscopy measurements of atomic and molecular spectra following laser-induced breakdown in selected gas mixtures. Integral inversions reveal the distributions of the excited species along the line of sight. The work also reviews applications of laboratory plasma spectroscopy for analysis of astrophysical spectra from white dwarf stars. Comparisons with readily available astrophysical signatures from the white dwarf stars α CMa B, Sirius B, and α CMi B, Procyon B, at temperatures, T_{eff}, of 8 kK and 26 kK, respectively, indicate hydrogen Balmer series and C_2 Swan band absorption spectra. Figure 1 (a) illustrates the pseudo-colored image of 100 accumulated hydrogen-beta lines, H_β, versus slit height of a Czerny-Turner spectrometer equipped with an intensified charge coupled device [1]. Fig. 1 (b) displays the single-shot equivalent spectrum obtained by averaging along the slit height, and H_β indicates a central dip-shift of $\Delta\delta_{ds} = 0.24 \pm 0.05$ nm.

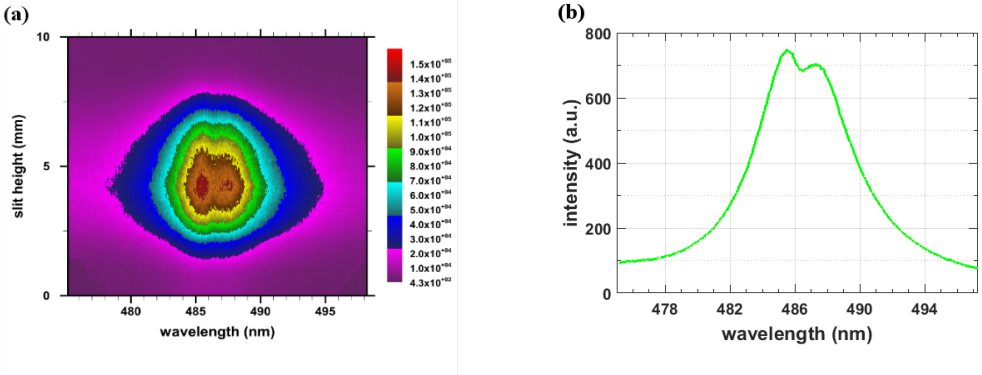

Figure 1. Balmer series H_β from laser-induced plasma in 0.76×10^5 Pa (11 psi) hydrogen, $\tau = 275$ ns time delay. (a) Recorded image of slit height vs. wavelength, and (b) averaged H_β spectrum

The central dip-shift of 0.24 nm implies an electron density of $N_e = 2.2\times10^{17}$ cm^{-3} [1, 2], consistent with H_β peak-separation and full-width-at-half-maximum diagnostics. An electron temperature, $T_e = 55$ kK, is inferred from the ratio of line to 10-nm continuum. H_β spectra at $\tau = 25$ ns reveal $\Delta\delta_{ds} \sim 1$ nm and $T_e \sim 110$ kK. For comparison, gravitational red-shifts of white dwarf stars [3], $\Delta\lambda = (v_g/c)\,\lambda$, amount to $\Delta\lambda = 0.049$ nm at a wavelength of $\lambda = 486.14$ nm and for a mean velocity of $\langle v_g \rangle = 30$ km/s, c is the speed of light. White dwarf stars that are categorized as DA's have hydrogen-dominated atmospheres and typically show Balmer series lines in absorption. White dwarf stars with $T_{eff} \sim 8$ kK may be labelled as DQ's and DQp's indicating C_2 Swan molecular and blue-shifted Swan-like bands in absorption, respectively.

References

[1] Parigger CG, Helstern CM, Drake KA, Gautam G 2017 *Int. Rev. At. Mol. Phys.* **8** 53.
[2] Halenka J, Vujičić B, Djurović S 1989 *J. Quant. Spectrosc. Radiat. Transfer* **42** 571.
[3] Falcon RE, Winget DE, Montgomery MH, Williams KA 2010 *Astrophys. J.* **712** 585.

Optical Clock Transitions in Weakly Bound Molecules

Mateusz Borkowski[a]

[a]*Institute of Physics, Faculty of Physics, Astronomy and Informatics, Nicolaus Copernicus University, Grudziadzka 5, 87-100 Torun, Poland; mateusz@fizyka.umk.pl*

Molecular optical clocks promise unparalleled sensitivity to proton-to-electron mass ratio and in searches for physics beyond the Standard Model. We propose to observe clock $^1S_0$-$^3P_0$ transitions in weakly bound bosonic $^{174}Yb_2$ molecules [1]. As in bosonic atomic clocks, a small transition dipole moment could be induced by means of a weak external magnetic field (Fig. 1a) [2]. The positions of molecular clock lines (Fig. 1b) can be determined to high accuracy: ground bound state positions have been measured with two-color photoassociation spectroscopy [3], while excited $^1S_0$+$^3P_0$ 0_u^- vibrational states can be predicted accurately using an interaction potential with *ab initio* long range parameters [4] and fitted to the recently measured ^{174}Yb $^1S_0$-$^3P_0$ scattering length [5]. The necessary ground state Yb_2 molecules could be efficiently produced by STIRAP. Thanks to favorable Franck-Condon factors (Fig. 1c) the magnetically induced molecular Rabi frequencies can be comparable to the atomic Rabi frequencies under same laser intensities and magnetic fields (Fig. 1d). A successful observation of clock transitions could pave the way towards Hz-level molecular spectroscopy.

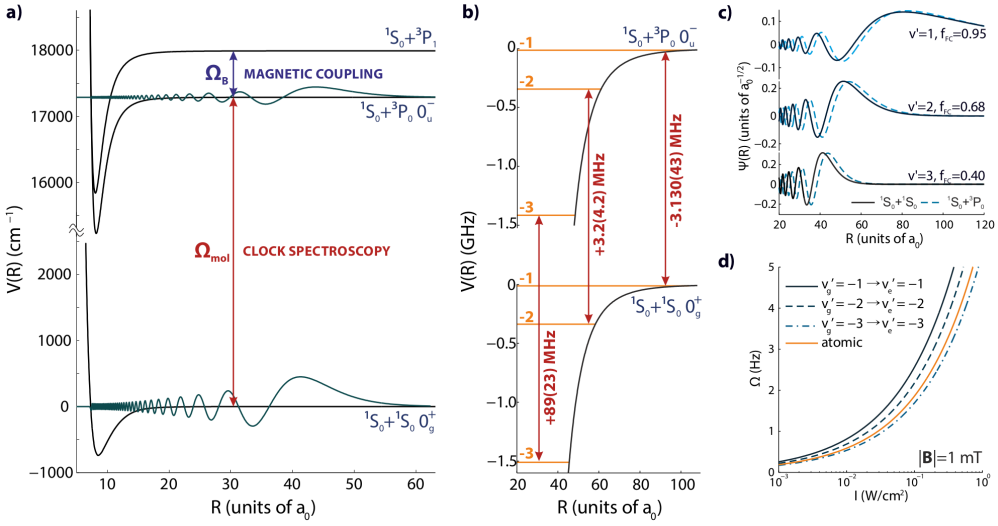

Figure 1. a) Relevant molecular states and potentials; b) molecular clock line positions in $^{174}Yb_2$; c) ground and excited state radial wavefunctions and Franck-Condon factors; d) magnetically induced molecular Rabi oscillation frequencies as a function of laser intensity

References

[1] Borkowski M 2018 *Phys. Rev. Lett.* **120** 083202
[2] Taichenachev AV, Yudin VI, Oates CW, Hoyt CW, Barber ZW, and Hollberg L 2006 *Phys. Rev. Lett.* **96** 083001
[3] Borkowski M, Buchachenko AA, Ciuryło R, Julienne PS, Yamada H, Kikuchi Y, Takahashi K, Takasu Y, and Takahashi Y 2017 *Phys. Rev. A* **96** 063405
[4] Porsev SG, Safronova MS, Derevianko A, and Clark CW 2014 *Phys. Rev. A* **89** 012711
[5] Franchi L, Livi LF, Cappellini G, Binella G, Inguscio M, Catani J, and Fallani L 2017 *New J. Phys.* **19** 103037

24th ICSLS 2018
Dublin, Ireland

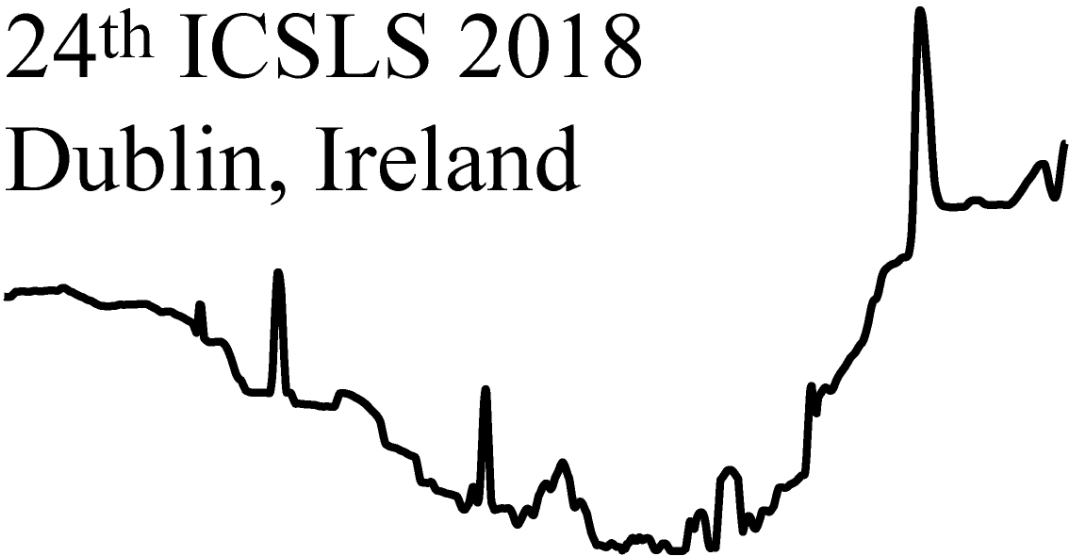

Monday Oral Session 2
Mo.O.2

Stark Broadening In Stellar Spectra

Milan S. Dimitrijević

Astronomical Observatory, Volgina 7, 1100 Belgrade, Serbia, mdimitrijevic@ aob.rs

In astrophysical plasmas the plasma conditions, first of all temperatures (T) and electron densities (N) are incomparably more various comparing to plasmas in laboratory and one can find many different cases when broadening due to interaction between emitter and charged particles (Stark broadening) is of interest. It could be significant in cosmical plasmas of such extreme conditions like in the interstellar molecular clouds, where T is around 30 K or smaller, and typical N is 2-15 cm^{-3} or in atmospheres of neutron stars, where T is 10^6 - 10^7 K and N is of the order of 10^{24} cm^{-3}. White dwarf and pre-white dwarf atmospheres are an excellent example for the importance of Stark broadening of spectral lines in astrophysics, since there, plasma conditions are very favorable for this mechanism of line broadening. For analysis and synthesis of spectra of A and late B type stars, contribution of Stark broadening may also be significant, as well as for cooler star atmospheres as e.g. Solar one, since the Stark line width within a spectral series increases with the increase of the principal quantum number of the upper level. Moreover, it is important and for modelling and investigation of subphotospheric levels. There is a variety of problems in astrophysics where Stark broadening is of interest as for example: stellar spectra analysis and synthesis, modelling of stellar atmospheres, stellar elemental abundances determination from equivalent widths of absorption lines, radiative transfer through the stellar plasmas, opacity calculations. radiative acceleration considerations, nucleosynthesis research etc. The need for reliable Stark broadening data even for atoms and ions previously without some special astrophysical interest, increased with the space missions with on board telescopes and spectrographs providing high resolution spectra and also with the development of computers computing facilities.

Here will be reviewed and discussed astronomical importance of Stark broadening, as well as the applications of Strak broadening data for various astrophysical problems with an emphasis on broadening of non-hydrogenic spectral lines. We will also discuss theoretical methods for the determination of Stark broadening parameters, astrophysical applications of obtained results and organisation of available Stark broadening data in on-line databases, with the particular attention to STARK-B database (http://stark-b.obspm.fr), which is a part of VAMDC (Virtual Atomic and Molecular Data Center – http://www.vamdc.org/).

Line Shape Modeling For Magnetic White Dwarf And Tokamak Edge Plasmas: Common Challenges

J. Rosato[a], M. Meireni[a], M. Koubiti[a], Y. Marandet[a], R. Stamm[a], J. Kovačević-Dojčinović[b], M. S. Dimitrijević[b], L. Č. Popović[b], Z. Simić[b]

[a]*PIIM, Aix-Marseille Université / CNRS, 13397 Marseille Cedex 20, France*
[b]*Astronomical Observatory, Volgina 7, 11060 Belgrade 38, Serbia*

About 10% of white dwarfs are known to have a magnetic field strength of 10^5 to 5×10^8 G, as indicated from spectroscopic observations and models [1 – 3]. An interpretation of the shape of absorption lines requires the Zeeman effect be accounted for in line broadening models, in addition to the Stark effect associated to the plasma microfield. Under specific conditions, the plasma located at the edge of tokamaks has conditions close to white dwarf stellar atmospheres (T_e and T_i are of the order of 10^4 K and N_e can be higher than 10^{14} cm^{-3} in divertor configurations [4]) and the magnetic field can be strong enough so that line shapes are affected both by the Zeeman effect and Stark broadening. In this work, we present new line shape calculations accounting for the simultaneous action of electric and magnetic fields, in conditions relevant to tokamak edge plasmas and white dwarf stellar atmospheres. A focus on the Balmer series is done. We perform fittings of observed spectra and infer the electron density from the Stark broadening.

References

[1] Kepler S O, et al. 2013 *Mon. Not. R. Astron. Soc.* **429** 2934.
[2] Landstreet J D, et al. 2012 *Astron. Astrophys.* **545** A30.
[3] Külebi B, et al. 2009 *Astron. Astrophys.* **506** 1341.
[4] Rosato J, et al. 2017 Atoms **5** 36.

Effect of Gamma Ray and Signal Line Shapes on the Spectral Performance of Fiber Bragg Grating

Roston G D, Mahran O, Helmi M S and Ellsaid N

Physics Department, Faculty of Science, Alexandria University, Egypt
dr.gamal_daniel@yahoo.com

The reflectivity power of the fiber Bragg grating (FBG) with wavelength and FBG lengths were studied at different signal profiles (sine and Gaussian) with the effect of gamma radiation. Firstly, for the sine signal profile, the reflectivity power in the case non-irradiated gives a maximum value at the FBG wavelength λ = 155 μm, but for gamma irradiated case the peak disappear and distorted. Secondly, for the Gaussian signal profile, the reflectivity powers are the same for irradiated and non-irradiated cases. It is founded that the Gamma radiation decreases the performance of FBG, so the fiber cable must putted out of gamma radiation.

Results:

The effect of the signal wavelength and FBG length on the reflectivity power of the fiber Bragg grating at signal profile (sine and Gaussian) were studied as seen in Fig. (1,2).

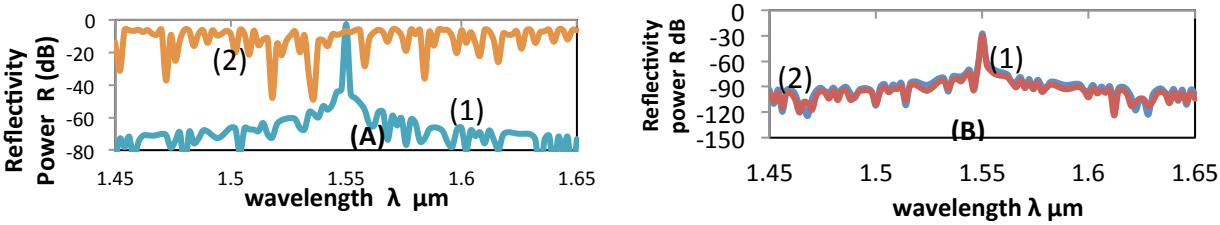

Fig. 1. (A) The reflectivity power of FBG for the sine **(A)** and Gaussian **(B)** profiles versus the wavelength of the signal (μm) ,for (, at lengths of the grating (L = 10) for the normal case (1) and under the effect of radiation (2), with Dose 0.6 MGy.

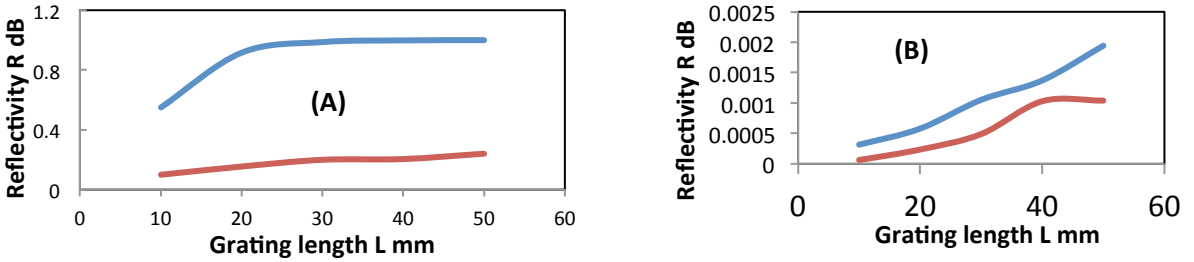

Fig. 2 The reflectivity with the length of the FBG in cases of radiated and non-radiated for sine (A) and Gaussian (B) profiles, at λ = 1550 nm and dose = 0.6 MGY**.**

References

[1] Kao C.K and Hockham G.A, Proc. 1966 IEE, , vol. 113, 1151.
[2] Hill K. O, Fujii Y, Johnson D. C and Kawasaki B. S, 1978 Appl. Phys. Lett, vol.32 , pp. 647–649.
[3] Meltz G, Morey W. W. and Glenn W. H, 1989 Opt. Lett., vol.14, 823–825,
[4] Mahran O, Hamdallah T A, Moustafa H. Aly and Ahmed E. El- Samahy 2009 Journal of Applied Sciences Research, 5(10): 1604-1610
[5] Taymour A. Hamdalla 2013, research Journal of physics 7(1), ISSN1819_3463 DOL:10.3923 /Rjp. 2013.9.16. Academic Journals Inc.

24th ICSLS 2018
Dublin, Ireland

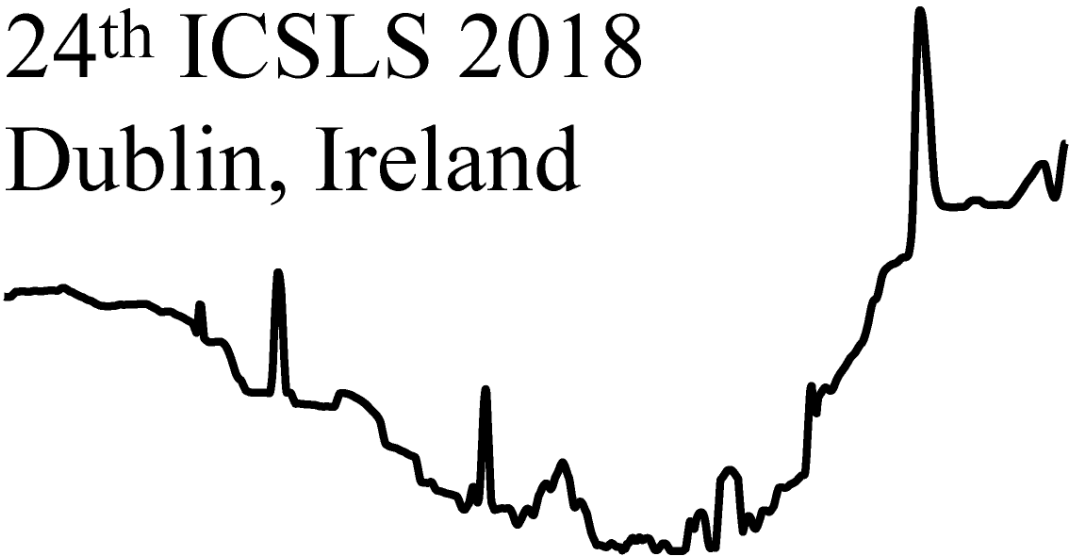

Monday Oral Session 3
Mo.O.3

Plasmon-enhanced Fluorescence for Improved Bioassay Performance

Colette McDonagh[a] and Daragh Byrne[a]

[a]*School of Physical Sciences, Irish Photonic Integration Centre (IPIC), Dublin City University, Glasnevin, Dublin 9.*
Email: Colette.mcdonagh@dcu.ie

Metal enhanced fluorescence presents numerous possibilities for the development of sensitive chemical and biological sensors. The presence of metals in proximity to a fluorophore can dramatically alter its excitation and emission properties, due to the interaction of the light with surface plasmon polaritons (SPP), leading to significant enhancement. In this work we examine the use of both Au diffraction gratings and in-situ grown plasmonic cavities for enhancement of fluorescence in bioassays.

When light is coupled into a diffraction grating at a momentum matching angle, SPPs are generated which alter the strength of the electric field above the surface. The absorption rate of fluorophores near the surface is directly proportional to the square of this modified electric field which leads to a corresponding enhancement in the emission rate. For compact device configurations, coupling can also be achieved by rotating the grating about the azimuth, thereby reducing the component of the grating vector coupling to the in plane component of the light.[1] Finite difference time domain modeling was used to determine the optimal conditions to maximize the strength of the field generated when coupling into a grating. A fluorescence enhancement of ~30 was obtained for a model bioassay, when coupling into the grating via azimuth rotations, which agreed well with the model shown in Figure 1(left).

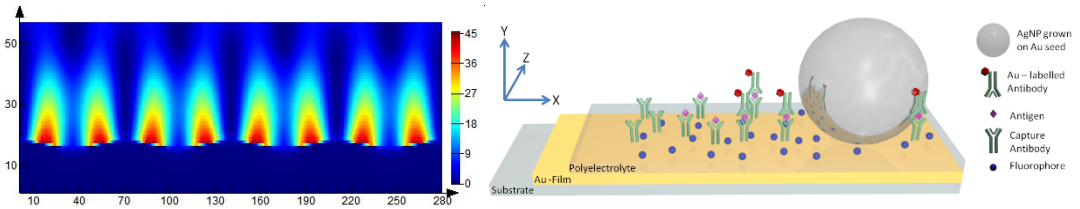

Figure 1. FDTD model of E-field of a plasmonic grating (left) and schematic of in-situ growth of plasmonic cavity for bioassay application (right)

Plasmonic cavities are widely studied for the large amplifications in fluorophore emission intensity that they can achieve. Exploiting these properties for biological sensing applications requires strategies to selectively insert the target antigen into the resonant cavities, which are often of similar size or smaller than the target molecule. Here we demonstrate that using relatively simple solution processing, cavity structures can be grown at the stochastic locations where antigen binding takes place, which yields enhanced fluorophore emission intensities and improved bioassay responses. The fluorescence amplification generated by the in situ growth structures is sufficiently large to enable both single antigen and fluorophore detection and negates the requirement for complex surfaces or geometries.

References

[1] Byrne, D.;Duggan, P.; McDonagh, C. Controlled surface plasmon enhanced fluorescence from 1D gold gratings via azimuth rotations. *Methods Appl Fluoresc* **2017**, *5*, 015004.

[2] Flauraud V, Regmi R, Winkler PM, Alexander DTL, Rigneault H, van Hulst NF, *et al.* In-Plane Plasmonic Antenna Arrays with Surface Nanogaps for Giant Fluorescence Enhancement. *Nano Letters* 2017, **17**(3)**:** 1703-1710

Asymmetric Photoelectron Emission From Chiral Molecules Using A High Repetition Rate Laser

Jason B. Greenwood, Caoimhe Bond

Centre for Plasma Physics, School of Maths and Physics, Queen's University Belfast, BT7 1NN, UK

j.greenwood@qub.ac.uk

The use of polarized light to identify the handedness of chiral chemicals has been employed for more than 200 years, but recently a completely new chiro-optical phenomenon has been discovered. Known as photoelectron circular dichroism, the angular distribution of electrons ionized from chiral molecules by circularly polarized light pulses has been found to be anti-symmetric with respect to the direction of the light propagation [1,2].

To study this phenomenon, chiral molecules were multiphoton ionized with a femtosecond laser in our laboratory. Using a magnetic field to confine electrons along the laser direction, the electrons emitted in the forward and backward hemispheres were separated and directed onto two detectors. This simple stereo-detection setup allows direct measurements of the asymmetry and demonstrates that the instrument can be used to measure the relative proportion of left-handed to right-handed chiral molecules in samples [3].

Using 260 nm pulses produced at a rate of 1 MHz to efficiently ionize the exemplar aromatic chiral molecule 1-phenylethanol, Figure 1 shows how the photoelectron asymmetry value G changes as the proportion of the circular polarisation in the pulse (the Stokes S_3 parameter) is varied. The linear dependence indicates that the photoelectron circular dichroism originates due to a single photon process from the excited state of the molecule. This is in contrast to previous results for camphor where a more complex dependence on S_3 suggested that selective excitation of molecules with certain orientations was influential [3].

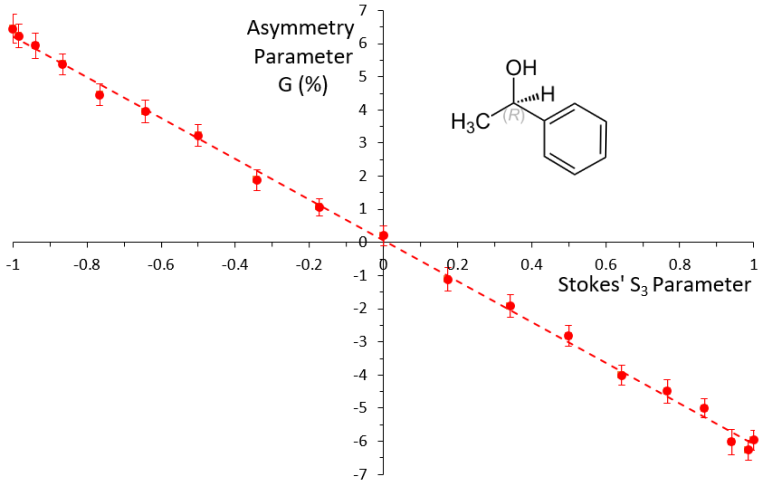

Figure 1. Photoelectron circular dichroism asymmetry parameter G of 1R-Phenylehanol as a function circularly polarised fraction of the pulse (the S_3 Stokes parameter). The ionising laser pulses were 300 fs long, at a wavelength of 260nm and an intensity of approximately 5 x 10^9 Wcm^{-2}.

References

[1] L. Nahon et al., J. Elect. Spect. Rel. Phen. **204**, 322 (2015)
[2] C. Lux et al, Angew. Chem. Int. Ed., **51**, 1(2012)
[3] J. Miles et al., Anal. Chim. Acta, 984, 134 (2017)

24th ICSLS 2018
Dublin, Ireland

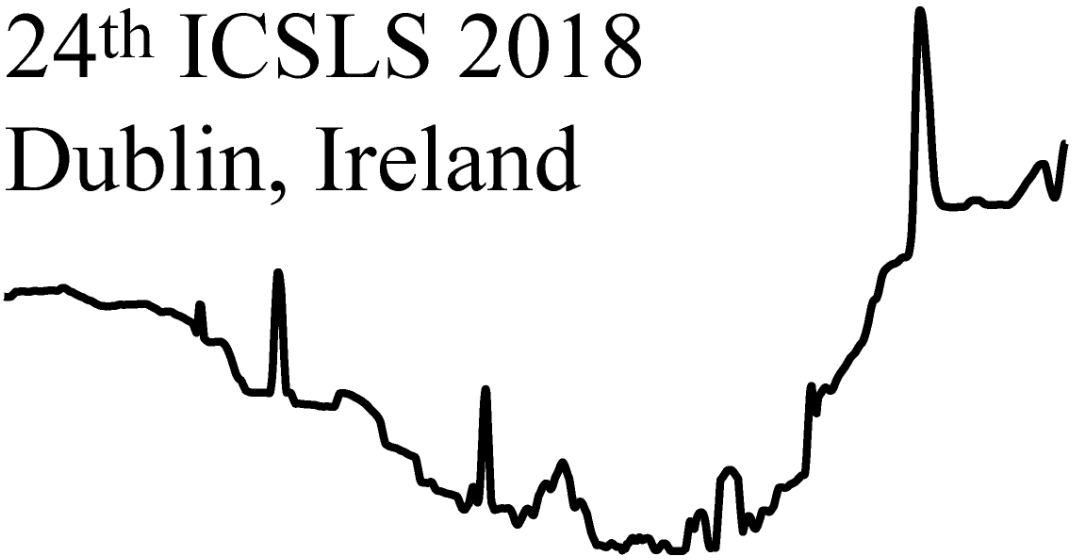

Monday Oral Session 4
Mo.O.4

Determining Molecular Orientation via Single Molecule SERS in a Plasmonic Nano-gap

Addison R. L. Marshall[1], Jamie Stokes[1], Francesco N. Viscomi[1], John E. Proctor[1,2], Johannes Gierschner[3], Jean-Sebastien G. Bouillard[1,4,5], and Ali M. Adawi[1,4]*

[1]*School of Mathematics and Physical Sciences, Department of Physics and Mathematics, University of Hull, Cottingham road, HU6 7RX, UK*
[2]*Materials and Physics Research Group, School of Computing, Science and Engineering, University of Salford, Manchester M5 4WT, United Kingdom*
[3]*Madrid Institute for Advanced Studies - IMDEA Nanoscience Calle Faraday 9, Ciudad Universitaria de Cantoblanco, 28049 Madrid, Spain*
[4]*G. W. Gray Centre for Advanced Materials, University of Hull, Cottingham road, HU6 7RX, UK*
[5]*Department of Physics, King's College London, Strand, London, WC2R 2LS*
**a.adawi@hull.ac.uk*

In this work we report on the design and fabrication of plasmonic nano-gaps for surface-enhanced Raman (SERS) spectroscopy. We present an optimized plasmonic nano-gap formed between a silver nanoparticle and an extended silver film with a 5 nm gap width for which the effect of near-field enhancement and photon scattering efficiency to the far-field on the SERS signal have been investigated as a function of particle size. Finite difference time domain (FDTD) calculations revealed that the enhancement in the SERS signal is mainly associated with the dipolar mode of the nano-gap and strongly affected by the particle size which was found to be in direct agreement with our SERS measurements.

Concentration dependent SERS measurements from our optimized nano-gaps doped with molecular dye Rhodamine 6G showed clear differences in the relative SERS peaks intensity at concentrations of $2x10^{-7}$ M compared to the SERS spectra measured from gaps doped with the same dye at higher concentrations $2x10^{-5}$ M. Those differences can be attributed to the random orientation of the single molecular dye in the plasmonic gap, therefore highlighting the single molecule sensitivity of the optimised nanogaps.

In the single molecule regime, the SERS signal is dependent on the molecule orientation with regards to the field in the plasmonic nanostructure. The dipole moment derivative of the various Raman modes of the analyte were determined using DFT (Density Function Theory) calculations, and by convoluting this information with the known dipole moment of the plasmonic nanogap, we were able to recover the orientation of the single molecule within the nanogap.

References

[1] Addison R. L. Marshall, Jamie Stokes, Francesco N. Viscomi, John E. Proctor, Johannes Gierschner, Jean-Sebastien G. Bouillard and Ali M. Adawi, 2017, *Nanoscale*, **9**, 17415–17421

Near-perfect absorption in the visible range using metal-dielectric-metal nanostructure plasmonic array

K. Wilson, C. Hrelescu and A. L. Bradley

School of Physics and CRANN, Trinity College Dublin, College Green, Dublin 2, Ireland.
Email: HRELESCC@tcd.ie.

Metal-dielectric-metal structures comprised of an nanoparticle separated by a dielectric from a continuous metallic film are capable of generating narrow bands of near-perfect absorption [1–3]. A structure consisting of an array Au nanodiscs on a polymer layer above a Ag backreflector has been numerically and experimentally investigated. The structures, characterized by reflectance spectroscopy, exhibit a near-perfect absorption feature in the visible spectrum. An example of a typical structure is an array of 100 nm thick and 150 nm diameter Au disks with a 300 nm periodicity, fabricated on a 100 nm thick polymer film deposited on a 100 nm optically thick Ag layer (Fig. 1a). The full structure is fabricated on a Si substrate. The reflectance spectrum has near-zero reflectance dip at 583 nm, producing a green colour when viewed in reflectance (Fig. 1b). At this wavelength, the electric and magnetic field distributions along the vertical cross section through one unit cell of the structure show very strong localization of light under the nanodisk. The disks alone in free space have a scattering peak at approximately 565 nm.

The presence and tuneablity of such a feature is of interest for the generation of structural colour, which can be tuned across the visible spectrum. Finite difference time domain numerical simulations have been used to uncover the origin of the feature, and it is attributed to the generation of higher order multipoles, also known as magnetic resonances[1–3]. The simulations show the strong influence of the dielectric layer and the metallic back-reflector on these modes. The position of the near-zero reflectance feature can be tuned by varying the periodicity of the structure and/or the thickness of the polymer film. Colour generation is highly sensitive to the different features in the reflectance spectrum, and in this presentation the mechanisms producing the various features and the interplay between them will be elucidated.

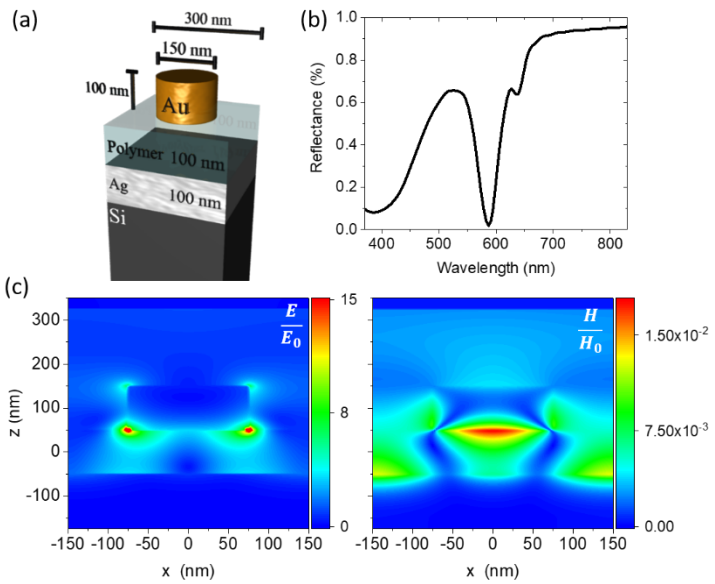

Figure 1. (a) A typical unit cell of the metal-dielectric-metal array. (b) The reflectance spectrum and (c) the electric and magnetic field distributions along the vertical cross-section of the unit cell.

References

[1] Kim W., Simpkins B. S., Long J. P., Zhang B., Hendrickson J., and Guo J., 2015 *J. Opt. Soc. Am.*, **32**(8), 1686.
[2] Zhang B., Zhao Y., Hao Q., Kiraly B., Khoo I.-C., Chen S., and Huang T. J., 2011 *Opt. Express*, **19**(16), 15221.
[3] Zhang B., Hendrickson J., and Guo J., 2013 *J. Opt. Soc. Am. B*, **30**(3), 656–662.

Fano Resonances in Plasmonic Systems: Bright Modes, Dark Modes and Critical Coupling

Olivier J.F. Martin

[a]*Nanophotonics and Metrology Laboratory, Swiss Federal Institute of Technology Lausanne (EPFL), CH-1015 Lausanne, Switzerland (olivier.martin@epfl.ch www.nanophotonics.ch)*

Asymmetric resonances display unique features compared to their symmetric Lorentzian counterpart, and are currently the subject of considerable research efforts in photonic and plasmonic nanostructures. A theoretical derivation was first proposed by Fano to explain autoionization of atoms and the asymmetric shape of these resonances that now bear his name [1]. In fact, the interference phenomenon underlying Fano resonances is a general wave phenomenon, appearing in particular as Wood anomalies in gratings; in extraordinary optical transmission, dielectric, and metallic photonic crystals; and more recently in optomechanical systems, plasmonic nanostructures, or as the plasmonic analog of electromagnetically induced transparency (EIT) in metamaterials [2].

The recent interest for Fano resonances in plasmonic stems on the one side from the underlying modal structure associated with multiparts plasmonic nanosystems that support both radiating modes (*viz.* bright modes, like a dipolar electric mode) and non-radiating modes (*viz.* dark modes, like a quadrupolar electric or a dipolar magnetic mode). On the other side, there is hope that through appropriate Fano resonance tuning, one might mitigate the intrinsic losses associated with the metals in plasmonic systems.

Although Fano resonances have been studied in a broad variety of complex plasmonic nanostructures and metamaterials, their analysis relies either on a classical oscillator model, phenomenological models, a coupled-mode formalism, or the quantum-mechanical approach used by Fano to fit experimental data and to understand the mechanisms behind the resonance shape. Here, we will present an *ab initio* theory for asymmetric resonances for electromagnetic scattering in general dispersive and lossy media and use it to explore different coupling regimes in a plasmonic system. In particular, we will show that by tuning the geometry of simple periodic plasmonic nanostructures fabricated by extreme-ultraviolet lithography, Fig. 1(a), it is possible to reach a critical-coupling state, Fig. 1(b), which is associated with a dramatic near-field enhancement in the nanostructure and can be evidenced through surface-enhanced Raman spectroscopy measurements [3].

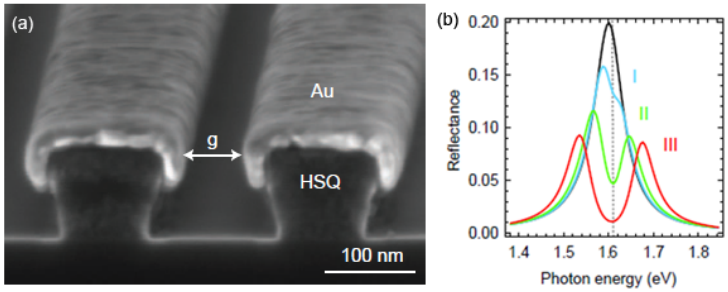

Figure 1. (a) Periodic plasmonic nanostructure and (b) the different coupling regimes it can achieve; I: under-coupled, II: critically-coupled and II: over-coupled.

[1] Fano U. *Phys. Rev.* 1961 **124**, 1866.
[2] Gallinet B., Martin O.J.F. 2011 *Phys. Rev. B* **83** 235427.
[3] Gallinet B. *et al.* 2013 *Nano Lett.* **13**, 497.

24th ICSLS 2018
Dublin, Ireland

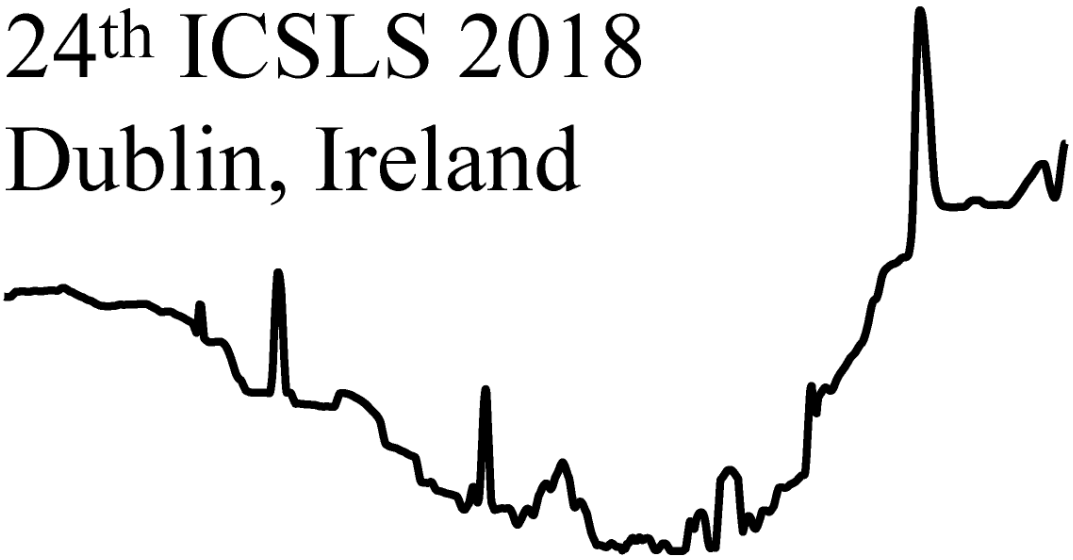

Tuesday Oral Session 1
Tu.O.1

Free Electron Streaking Reveals Attosecond Dynamics On Surfaces And Layered Systems

Reinhard Kienberger[a,b]

[a]*Fakultät für Physik, E11, Technische Universität München, James Franck Straße, 85748 Garching, reinhard.kienberger@tum.de,*

The generation of single isolated attosecond pulses in the extreme ultraviolet (XUV) together with fully synchronized few-cycle infrared (IR) laser pulses allowed to trace electronic processes on the attosecond timescales. A pump/probe technique was used to investigate electron dynamics on surfaces and layered systems with unprecedented resolution.

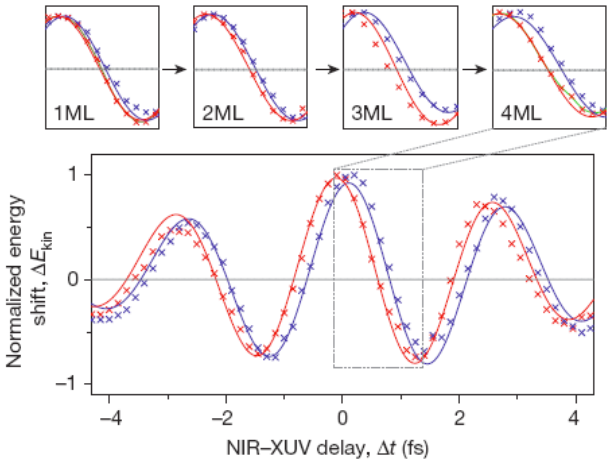

Figure 1. Delay of W 4f electron with respect to Mg electrons depending of the number of Mg adlayers (from [4]).

The attosecond streaking method [1] is the most established technique in attosecond science. Photoelectrons generated by laser based attosecond extreme ultraviolet pulses (XUV), are exposed to a dressing electric field from well synchronized laser pulses. The energy shift experienced by the photoelectrons by the dressing field is dependent on the delay between the XUV pulse and the dressing field and makes it possible to measure the respective delay in photoemission between electrons of different type (core electrons vs. conduction band electrons). The information gained in such experiments on tungsten [2] triggered many theoretical activities leading to different explanations on the physical reason of the delay. Attosecond streaking experiments have been performed on different solids [3], leading to different delays – also depending on the excitation photon energy. We show measurements of time-resolved transport of different types of electrons through a defined number of adlayers on a bulk material on an attosecond timescale (Fig 1) [3]. Finally, using a sophisticated sub-monolayer-extrapolation, we were able to measure not only relative delays but the absolute time an electron needs to travel from A to B.

References

[1] R. Kienberger et al., Nature **427**, 817 (2004).
[2] A. Cavalieri et al., Nature **449**, 1029 (2009)
[3] S. Neppl et al., Nature **517**, 342 (2015)

Switching Lorentzian To Fano Line Shapes With Intense Lasers — From Attosecond Electronics To Sub-Ångstrom Nuclear Resonance Metrology

Thomas Pfeifer[a,b]

[a]*Max-Planck-Institut für Kernphysik, Saupfercheckweg 1, 69117 Heidelberg, Germany*
[b]*Center for Quantum Dynamics, Ruprecht-Karls-Universität Heidelberg, 69120 Heidelberg, Germany*

The spectral line shape encodes dynamical information about a sample or system of interest. The symmetric Lorentzian resonance line shape encodes a lifetime or coherence time of an excited state in the width of the resonance line. The asymmetric Fano resonance comes about by an interference of two channels, a continuum and a bound excitation which are coupled to one another. In physics, metrology of Fano resonances is used to study correlation effects (i.e. configuration interaction) of two or more electrons to test and further develop few- and many-body quantum theory for the understanding of progressively more complex systems.

We observed that Fano resonances can be modified by interaction with intense (femtosecond pulsed) laser fields: Fano resonances are converted to Lorentzian resonances and vice versa [1]. The understanding of this phenomenon by a laser-induced quantum-mechanical phase-shift, encoded in the modified Fano profile, allows the precise quantification of ultrashort strong-field laser–matter interactions for sensitive tests of quantum-dynamics theory [2].

Generalization of the Fano phase control mechanism to general modifications of a system's temporal response function [3] allowed for a novel scheme for few-cycle laser pulse metrology [4], and the time-resolved observation of the emergence of a Fano resonance [5].

Application of Fano-phase control to nuclear resonances recently enabled the resonant amplification of hard-x-ray light by passing through a ^{57}Fe Mössbauer sample. The result is a laser-like bright and narrow 14.4 keV emission line [6]. This x-ray control approach opens new routes not only for Mössbauer-spectroscopy, but could unlock the x-ray domain for precision spectroscopy.

References

[1] Ott C, Kaldun A, Raith P, Meyer K, Laux M, Evers J, Keitel CH, Greene CH, and Pfeifer T 2013 *Science* **340**, 716.
[2] Ott C, Kaldun A, Argenti L, Raith P, Meyer K, Laux M, Zhang Y, Blättermann A, Hagstotz S, Ding T, Heck R, Madronero J, Martín F, and Pfeifer T 2014 *Nature* **516**, 374.
[3] Blättermann A, Ott C, Kaldun A, Ding T, and Pfeifer T 2014 *J. Phys. B* **47**,124008.
[4] Blättermann A, Ott C, Kaldun A, Ding T, Stooß V, Laux M, Rebholz M, and Pfeifer T 2015 *Opt. Lett.* **40**, 3464.
[5] Kaldun A, Blättermann A, Stooß V, Donsa S, Wei H, Pazourek R, Nagele S, Ott C, Lin CD, Burgdörfer J, and Pfeifer T 2016 *Science* **354**, 738.
[6] Heeg KP, Kaldun A, Strohm C, Reiser P, Ott C, Subramanian R, Lentrodt D, Haber J, Wille HC, Goerttler S, Rüffer R, Keitel CH, Röhlsberger R, Pfeifer T, Evers J, 2017 *Science* **357**, 375.

24th ICSLS 2018
Dublin, Ireland

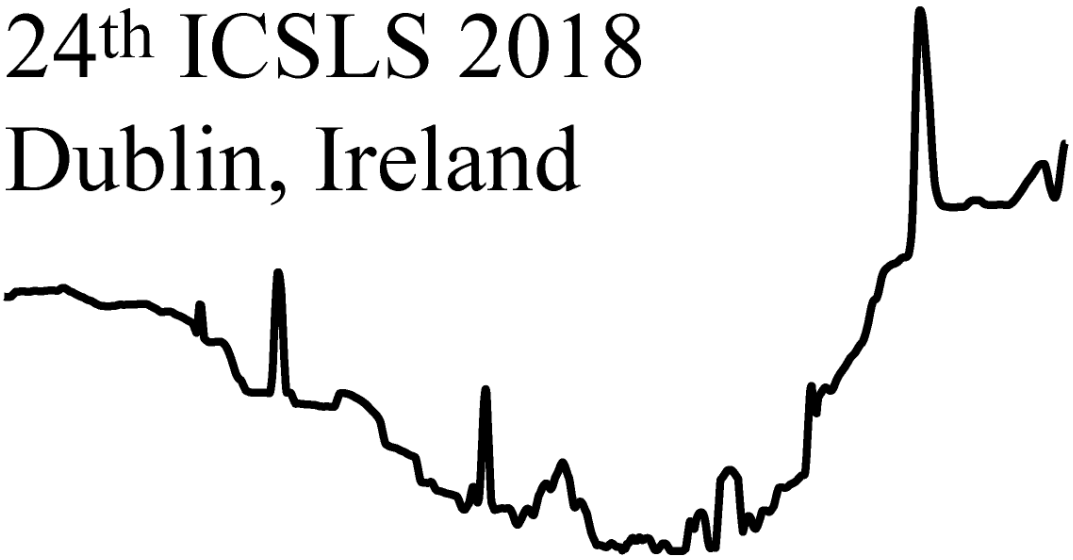

Tuesday Oral Session 2
Tu.O.2

Photoionization of Atomic and Molecular Ions

E.T. Kennedy[a], J.-P. Mosnier[a,] *, P. V Kampen[a], J-M Bizau[b,c], D. Cubaynes[b,c], S. Guilbaud[b], S. Carniato[d], A. Puglisi[d], N. Sisourat[d]

[a]*School of Physical Sciences and NCPST, Dublin City University, Dublin 9, Ireland(Eugene.kennedy@dcu.ie)*
[b]*Institut des Sciences Moléculaires d'Orsay, CNRS, Université Paris–Sud, and Université Paris-Saclay, F-91405 Orsay, France*
[c]*Synchrotron SOLEIL, L'Orme des Merisiers, Saint-Aubin, BP 48, F-91192 Gif-sur-Yvette Cedex, France*
[d]*Sorbonne Universités, UPMC Univ Paris 06, CNRS, UMR 7614, Laboratoire de Chimie Physique-Matière et Rayonnement, F-75005 Paris, France*

Measurements of photoionization cross-sections of free ions are challenging, as a suitable ion beam must be produced and illuminated by an appropriate, short wavelength, light source. Versatile techniques are required, as photoabsorption and/or photoionization experiments can provide physical insight into the interaction of short wavelength photons with ions and correspondingly useful data for plasmas and astrophysics. Early survey investigations of a wide range of *atomic* ions were achieved with the Dual Laser Plasma technique [1], which combined a broad-bandwidth, backlighting source coupled with the ability to produce a range of atomic ions. Developments at synchrotrons utilizing *atomic* ion sources coupled with monochromatized synchrotron radiation in merged-beam configurations provide absolute cross sections, higher spectral resolution, photoionization channel discrimination and detection varying linearly with the ion beam density [2].

This talk outlines some recent results in the study of positively charged ions, in particular *molecular* hydride ions. For example, we describe complementary measurements of the 2p photoexcitation cross sections for the atomic-molecular-ion series SiH_n^+ (n = 0,1,2,3) near the L-shell threshold [3]. The experiments, carried out at the Soleil synchrotron, used an electron cyclotron resonance (ECR) plasma ion source. For the molecular ions, the Si^{2+} decay channel appeared dominant, implying similar electronic Auger and nuclear relaxation dissociation patterns. The Si^{2+} yields were recorded for the molecular ions and put on absolute cross-section scales by comparing with the yields for the Si^+ parent atomic ion. Theoretical cross-sections were calculated using ab initio configuration interaction method (CI), inclusive of spin-orbit coupling/vibrational dynamics and contributions from inner-shell excitations, from both ground and valence-excited electronic states. The broadly similar experimental spectra moved towards lower energies as the number of screening hydrogen atoms increased. They featured a region below ~107 eV due to $2p \rightarrow \sigma*$ transitions to dissociative states, intense and broadened peaks in the ~107–113-eV region and relatively sharp Rydberg series due to $2p \rightarrow n\delta,n\pi$ transitions converging on the $L_{II,III}$ limits above ~113 eV. The overall spectral shape was broadly replicated by theory in each case, but the level of agreement did not extend to individual resonance structures.

Other examples will also be discussed to further illustrate the additional complexity introduced when moving from atomic to molecular ions.

References

[1] Kennedy ET *et al* 1994 *Optical Engineering,* **33** 3984-3992.
[2] Kjeldsen H 2006 *J. Phys. B* **39** R325-R377: Schippers S, Kylcoyne ALD, Phaneuf RA and Müller A 2016 *Contemp. Phys.* **57** 215-229
[3] Kennedy ET *et al* 2018 Phys. Rev A, **97** 043410

Investigation of the double photoionization mechanism in benzene

Emma Sokell[a], Jason Howard[a], Paola Bolognesi[b], Lorenzo Avaldi[b]
[a] *School of Physics, University College Dublin, Belfield, Dublin 4, Ireland*
[b] *CNR-ISM, Area della Ricerca di Roma 1, Monterotondo Scalo, Italy*

The mechanisms leading to the emission of an electron pair from an atom/molecule due to the absorption of a single VUV or soft X-ray photons has attracted interest because it is completely governed by electron correlation. In atoms the dynamics is determined by the symmetry of the pair wavefunction and the Coulomb interaction among the two electrons in the field of the double charged ion. Less is known in molecules, apart from the studies on the simplest two-electron molecule H_2.

A recent work [1], where the ratio of doubly to single charged parent ions was measured as a function of photon energy using time-of-flight, TOF, spectroscopy, revealed a resonant contribution at a photon energy of ~40eV above the double ionization threshold of aromatic hydrocarbons, like benzene, naphthalene, anthracene and coronene. A mechanism beyond the usual direct 'knock-out' was invoked to explain those data. By analogy to similar observations in the single photoemission on C_{60} [2], where the energy of the enhancement occurred when the de Broglie wavelength of an electron fitted between certain carbon-carbon spacings [1], it was suggested that in these ring-based molecules the resonant enhancement was caused by the excitation of a particle of twice the electron mass, i.e. an electron Cooper pair, whose de Broglie wavelength forms a closed loop structure in the system of overlapping π orbitals. The TOF ion ratios were complemented by photoelectron measurements, either recorded at the magic angle [1] or integrated over 2π using a magnetic bottle TOF [3].

Here we used the electron-electron multicoincidence set-up available at the Gas Phase Photoemission beamline at Elettra to investigate the double photoionization of benzene. The multicoincidence end station is equipped with ten independent analyzers, which allow the detection of twenty one pairs of electrons simultaneously. Two types of coincidence measurements have been performed. In the first one the energy of each electron is fixed and the photon energy is scanned. In this way the binding energy spectrum of the benzene dication has been studied in two regions, one below and one around the energy where the enhancement has been observed. In the second type of measurements the photon energy has been fixed and three independent coincidence angular distributions were measured, fixing the direction of one electron at 0, 30 and 60° with respect to the direction of the linear polarization of the incoming radiation. Two values of excess energy, corresponding to where the Cooper pair formation was expected to occur and a lower one, were chosen.

Finally to complement the measurements presented in [1], a set of full photoelectron spectra, at hv=75 and 80eV, due to the double ionization of benzene at several emission angles have been recorded. The analysis of all the data obtained is on-going and it is envisaged that this will provide further information on the mechanism responsible for the resonant enhancement observed in the photo double ionisation in symmetrical aromatic hydrocarbons.

References

[1] R. Wehlitz et al, Phys. Rev. Lett. **109**, 193001 (2012)
[2] P. N. Juranic et al, Phys. Rev. Lett. **96**, 023001 (2006)
[3] K. Jankala et al, Phys. Rev. Lett. **112**, 143005 (2014)

First Comprehensive Dataset Of Beyond-Voigt Line-Shape Parameters From *Ab Initio* Quantum Scattering Calculations For The HITRAN Database

P. Wcisło[a], F. Thibault[b], N. Stolarczyk[a*], H. Jóźwiak[a], M. Słowiński[a], M. Konefał[a,c,d], S. Kassi[c,d], A. Campargue[c,d], Y. Tan[e,g], J. Wang[e], A.-W. Liu[e], S.-M. Hu[e], K. Patkowski[f], R. Ciuryło[a], D. Lisak[a], R.V. Kochanov[g], I.E. Gordon[g]

[a] *Institute of Physics, Faculty of Physics, Astronomy and Informatics, Nicolaus Copernicus University, Grudziadzka 5, 87-100 Torun, Poland (*Corresponding author: 280301@stud.umk.pl)*
[b] *Institut de Physique de Rennes, UMR CNRS 6251, Université de Rennes 1, Campus de Beaulieu, Bât.11B, Rennes F-35042, France*
[c] *University of Grenoble Alpes, LIPhy, F-38000 Grenoble, France*
[d] *CNRS, LIPhy, F-38000 Grenoble, France*
[e] *Hefei National Laboratory for Physical Sciences at Microscale, iChEM, University of Science and Technology of China, Hefei, 230026 China*
[f] *Department of Chemistry and Biochemistry, Auburn University, Auburn, AL 36849 USA*
[g] *Atomic and Molecular Physics Division, Harvard-Smithsonian Center for Astrophysics, Cambridge, Massachusetts 02138, USA*

Molecular collisions are manifested as a perturbation of the shapes of molecular optical resonances. Therefore, on the one hand, the line-shape analysis of accurate molecular spectra constitutes an important tool for studying quantum scattering and testing *ab initio* molecular interactions [1]. On the other hand, the collisional effects can deteriorate the accuracy of atmospheric measurements of the Earth and other planets, modify the opacity of the exoplanetary atmospheres as well as influence the accuracy in optical metrology based on molecular spectroscopy [2,3]. Recently a new relational structure has been introduced to the most extensively-used line-by-line spectroscopic database HITRAN [4,5], enabling the collisional, beyond-Voigt line-shape effects to be represented. It is, however, extremely challenging to populate the entire database with purely experimental parameters for all the molecular transitions and thermodynamical conditions (all the bands, branches and temperature ranges).

We demonstrate a new methodology of generating a comprehensive dataset of the beyond-Voigt line-shape parameters from fully *ab initio* quantum-scattering calculations. We also demonstrate first such a complete dataset for the benchmark system of helium-perturbed H_2 line. We provide the temperature dependences for the pressure broadening and shift parameters, as well as for the Dicke parameter using generalized spectroscopic cross sections resulting from quantum scattering calculations on accurate *ab initio* potential energy surfaces. The results are consistent with the recently adapted HITRAN parameterisation of the Hartmann-Tran profile [4]. The calculations and methodology are also validated on the ultra-accurate experimental data of the H_2-He system.

References

[1] Wcisło P et al. 2015 Phys. Rev. A **91**, 052505.
[2] Moretti L et al. 2013 Phys. Rev. Lett. **111**, 060803.
[3] Wcisło P et al. 2016 Phys. Rev. A **93**, 022501.
[4] Wcisło P et al. 2016 J. Quant Spectrosc. Radiat. Transfer **177**, 75-91.
[5] Gordon I E et al. 2017 J. Quant. Spectrosc. Radiat. Transfer **203**, 3 – 69. 3

24th ICSLS 2018
Dublin, Ireland

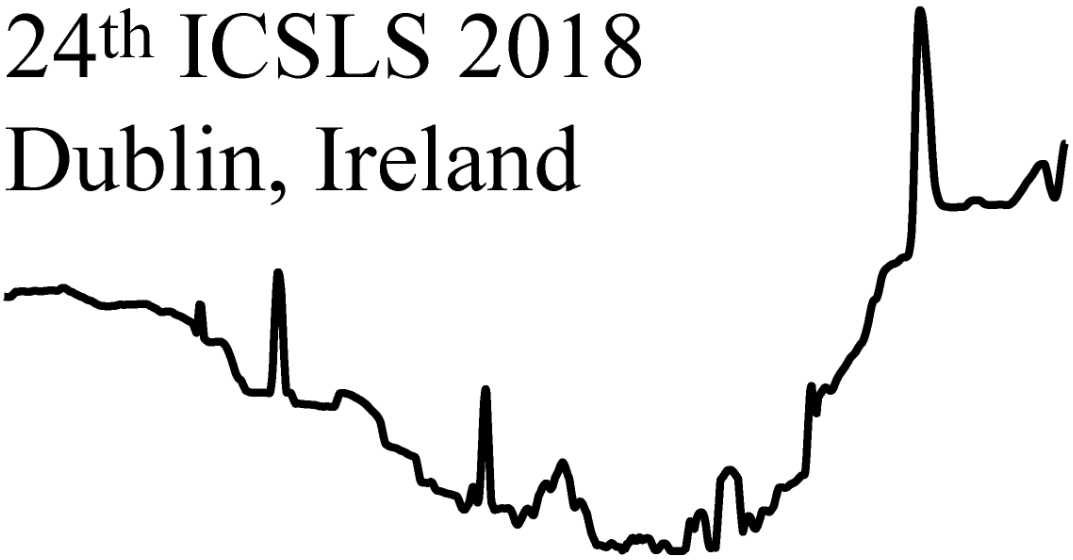

Tuesday Oral Session 3
Tu.O.3

Ab Initio Line Shape Parameters For Speed Dependent Hard Collision Profiles: Applications To Rovibrational Lines Of H_2, D_2, HD In He Or H_2

Franck Thibault[a], Piotr Wcisło[b]

[a]*Institut de Physique de Rennes, UMR CNRS 6251, Université de Rennes1, Campus de Beaulieu, Bât.11B, F-35042 Rennes, France (Franck.Thibault@univ-rennes1.fr)*
[b]*Institute of Physics, Faculty of Physics, Astronomy and Informatics, Nicolaus Copernicus University, Grudziadzka 5, 87-100 Torun, Poland*

Recently [1], some of us have tested various H_2-He potential energy surfaces on H_2 state to state rates and pressure broadening and shifting of the isotropic Raman Q(1) line of the fundamental of D_2 and H_2, as well purely rotational Stokes $S_0(1)$ line of H_2. The inclusion of the effects of the translational motion on the line shape allowed us, unequivocally, to conclude that the Bakr et al [2] PES was the most accurate to date. However, this PES was determined on a too small intramolecular interval to be used for studying overtones. It has thus been extended [3] allowing calculations for transitions up to the 9-0 band. From close coupling dynamics performed on this PES, we provided [3], in a first step, pressure broadening and shifting parameters for isotropic Raman lines and Raman anisotropic lines (or electric quadrupole lines) from $v = 0$ up to $v = 5$ and $j = 0$ up to 5 and for temperatures varying from 5 to 2000 K. In addition, making use of the generalized Hess method the Dicke parameters for these lines were provided. The real part of the latter parameter is the frequency of the velocity-changing collisions. For H_2 perturbed by helium, a "complete" dataset of beyond-Voigt line-shape parameters from *ab initio* quantum scattering calculations for the HITRAN database will be soon presented [4]. This dataset will be consistent with the new structure of the HITRAN database and hard-collisions profiles, in particular with the Hartmann-Tran profile recommended by the IUPAC and adopted by HITRAN.

In addition, we have tested the PES of Ref. [3] and our dynamical calculations for the D_2-He benchmark system [5]. Indeed, pure rotational D_2 Raman spectra, obtained using stimulated Raman spectroscopy (SRS) in Madrid between 77 and 300 K, allowed us to compare the results of our calculations with measured line shifts and broadening of the very first Stokes lines. Experimental and calculated values agree well with each other. Moreover, our calculations including both the speed dependence of the line shape parameters and the narrowing effect permit to explain the evolution with the pressure of the recorded line shapes.

Finally, I will present new accurate spectra, measured with a frequency-stabilized cavity ring-down spectrometer linked to an optical frequency comb referenced to a primary time standard, of the 2-0 S(2) electric quadrupole line of D_2 self- and helium- perturbed [6-7].

References

[1] Thibault F., Wcisło P., Ciuryło R., 2016 *Eur. Phys. J. D*, **70**, 236.
[2] Bakr B.W., Smith D.G.A., Patkowski K., 2013 *J. Chem. Phys.*, **139**, 144305.
[3] Thibault F., Patkowski K, Żuchowski P.S., Jóźwiak H., Ciuryło R., Wcisło P., 2017 *J. Quant. Radiat. Transfer*, **202**, 308-320.
[4] Wcisło P., Thibault F., Stolarczyk N. et al, 2018 *J. Quant. Radiat. Transfer,* in preparation.
[5] Martínez R.Z., Bermejo D., Thibault F., Wcisło P., 2018 *J. Raman Spectrosc.*, in press
[6] Wcisło P., Thibault F., Zaborowski M., 2018 *J. Quant. Radiat. Transfer*, submitted.
[7] Nishiyama A., Thibault F., Słowiński M., Zaborowsk M. et al, poster session

Spectral Line Shapes and Angular Momentum

JF Williams, S Samarin, L Pravica

ARC Centre of Excellence for Antimatter and Matter Studies Centre for Atomic, Molecular and Surface Physics Physics Department, Faculty of Engineering, University of Western Australia, Perth. WA 6009. Australia.
jim.williams@uwa.edu.au

The spectra of zinc atoms, when excited by spin-polarized electrons, reveal line shapes from open and closed shell transitions. The electron energy loss spectra and the Stokes polarization parameters of the emitted photons indicate markedly different effects of electron exchange and spin-orbit interactions reflecting the angular momentum of closed and open core states. The interpretations of the spectra indicate autoionizing phenomena near multiply excited states of the neutral atom with Fano resonances and post-collision interactions (PCI). Also zinc negative-ion resonances have been observed above the first ionization threshold at 9.39 eV. The decay of such features into many states below the ionization threshold with a range of n, L, and S quantum numbers has been investigated with the aims of determining structure and exchange and spin-orbit interaction processes. Representative studies are described in [1].

Sample results in the figure indicate the photon excitation functions with resonance and PCI structure contributions identified as a percentage of the total signal for 4d (upper) and 5d (lower) $^1D_2$ excitations. The small letters (a, b, c) indicate resonance structures and large letters (S) indicate individual peaks.

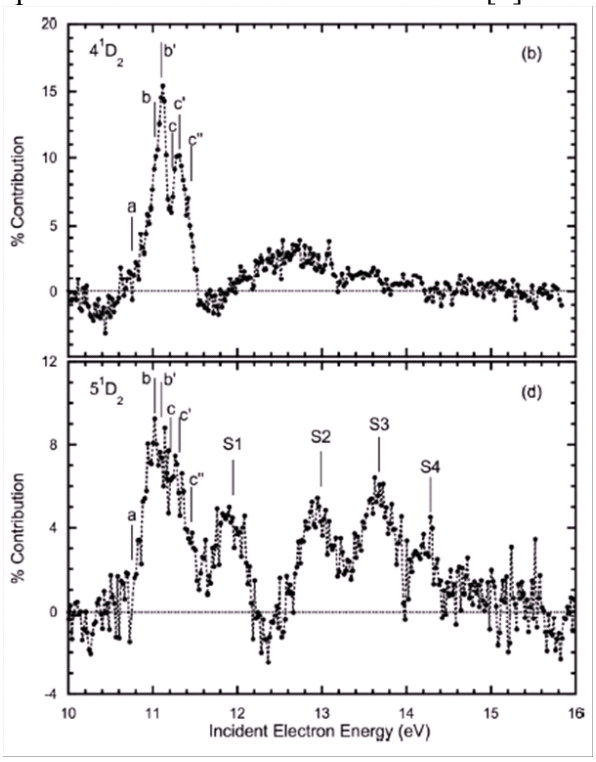

Relative to non-resonance scattering, the resonance contribution to the observed signal is largest for decay to the $4p\ ^3P_1$ and $4d$, $5d$, $6d\ ^3D_{1,2,3}$ states. PCI has been observed to affect the excitation of the higher-energy states, and in particular its influence on the nd $^3D_{1,2,3}$ state excitation is large. The structure of zinc, in the incident energy range, shows Wannier-type correlations and large PCI orbital angular momentum transfer associated with excitation of a 3d electron, which causes significant electron correlations.

Further experiments with spin-polarized electrons can test the role of spin-orbit and exchange scattering in the resonance region, and angle differential electron excitation function measurements can provide information regarding the resonance symmetry and predominant partial waves to aid the resonance assignments. The spectral line shapes indicate the different LS-coupling properties of the intermediately coupled states; the triplet components make exchange and spin-orbit interaction important. For states with a large singlet component the spin-orbit interaction may be dominant.

References.

[1] Williams, JF, Pravica L and Samarin SN 2012 *Phys Rev A* 85, 022701

24th ICSLS 2018
Dublin, Ireland

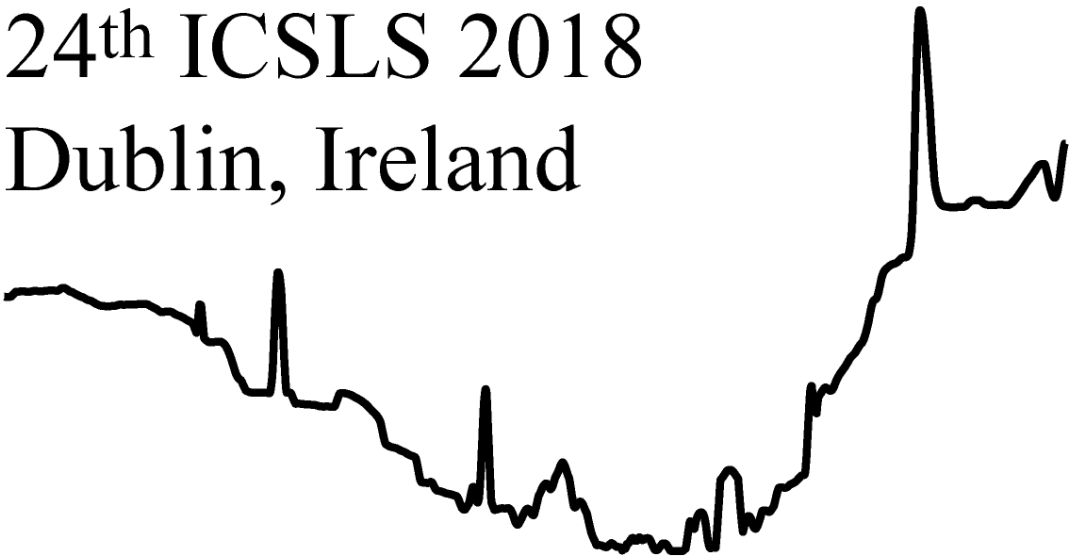

Tuesday Oral Session 4
Tu.O.4

Collision-Induced Absorption By Oxygen And Nitrogen Molecules

Tijs Karman[a], Ad van der Avoird[b], Gerrit C. Groenenboom[b]

tijs.karman@durham.ac.uk
[a]*Department of Chemistry, Durham University, South Road, Durham DH1 3LE, United Kingdom*
[b]*Theoretical Chemistry, Institute for Molecules and Materials, Radboud University, Nijmegen, The Netherlands*

Collision-induced absorption is the phenomenon in which interactions between colliding molecules lead to absorption of light, even for transitions that are forbidden for the isolated molecules. Collision-induced absorption contributes to the atmospheric heat balance and is important for the electronic excitations of O_2 that are used for remote sensing. Absorption by O_2–O_2 pairs has been put forward as a biomarker to be observed in exoplanetary transit spectra.

We study the roto-translational spectrum of N_2–N_2 collisional pairs using quantum mechanical line-shape calculations. Such calculations are usually performed in the approximation of isotropic interactions between the colliding molecules. We included interaction anisotropy for the first time – apart from earlier work on effectively isotropic systems such as H_2–H_2 and H_2–He – and show that interaction anisotropy increases the line strength, bringing our calculations in closer agreement with the experiment.

Furthermore, we present an *ab initio* study of the X $^3\Sigma_g^- \rightarrow$ a $^1\Delta_g$ and X $^3\Sigma_g^- \rightarrow$ b $^1\Sigma_g^+$ electronic transitions of O_2, which are electric-dipole forbidden by both spin and spatial selection rules. We unambiguously identify the underlying absorption mechanism, which is shown to depend explicitly on the collision partner – contrary to text-book knowledge. This explains experimentally observed qualitative differences between O_2–O_2 and O_2–N_2 collisions in the overall intensity, line shape, and vibrational dependence of the absorption spectrum.

References

[1] Karman, T., Miliordos, E., Hunt, K.L.C., Groenenboom, G.C., and van der Avoird, A. 2015 *J. Chem. Phys.* **142** 084306.
[2] Karman, T., Koenis, M.A.J., Banerjee, A., Parker, D.H., Gordon, I.E., van der Avoird, A., van der Zande, W.J., and Groenenboom, G.C., 2018 *Nature Chemistry* **10** 549.

Fragmentation Of Anthracene And Phenanthrene By Low Energy Electron Impact

Peter J. M. van der Burgt [a], Melissa Dunne [a], and Marcin L. Gradziel [a]

[a] *Department of Experimental Physics, National University of Ireland Maynooth, Maynooth, Co. Kildare, Ireland, email: peter.vanderburgt@mu.ie*

Polycyclic aromatic hydrocarbons have environmental relevance, because they are formed as by-products in the combustion of organic materials. They are believed to be a major component of the interstellar medium, because they are considered to be responsible for the emission features that dominate the infrared spectra of many galactic and extragalactic sources.

We have measured sets of mass spectra of positive ions of anthracene ($C_{14}H_{10}$) and of its isomer phenanthrene, with electron energies ranging from 5 to 100 eV in steps of 0.5 eV. A beam of molecules is generated using a resistively heated oven, and is crossed by a pulsed electron beam (0.3 μs, 8 kHz). Positively charged fragments are extracted into a reflectron time-of-flight mass spectrometer. LabVIEW based data acquisition techniques are used to measure mass spectra as a function of electron impact energy. Ion yield curves and appearance energies for most fragment ions of anthracene have been obtained [1].

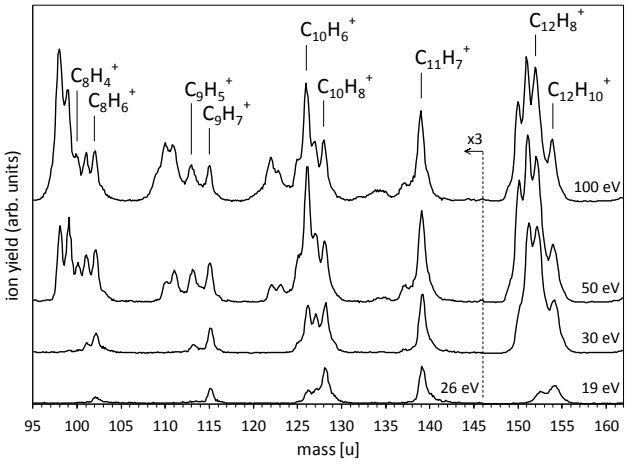

Figure 1. Mass spectra of anthracene, showing evidence for hydrogen rearrangements in the formation of fragments with 8 to 12 carbon atoms.

The groups of anthracene fragments containing 8-13 carbon atoms provide evidence for hydrogen rearrangements during the fragmentation, involving retention or loss of one or two additional hydrogen atoms. Groups of fragments with 6 and 7 carbon atoms clearly show the presence of doubly-charged fragments. The smaller fragments with 1-4 carbon atoms all show broadened peaks, and these fragments may be partly or mostly due to energetic charge-separation fragmentations of doubly-charged anthracene. The mass spectra of phenanthrene are very similar to those of anthracene, and a more detailed comparison will be provided at the conference.

References

[1] van der Burgt P J M, Dunne M, and Gradziel M L, 2018 *Eur. Phys. J. D* **72** 31.

24th ICSLS 2018
Dublin, Ireland

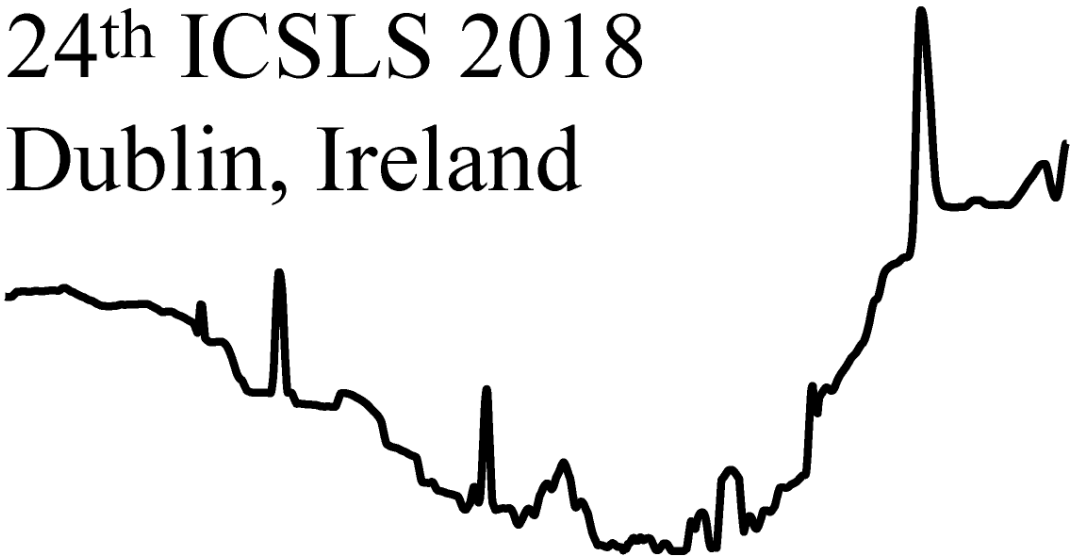

Wednesday Oral Session 1
We.O.1

Optical Isotopic Analysis with Laser Induced Plasmas

Richard E. Russo[a,b], George C. Chan[a], Xianglei Mao[a], Vassilia Zorba[a]

[a]*Lawrence Berkeley National Laboratory, 1 Cyclotron Road, Berkeley, CA 94720 (rerusso@lbl.gov)*
[b]*Applied Spectra, Inc. 46665 Fremont Blvd, Fremont, CA 94538.*

The interaction of a pulsed laser beam with any sample (laser ablation) creates a transient optical source (plasma), in which chemical information of the sample is contained. Laser-ablation based optical-emission methods [e.g., laser induced breakdown spectroscopy (LIBS) and laser-ablation molecular isotopic spectrometry (LAMIS)] are versatile tools for direct and fast chemical analysis at atmospheric pressure, for virtually any type of sample with minimal sample preparation. Furthermore, the ability to perform standoff or remote analysis is a unique advantage of photon-emission based measurement over other analytical techniques (e.g., mass spectrometry).

It has been recognized long ago that atomic transitions of the same element but from different isotopes emit light at slightly different wavelengths. This isotopic shift allows the different isotopes to be analyzed by means of atomic optical spectrometry. Currently, most LIBS measurements are utilized only for elemental analyses; however, LIBS also can provide isotopic information, at least for elements that exhibit large isotopic shifts (e.g., uranium). The development of the LAMIS technique further enhances the capability of laser-induced plasma for isotopic analysis.

LAMIS measures the molecular emission spectra of those radicals that are formed at a late time scale in the plasma, when ablated atoms begin interacting with atmospheric species to create excited-state molecules (e.g., oxides). As molecular spectra typically exhibit two to three orders of magnitude increase in isotopic shift compared to atomic transitions, the shift can be readily measured with a relatively low-resolution optical spectrometer.

In this presentation, the theoretical principles of LIBS and LAMIS for isotopic analysis will be overviewed, the current status (e.g., analytical figures of merit as well as challenges) of the techniques will be examined, and some application examples will be discussed.

Applications Of Vacuum Ultraviolet Laser Induced Breakdown Spectroscopy (VUV-LIBS) – Analysis Of Pharmaceuticals.

Paddy Hayden[a*], Muhammad Bilal Alli[a], and John T. Costello[a]

[a]*School of Physical Sciences and the National Centre for Plasma Science and Technology, Dublin City University, Dublin 9, Ireland.*
**patrick.hayden@dcu.ie*

As Laser Induced Breakdown Spectroscopy (LIBS) matures as an analytical technique, particularly with the expansion beyond elemental characterization provided by advanced chemometric techniques, the range of potential applications has grown steadily. One such area where the ease of measurement, robustness and accuracy of LIBS can have a significant impact is in the analysis, development and production of pharmaceutical and nutraceutical products.

This presentation will introduce Vacuum Ultraviolet LIBS (VUV-LIBS) [1, 2], utilizing emission in the 35–120 nm range, and its usefulness in meeting the off-line requirements at the design stage. VUV-LIBS has a number of advantages, such as increased access to resonance transitions, higher ion stages, less complex spectra, reduction of plamsa interference effects etc.

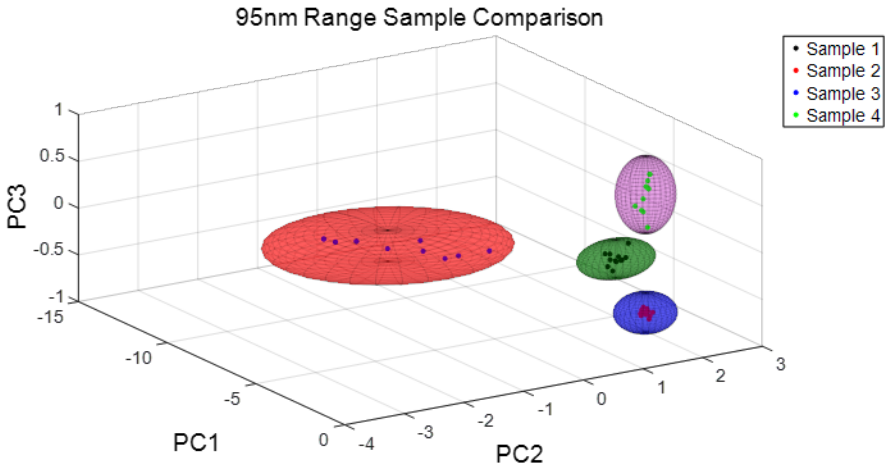

Figure 1. Correct separation and identification of VUV-LIBS spectra of pharmaceutical samples, using Principal Component Analysis.

In addition to traditional spectral analysis, the information rich spectra are interrogated with more complex chemometric techniques, such as Principal Component Analysis (PCA) [3], Convolutional Neural Networks (CNN) [4], Self-Organizing Maps (SOM) [5] and Support Vector Machines (SVM) [6]. This leads to enhanced performance in the identification and classification of the LIBS spectra, allowing improvements in the correct separation of the pharmaceutical samples.

References

[1] Jiang X, et al., *Spectrochimica Acta Part B B* **86** 66 (2013).
[2] Jiang X, et al., *Spectrochimica Acta Part B* **101** 106 (2014).
[3] Myakalwar A K, et al *Talanta* **87** 53–59 (2011).
[4] Pagnotta S, et al. *Spectrochimica Acta Part B* **103–104** 70–75 (2015).
[5] Campanella B, et al. *Spectrochimica Acta Part B* **134** 52–57 (2017).
[6] Luna A S, et al., *Spectrochimica Acta Part B* **139** 20-26 (2018).

Time Resolved Studies of Optical Emission Spectroscopy from Aluminum Oxide formed by Laser Induced Plasma

N. Walsh[a], T.J Kelly[b], P.Hayden[a] J.T Costello[a]

[a]*School of Physical Sciences, Dublin City University, Glasnevin, Dublin 9, Ireland*
[b]*School of Mathematics and Physical Sciences, University of Hull, Hull, United Kingdom, HU67RX*

We report on a series of studies on the emission spectroscopy of Aluminum Oxide (AlO) formed in the condensation phase of laser produced ablation of aluminum in air. For many applications, laser ablation of complex targets must preserve the stoichiometry and so a detailed investigation of molecular formation with background gases is of scientific interest. Similarly, the specific formation of AlO molecules is of interest because it represents a possible chemical intermediate in the formation of clusters and nano-particles.

Previous studies have reported on the evolution of the AlO spectrum have shown that a mixture of plasma diagnostics can be used to track the temperature and density of the AlO formed from laser ablation of aluminium in air [1],[2]. In particular, previous studies have shown that there is a minimum time, or maximum temperature after which the plasma under goes rapid change in terms of molecular formation, making LIBS analysis difficult [1].

In this talk, I report on the results and analysis of two experiments. The first, is a space-averaged, time-resolved study of emission spectroscopy from a laser plasma formed in air on an aluminium target. The plasma was formed using an Nd:Yag laser operating at it's fundamental wavelength, with a pulse duration of 10ns. The emission spectrum was measured using a fibre-optic coupled Czerny-Turner spectrometer connected to an ICCD camera of ~10ns resolution. The method of constructing Deslandres tables was used to assign vibrational transitions to the spectrum lines and estimate dissociation energies. Temperatures were also measured using existing molecular fitting models [3]. In a second experiment, a second laser was coupled to the plasma during the AlO formation phase. The laser wavelength was tuned to exactly the emission wavelength of the $\Delta v = 0$ vibrational band to increase resonant absorption. Here, we comment on the results in terms of how the presence of the second laser distorts the dominant pathways to AlO formation.

References

[1] X. Bai, V. Motto-Ros, W. Lei, L. Zheng and J. Yu, "Experimental determination of the temperature range of AlO molecular emission in laser-induced aluminium plasma in air", *Spectrochimica Acta A. Mol. Biomol. Spectroscopy,* vol 99, pp. 193-200, Sept. 2014.
[2] C.G. Parigger, A.C. Woods, D.M. Surmick, G. Gautam, M.J Witte and J.O Hornkohl, "Computation of diatomic molecular spectra for selected transitions of aluminium monoxide, cyanide, diatomic carbon, and titanium monoxide,", *Spectrochim. Acta Part B At. Spectroscopy,* vol 107, pp. 132-138, May 2015
[3] C.G Parigger and J.O Hornkohl, "Computation of AlO B2Σ+→X2∑+ emission spectra", *Spectrochimica Acta A Mol. Biomol. Spectoscopy,* vol 81, no. 1, pp. 404-411, Oct 2011

24th ICSLS 2018
Dublin, Ireland

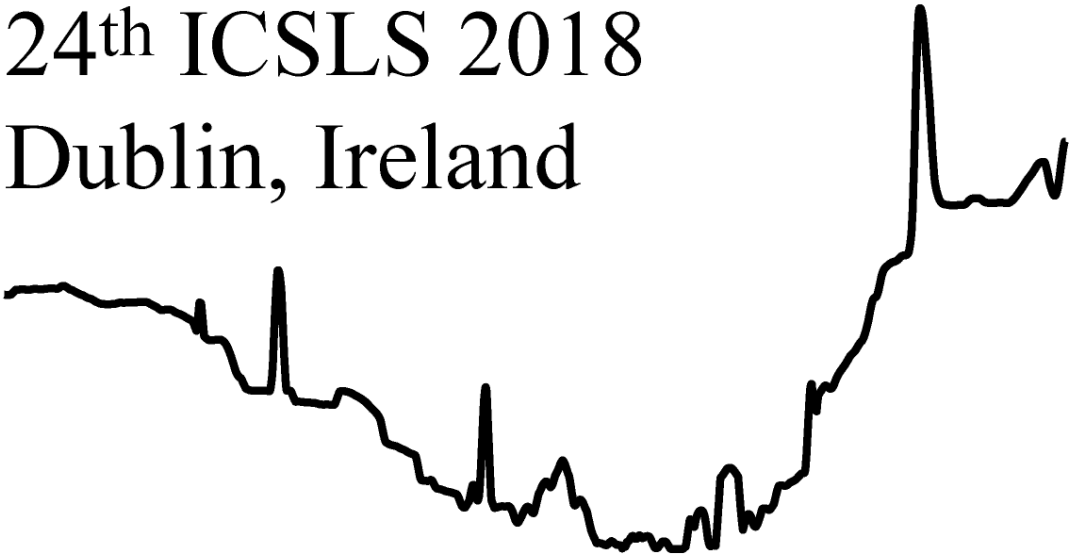

Wednesday Oral Session 2
We.O.2

Water Absorption Spectroscopy: From Doppler-Free Saturation Dips To Continuum

A. Campargue, S. Kassi, D. Mondelain

Univ. Grenoble Alpes, CNRS, LIPhy, 38000 Grenoble, France

Water vapor being the first greenhouse gas in the Earth's atmosphere, its absorption spectrum deserves to be accurately characterized. In the last years, we have used high sensitivity cavity-based laser absorption techniques to address different aspects of water spectroscopy.

Doppler-free saturated-absorption Lamb dips were measured at sub-Pa pressures on rovibrational lines of $H_2{}^{16}O$ near 7180 cm^{-1}, using optical feedback frequency stabilized cavity ring-down spectroscopy [1]. By referencing the laser source to an optical frequency comb, transition frequencies are determined down to 100 Hz precision and kHz accuracy. The developed setup allows resolving highly *K*-type blended doublets separated by about 10 MHz

The amplitude, the temperature dependence and the physical origin of the water vapor absorption continuum are a long standing issue in molecular spectroscopy with direct impact in atmospheric and planetary sciences. The self-continuum absorption of water vapor was determined at different spectral points of the atmospheric windows at 4.0, 2.1, 1.6 and 1.25 µm, by CRDS and OFCEAS (optical-feedback-cavity enhanced absorption spectroscopy) [2]. These accurate experimental constraints have been used to adjust the last version (V3.2) of the semi-empirical MT_CKD model (Mlawer-Tobin_Clough-Kneizys-Davies) widely incorporated in atmospheric radiative transfer codes.

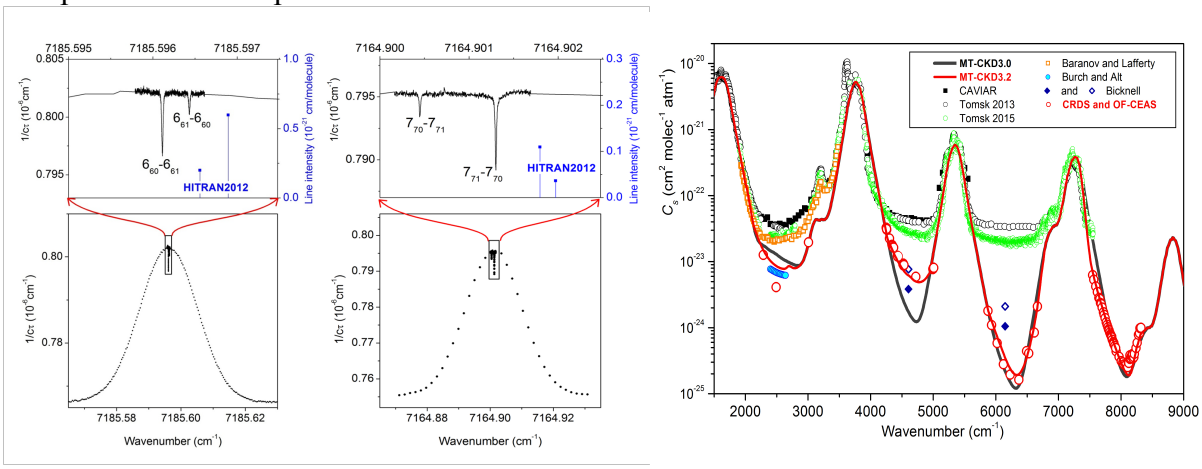

Figure 1. *Left panels*: Absorption line and Lamb dips for the $J_{J\,0} \leftarrow J_{J\,1}$ and $J_{J\,1} \leftarrow J_{J\,0}$ doublets of $H_2{}^{16}O$ (J= 6, 7). On the lower panels, individual measurements points are showed to illustrate the higher resolution to sampling the dips range.
Right panel: Comparison of the MT_CKD3.0 and 3.2 models (black and red solid lines, respectively) of the water vapor self-continuum cross-sections, C_S, in the 1500-9000 cm^{-1} range to an exhaustive collection of the experimental determinations.

References

[1] Kassi S, Stoltmann T, Casado M, Daëron M, Campargue A 2018 *J. Chem. Phys.* **148**, 054201.

[2] Campargue A., Kassi S, Mondelain D, Vasilchenko S, Romanini D, 2016 *J. Geophys. Res. Atmos.* 121, 13,180.

Non-Markovian relaxation matrix for two linear colliders in dense gas media

Andrei Sokolov[a,b], Jeanna Buldyreva[a], Alexander Kouzov[b]

[a]*Institut UTINAM, UMR CNRS 6213, Université Bourgogne Franche-Comté, 16 Route de Gray, 25030 Besançon cedex, France (andrei.sokolov@univ-fcomte.fr)*
[b]*Faculty of Physics, Saint-Petersburg State University, 3 Ulyanovskaya str,198504 Saint-Petersburg, Russia*

Progress in atmospheric physics and gas diagnostics requires urgently higher and higher accuracy of spectroscopic data modeling of various gaseous media. Different processes induced in these environments by collisional relaxation need flexible theoretical models taking account of fine features of collisional dynamics but easy to handle and convenient for practical use. Whereas for the spectral regions near the band centers this role is successfully played by the commonly employed Energy-Corrected Sudden (ECS) approximation introduced almost 40 years ago [1], theoretical description of absorbed (or scattered) intensities in the far spectral wings remains a major challenge.

Problems arise from the fact that for large frequency detunings from the band center the significant increase (or decrease) of the rototranslational energy by the extra photon energy during the transition process cannot be neglected and the use of off-energy-shell scattering amplitudes is required to account for incomplete (non-Markovian) collisions. Corresponding frequency-dependent relaxation matrices have been developed up to now solely for weak interactions treated by perturbation theory [2-4] and for linear rotors perturbed by structureless particles [5,6].

Here, we report rigorous non-Markovian relaxation matrix expressions obtained for collisions between pairs of linear molecules. Owing to a specific choice of symmetric metrics in the Liouville space, this matrix obeys all fundamental relations issued from first principles, corrects the neglect of initial correlations and avoids spurious effects on the computed spectra. All relaxation characteristics can be obtained when the Fourier-transforms of the time-correlation functions are known. These transforms can be either calculated directly from interaction potential energy surfaces (tedious and lengthy task) or modeled using *a priori* information and relaxation matrix properties. Moreover, they can be mimicked in terms of the leading spectral moments which are readily obtained from the tripolar expansions of the interaction potential and of the binary distribution function.

The proposed formulae represent a particular interest for accurate computations of broad-band high-density spectra of long anisotropic colliders like CO_2-CO_2. In the infrared absorption domain such spectra are strongly requested for radiative transfer models of CO_2-rich planetary atmospheres.

References

[1] DePristo AE, Augustin SD, Ramaswamy R, Rabitz H 1979 *J. Chem. Phys.* **71**, 850.
[2] Borysow A, Moraldi M 1989 *Phys. Rev. A* **40**, 1251-1261.
[3] Kouzov AP 1980 *Opt. Spectrosc. (USSR)* **49**, 1013.
[4] Kouzov AP, Buldyreva JV 1997 *Chem. Phys.* **221**, 103.
[5] Kouzov AP 1999 *Phys. Rev. A* **60**, 2931-2939.
[6] Buldyreva JV, Bonamy L 1999 *Phys. Rev. A* **60**, 370-376.

Hydrogen Dimers in Giant-planet Infrared Spectra

Leigh Fletcher[a], Magnus Gustafsson[b], Glenn Orton[c]

[a]*Department of Physics and Astronomy, University of Leicester, University Road, Leicester, LE1 7RH, UK*
[b]*Applied Physics, Department of Engineering Science and Mathematics, Luleå University of Technology, SE-97187 Luleå, Sweden, magnus.gustafsson@ltu.se*
[a]*Jet Propulsion Laboratory, California Institute of Technology, 4800 Oak Grove Dr, Pasadena, CA 91109, USA*

Despite being one of the weakest dimers in nature, low-spectral-resolution Voyager/IRIS observations revealed the presence of $(H_2)_2$ dimers on Jupiter and Saturn in the 1980s. However, the collision-induced H_2–H_2 opacity databases widely used in planetary science have thus far only included free-to-free transitions and have neglected the contributions of dimers. Dimer spectra have both fine-scale structure near the S(0) and S(1) quadrupole lines (354 and 587 cm^{-1}, respectively), and broad continuum absorption contributions up to ±50 cm^{-1} from the line centers. We compute new absorption coefficients for the free-to-bound, bound-to-free, and bound-to-bound transitions of the hydrogen dimer for a range of temperatures (40–400 K) and para-hydrogen fractions (0.25–1.0). The data are validated against low-temperature laboratory experiments (see Fig. 1), and used to simulate the spectra of the giant planets. The new collision-induced opacity database permits high-resolution (0.5–1.0 cm^{-1}) spectral modeling of dimer spectra near S(0) and S(1) in both Cassini Composite Infrared Spectrometer observations of Jupiter and Saturn, and in Spitzer Infrared Spectrometer (IRS) observations of Uranus and Neptune for the first time. Furthermore, the model reproduces the dimer signatures observed in Voyager/IRIS data near S(0) on Jupiter and Saturn, and generally lowers the amount of para-H_2 (and the extent of disequilibrium) required to reproduce IRIS observations.

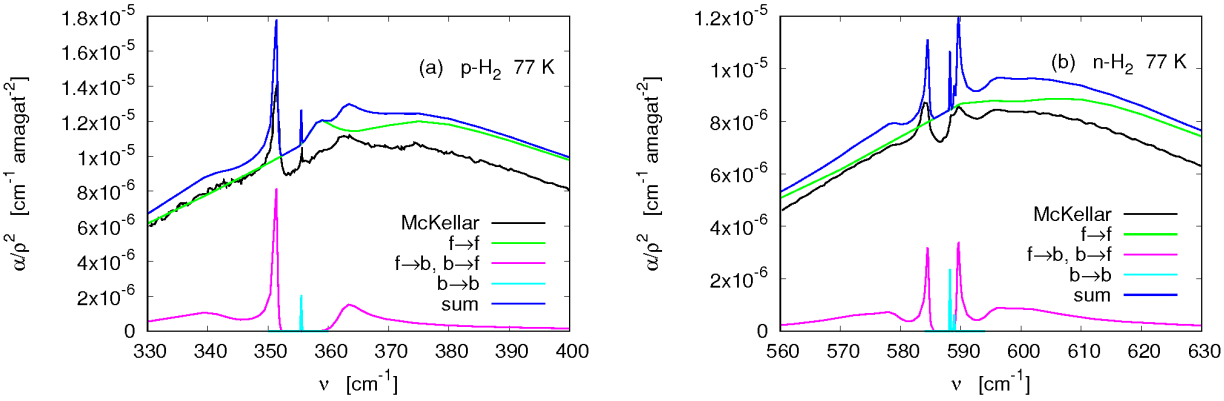

Figure 1. The absorption coefficient at 77 K, normalised by the square of the hydrogen density, around (a) the S(0) and (b) the S(1) transitions for pure para-hydrogen and for normal-hydrogen, respectively. The line labeled 'McKellar' represents the laboratory measurements in Ref. [2], which were taken at number densities of 1.30 amagats and 2.45 amagats for (a) and (b), respectively.

References

[1] Richard C. et al. 2012 *J. Quant. Spectro. Rad. Transf.* **113** 1276.
[2] McKellar, A. R. W. 1988 *Astrophys. J. Lett.* **326** L75.

24th ICSLS 2018
Dublin, Ireland

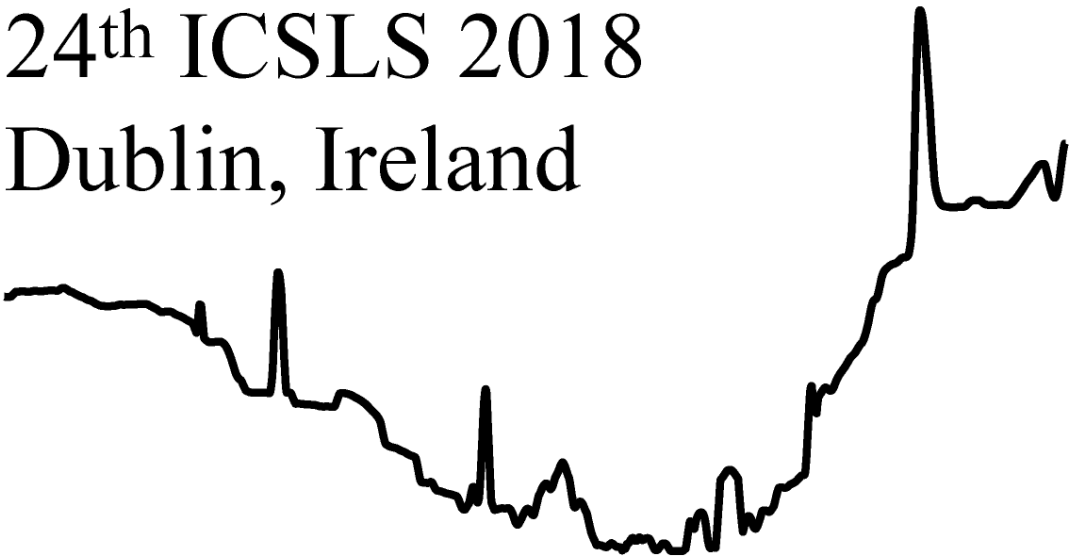

Wednesday Oral Session 3
We.O.3

Quantitative analysis on tungsten spectra of W^{6+} to W^{45+} ions

Shigeru Morita[a], Chunfeng Dong[b], Daiji Kato[a], Yang Liu[c], Ling Zhang[d], Zhengying Cui[b], Motoshi Goto[a], Izumi Murakami[a] and Tetsutaro Oishi[a]

[a]*National Institute for Fusion Science, Toki 509-5292, Gifu, Japan (morita@nifs.ac.jp)*
[b]*Southwestern Institute of Physics, P. O. Box 432, Chengdu 610041, China*
[c]*SDepartment of Fusion Science, School of Physical Sciences, SOKENDAI (The Graduate University for Advanced Studies), Toki 509-5292, Gifu, Japan*
[d]*Institute of Plasma Physics Chinese Academy of Sciences, Hefei 230031, Anhui, China*

In recent fusion research study of tungsten transport is very important in both edge and core plasmas because tungsten divertor is used in ITER. Based on the requirement tungsten spectra have been energetically studied in both fusion and EBIT experiments. So far several qualitative tungsten studies have been done based on the spectroscopic technique, while any quantitative study on the tungsten has not been done yet until very recently. Then, experiments on the quantitative study of tungsten ions are carried out in Large Helical Device (LHD: NIFS), EAST tokamak (ASIPP) and HL-2A tokamak (SWIP) as a collaborative work. In this report, recent progress on the quantitative analysis of tungsten spectra is reported for tungsten ions of W^{6+} to W^{45+} ions. The presentation includes the following five subjects;

1. Evaluation of tungsten influx from WVII (W^{6+}) spectrum in HL-2A [1]
2. Evaluation of tungsten ion density from UTA (W^{24+}, W^{25+}, W^{26+}) spectra in LHD [2] (Typical example of density evaluation is shown in Fig. 1)
3. Evaluation of tungsten ion density from WXLV (W^{44+}) and WXLVI (W^{45+}) spectra in LHD [3]
4. Evaluation of tungsten ion density from M1 (Magnetic dipole: W^{27+} at 3377Å) visible spectrum in LHD [4]
5. Evaluation of tungsten ion density from impurity transport code analysis in EAST [5]

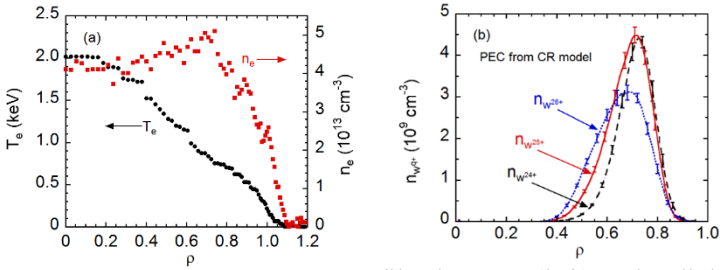

Figure 1. Electron density and temperature profiles in LHD (left) and radial profiles of tungsten ion density of W^{24+}, W^{25+} and W^{26+} evaluated from UTA (Unresolved Transition Array) lines (right)

References

[1] Dong C.F., Morita S., Cui Z.Y. et al., submitted to Nuclear Fusion.
[2] Liu Y., Morita S., Murakami I. et al., submitted to J. Appl. Phys.
[3] Morita S., Dong C.F., Goto M. et al., 2013 AIP Conf. Proc. **1545** 143.
[4] Kato D., Sakaue H.A., Murakami I. et al., 2016 Proc. 26th IAEA Fusion Energy Conference (17-22 October, 2016, Kyoto, Japan), EX/P8-14.
[5] Zhang L., Morita S., Xu Z. et al., Proc. 12th A3 Foresight Program Seminar (12-15 December, 2017, Chongqing, China), to be appeared in NIFS-PROC series.

Line shape modeling for the emission from carbon pellet ablation clouds in presence of a magnetic field

M. Koubiti[a] and M. Goto[b]

[a] *Aix Marseille Univ, CNRS, PIIM, Marseille, France; e-mail: mohammed.koubiti@univ-amu.fr*
[b] *National Institute for Fusion Science, Toki, 509-5292, Japan*

There are a number of reasons pleading in favor of the adoption of the pellet injection technique in future large-scale magnetic fusion devices like the ITER tokamak. Depending on their size, hydrogen isotope pellets are injected for (i) plasma fueling, (ii) control of MHD instabilities (iii) or even for disruption mitigation [1-3]. Additionally, pellets made from other materials like carbon, aluminum, titanium or even tungsten are often injected in magnetic fusion devices like the Japanese LHD stellarator [4-5]. We investigate in this paper from the spectroscopic point of view the ablation cloud of carbon pellets injected in LHD. We will consider in particular typical spectra of the C II 723-nm line measured perpendicularly to the magnetic field using linear polarizers. This line is broadened by Stark effect but is also affected by Zeeman effect which cannot be treated within the weak or the strong field approximations. In this model, we consider only the effect of the magnetic field on the structure of the emitter. This effect is taken into account prior to the line shape calculations in which a Lorentzian shape is used for each emission component of the line. This is because the Stark broadening of this line is dominated by the electronic contribution as has already been shown previously [6]. The theoretical profiles will be compared to the typical experimental spectra.

References

[1] Pégourié B 2007 PPCF, **49**, R87.
[2] Shiraki D et al. 2015 Nucl Fusion, **55**, 073029
[3] Commaux N et al. 2016 Nucl Fusion, **56**, 046007
[4] Nozato H et al. 2006 Phys Plasma, **13**, 092502
[5] Goto M et al 2010 J Phys B, **43**, 144023
[6] Koubiti M et al. 2014 Atoms, **2**, 319

24th ICSLS 2018
Dublin, Ireland

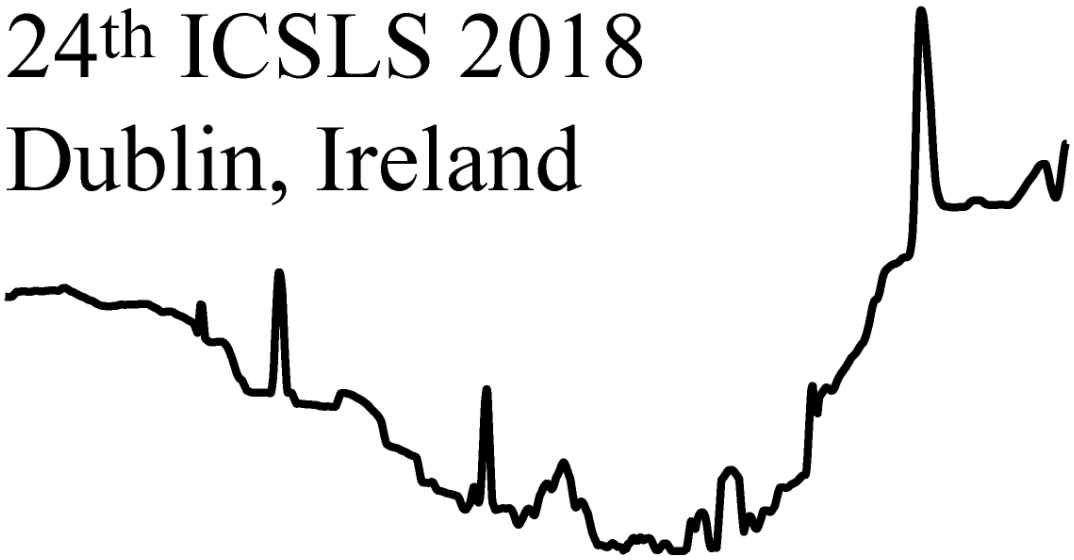

Wednesday Oral Session 4
We.O.4

Spectroscopic Analysis of Corona Discharge Cryoplasma in Helium with Molecular Nitrogen and Hydrogen Addivities

N. Bonifaci [a], Z. Li[b] J. Rosato[c], V. M. Atrazhev [d], V.A. Shakhatov[e] and J Eloranta[f]

[a]*Laboratoire G2Elab CNRS & Grenoble University. 25 rue des Martyrs, 38042 Grenoble, France*
[b] *Guizhou Institute of technology, 1,Rue Caiguan, 550003, Guiyang, Chine*
[c]*PIIM, UMR 7345 Aix-Marseille Université / CNRS, Centre de St-Jérôme, 13397 Marseille Cedex 20, France*
[d]*Joint Institute for High Temperatures, RAS, Moscow, Russia*
[e] *Topchiev of Petrochemical Synthesis Institute, RAS, Moscow, Russia*
[f] *Department of Chemistry and Biochemistry, University of Northridge, USA*
nelly.bonifaci@g2elab.grenoble-inp.fr

Fluorescence spectroscopy is a powerful tool to obtain information on microscopic processes in non-equilibrium discharge plasma (corona) in dense media such as high pressure supercritical gas and even liquids. Spectroscopic observations of the light emitted by electronically excited neutral and ionized gases can be used to determine structural information on the local environment of the emitting atoms or molecules. A microplasma of helium was formed by corona discharge in gaseous and liquid Helium at cryogenic temperatures. Experiments were performed at constant temperature, in a range from 300 K down to 4.2 K under high pressures, ranging from 0.1-10 MPa. Under these conditions, a wide region of densities covering the gas phase with density of 10^{20} cm^{-3} up to liquid phase of Helium with density of 2×10^{22} cm^{-3} could be studied. By putting nitrogen and hydrogen impurities into the helium gas optical emission spectra from not only the helium but also nitrogen and hydrogen can be observed. The most important spectrometric signatures of radiative transitions of diatomic as well as atomic species are discussed as well as simulations of the most important emissions. Results from the profiles of the high resolution emission spectral for several species such as H, N_2, N^+_2, He_2 and He are presented and compared.

Modeling of Lyman-α Line Polarization in Fusion Plasma due to Anisotropic Electron Collisions

M. Goto[a, b], N. Nimavat[b], T. Oishi[a, b], and S. Morita[a, b]

[a]*National Institute for Fusion Science, Toki 509-5292, Japan (goto@nifs.ac.jp)*
[b]*Department of Fusion Science, Sokendai, Toki 509-5292, Japan*

In LHD (Large Helical Device), a phenomenon called the density pump-out has been observed when a high-power ECH (electron cyclotron heating) is injected [1]. This is understood as an enhancement of loss of particles which are trapped in helical ripples because the cyclotron motion is selectively accelerated by ECH and particles having large pitch angle are increased. We attempt to detect a symptom of anisotropic velocity distribution function (VDF) of electrons in the polarization of atomic emission lines.

Excited states of atoms or ions in fusion plasmas are dominantly created by electron collisions. When electrons in a plasma have an anisotropic VDF, excited states may have an inhomogeneous population distribution over the magnetic sublevels in that state [2], and as a result, emission lines from such a state is polarized.

We have started a polarization measurement for the Lyman-α line in LHD and have obtained the polarization degree in the order of several percent. It has a tendency to decay with increasing electron density and this behavior qualitatively agrees with our understanding because a relaxation of anisotropy in the electron VDF should be more enhanced in a higher density condition.

For quantitative verification of our hypothesis, a theoretical model calculation is necessary. To this end, we have developed a code which simulates the polarization formation of the Lyman-α line in plasma. In actual analyses, we assume an electron VDF having different electron temperatures in the perpendicular and parallel directions with respect to the magnetic field, respectively, and attempt to find a solution giving the best agreement with the experimental data in terms of the polarization degree. The details on the theoretical formulation of the polarization formation for the Lyman-α line and some initial results of the data analysis will be presented.

References

[1] R. Makino, et al., Plasma and Fusion Research 8 (2013) 2402115
[2] T. Fujimoto and A. Iwamae (ed), Plasma Polarization Spectroscopy (2008) (Berlin: Springer)

The Stark Broadening Parameters of The Nitrogen HF RF-CCPs

Ümmügül Erözbek Güngör[a]

[a]*Physics Department of Middle East Technical University, 06800, Ankara, TURKEY*
e-mail: ummugul@metu.edu.tr

This paper presents the experimental Stark-broadening and shifting analysis of some selected NI and NII spectral line profiles of the 40.68 MHz RF-CCPs. The discharges were generated in a homemade stainless steel cylindrical parallel plate reactor (with radii R~500 mm and height H~400 mm). Two identical isolated aluminum electrodes with R~200 mm were placed in the reactor at a 4 cm gap distance. Additionally, an Ocean Optics High-Resolution HR2000 fiber optic spectrometer (200-1100 nm) was connected to the window of the discharge system. The applied RF power was in the range of 50-200 Watt and the gas pressure was in the range of 0.2-1 Torr. An optical emission spectrum (OES) of the system and the calculation of the excitation temperature (T_{exc}) can be seen in Figure 1.

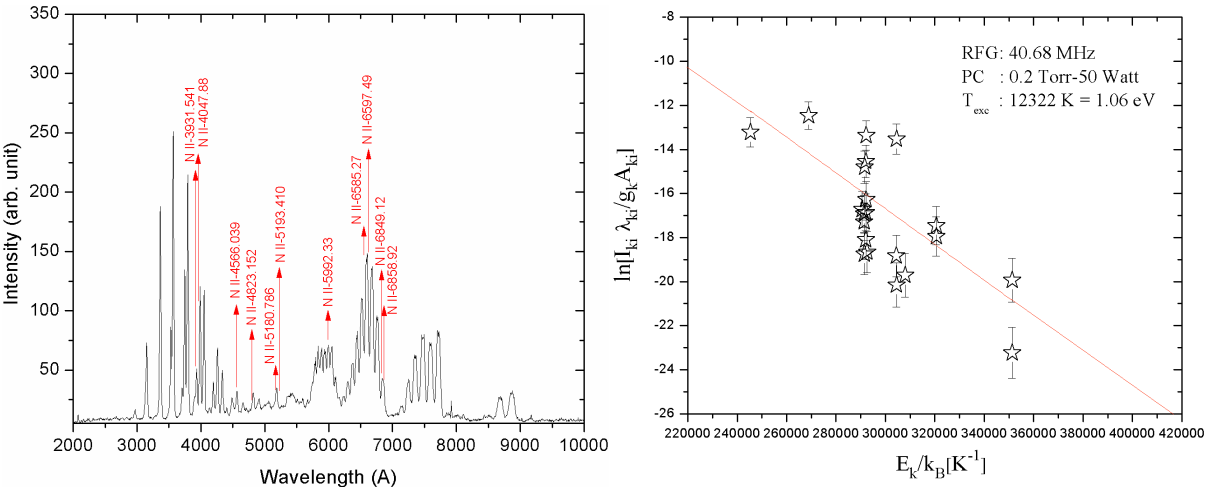

Figure 1. Optical emission spectroscopy-OES (left) and the linear Boltzmann plot (right) of the singly-ionized Nitrogen (NII) spectral transition lines of the 40.68 MHz RF-CCP at 0.2 Torr-50 Watt

I assumed that the discharge is in the local thermal equilibrium (LTE) and the excitation temperature is equal to the electron temperature (T_e). Then, I calculated the electron density (n_e) by using the Saha equation [1]. According to n_e and T_{exc} values, I calculated the $\Delta\lambda_s$ (Strak FWHM of the peaks) [2] and also the gas temperature of the system [3].

References

[1] Fridman A 2008 *Plasma Chemistry (New York: Cambridge University Press)*.
[2] Pellerin S, Musiol K, Pokrzywka B, Chapelle 1996 *J. Phys. B: At. Mol. Opt. Phys.*, **29**, 3911-3924.
[3] Yubero C, Rodero A, Dimitrijevic M S, Gamero A, Garcia M C 2017 Spectrochimica Acta Part B, **129**, 14-20.

24th ICSLS 2018
Dublin, Ireland

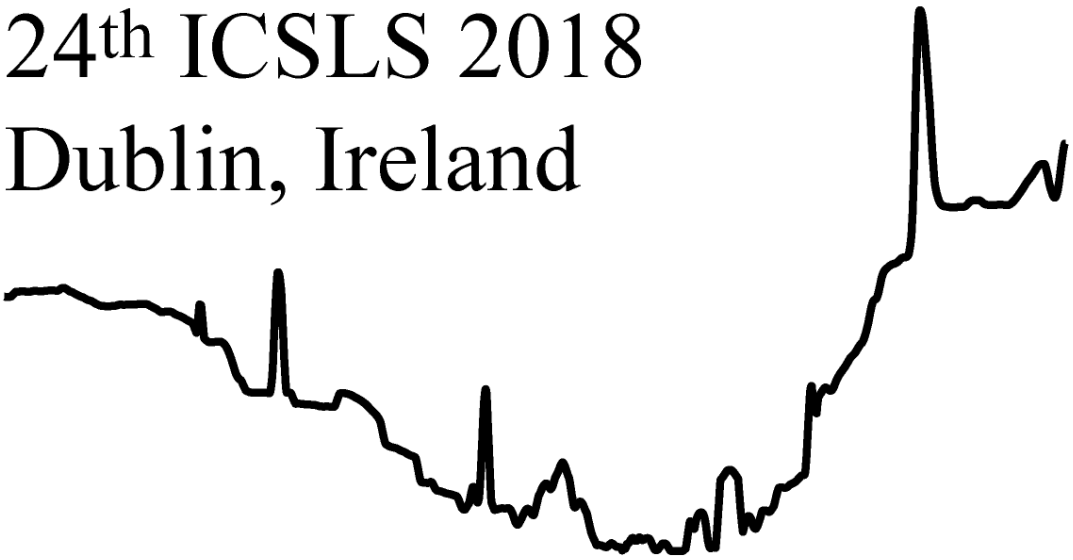

Thursday Oral Session 1
Th.O.1

Lineshapes In Photoprocesses Induced By Ultra Short Laser Pulses

Astapenko V.A.[a], Lisitsa V.S.[a,b,c], Khramov E.S.[a], Moroz N.N.[a]

[a]*Moscow Institute of Physics and Technology (State University), Dolgoprudnyi, Russia, astval@mail.ru*
[b]*National research Nuclear University MEPhI (Moscow Engineering Physics Institute), Moscow, Russia*
[c]*National Research Center "Kurchatov Institute", Moscow, Russia*

The effects of spectral line shapes on photo-processes induced by the interaction of ultrashort laser pulses (USP) with atomic systems are under consideration. The problem results in an appearance of additional parameter in the line broadening theory, namely, the time duration of USP (τ) together with standard parameters of line shape theory such as frequency shifts, line widths, electric field fluctuation times.

Two main processes are of specific interest, namely, absorption and scattering probabilities during all time of USP action [1, 2]. Probability W of atom excitation in dimensionless variables has the form [3]

$$W(\alpha,\delta)=\frac{\pi}{4}\,\frac{f_0 E_0^2}{\omega_0}\,\frac{\alpha^2}{\Delta}\int_{-\infty}^{\infty}\exp\left\{-\alpha^2(\beta-\delta)^2\right\}G(\omega_0+\Delta\beta)\,d\beta$$

$G(\omega')$ is the spectral lineshape of a radiative transition between atomic states. Here dimensionless variables are entered:

$$\beta=\frac{\omega'-\omega_0}{\Delta},\ \delta=\frac{\omega-\omega_0}{\Delta},\ \alpha=\Delta\tau$$

where Δ is the spectral width of the line, ω_0 , f_0 are the own frequency and oscillator strength of the electron transition, E_0 is the amplitude of electric field strength of the USP.

The modern USP generation technique makes it possible to obtain USP in ultraviolet and even X-ray spectral ranges making it actual to observe transition probabilities not from excited but also from ground atomic states. A number of standard line shape problems modified by the action of USP are considered, namely, Doppler broadening and the effects of slow far line wings decrease in Voigt spectra, static line shapes described by standard Holtsmark distribution with account for ion dynamics effects by application of kinetic version of frequency-fluctuation model, simplified static line shapes for radiative transitions from Rydberg atomic states with account of ion dynamic effects.

It is shown that new dimensionless parameter α being the product of line shape widths on pulse duration τ produces a large effect on both probability dependences on carrier frequency and duration of USP. The last one demonstrates a smooth evolution from nonlinear dependence upon τ to standard linear one corresponding to well know probability per unit time.

The general properties of USP interaction with atomic systems are illustrated by specific examples of hydrogen and highly charged ions line broadening in plasmas.

References

[1] Astapenko VA 2010 *Physics Letters A* **374 1**585-1590
[2] Astapenko VA 2011 *Journal of Experimental and Theoretical Physics* **139** 193-198
[3] Calisti A, Astapenko VA, Lisitsa VS 2017 *Contribution to Plasma Physics* **57** 414-420

Temperature Dependence of Half-Widths and Line Shifts for Molecular Transitions in The Microwave and Infrared Regions

Robert R. Gamache[a], Bastien Vispoel[a]

[a] *Department of Environmental, Earth, and Atmospheric Sciences, University of Massachusetts Lowell, Lowell, MA 01854, USA, Robert_Gamache@uml.edu*

An expression was derived from a power series expansion of the optical cross-sections in in the radiator-perturber relative velocity, cut off at second order, that correctly models the temperature, T, dependence of the half-width, γ, over large temperature ranges and the T dependence of the line shift, δ, even for cases where the shift changes sign. Data were collected for more than 100 thousand transitions and the power law (PL) expression for γ and δ when the shift doesn't change sign were compared with the new double power law expression. Figure 1 shows data (symbols) and fits (solid lines) for the $2_{2\ 0} \leftarrow 3_{1\ 3}$ rotation band transition of H_2O in collision with H_2; left-hand upper and lower panels are the PL fits for γ and δ, right-hand upper and lower panels are the DPL fits for γ and δ .

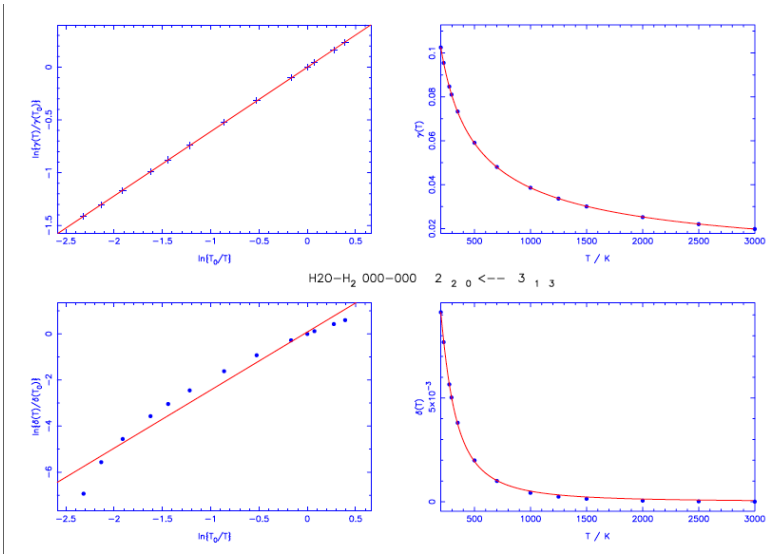

Figure 1. Power law and double power law fits to γ and δ for the $2_{2\ 0} \leftarrow 3_{1\ 3}$ rotation band transition of H_2O in collision with H_2.

The DPL model works well for all transitions, even those that exhibit unusual structure, which the standard power law cannot model. The DPL expression gives better results than the PL model for 99.997 and 99.475 percent of the transitions for γ and δ, respectively. The DPL model gives good results for the temperature dependence of δ when δ changes sign. The DPL model for the T dependence of δ was compared with the linear model, which is currently used on the HITRAN database. In all cases the DPL model gave much better results than the linear model no matter what temperature range was studied. The new formalism allows a substantial reduction in the number of parameters that need to be stored in databases and the same expression can be utilized in radiative transfer and simulation codes for both the half-width and line shift.

Exited Atoms-Surface Collisions and Their Manifestations in the Fluorescence Excitation Line Shapes

Tigran A. Vartanyan

ITMO University, St. Petersburg, 197101, Russian Federation, e-mail Tigran.Vartanyan@mail.ru.

Since the invention of the extremely thin cell (ETC) which sustains prolonged action of hot and dense alkali vapors [1], a number of spectroscopic problems have been solved with its aid. As the width of the cell is comparable to or smaller than the wavelength of the actual atomic transition, Doppler width of the fluorescence light is substantially reduced due to the cage effect. Selective reflection and transmission spectra of the alkali vapor filled ETC are even more intriguing. The widths and the shapes of both lines depend periodically on the vapor slice thickness. The period of this dependence is twice as large as compared to the periodicity characteristic for the Fabry-Perot cavity [2]. As a unique linear Doppler-free spectroscopic tool, ETC found numerous applications in atomic spectroscopy and magnetometry [3].

ETC keeps also great promises in the studies of excited atoms-surface collisions. As the distance between the cell walls is very small, in particular, it may be much smaller than the wavelength of the resonant transition, interaction of all atoms with the walls is significant. Hence the measurements based on the ETC has a definite advantage as compared to the well-developed technique for atom-surface interaction investigations based on the careful analysis of the selective reflection line shapes [4]. In the last case the distances from the surface probed by the technique is fixed by the wavelength of resonant light and cannot be changed.

Stimulated by the recent precise measurements of the fluorescent excitation line shapes in the ETC [5] and the criticism [6] about their interpretation we applied to this case the standard approach of optical collisions accompanied by free-free transitions between the ground and excited electronic states [7]. Indeed, the atomic transition frequency varies in the course of the atomic free flights between the cell walls. Hence the excitation dynamics is similar to the Landau-Zener transition between the potential curves with avoided crossing. Thus, the fluorescent excitation line profiles are governed by the slopes of the potential energy curves in addition to the shifts themselves.

This work was supported by RFBR (17-52-18037) and the Ministry of Education and Science of Russian Federation (3.4903.2017/6.7).

References

[1] Sarkisyan D., Bloch D., Papoyan A., Ducloy M. 2001 Opt. Comm. **200** 201.
[2] Vartanyan T.A., Lin D.L. 1995 Phys. Rev. A **51** 1959.
[3] Mariotti E., Bevilacqua G., Biancalana V., Cecchi R., Dancheva Y., et al. 2017 Proc. SPIE **10226** 102260K.
[4] Chevrollier M., Bloch D., Rahmat G., Ducloy M. 1991 Opt. Lett. **16** 1879
[5] Whittaker K.A., Keaveney J., Hughes I.G., Sargsyan A., Sarkisyan D., Adams C.S. 2015 Phys. Rev. A **92** 052706.
[6] Bloch D. 2015 Phys. Rev. Lett. **114**, 049301.
[7] Szudy J., Baylis W. E. 1996 Phys. Rep. **266** 127.

24th ICSLS 2018
Dublin, Ireland

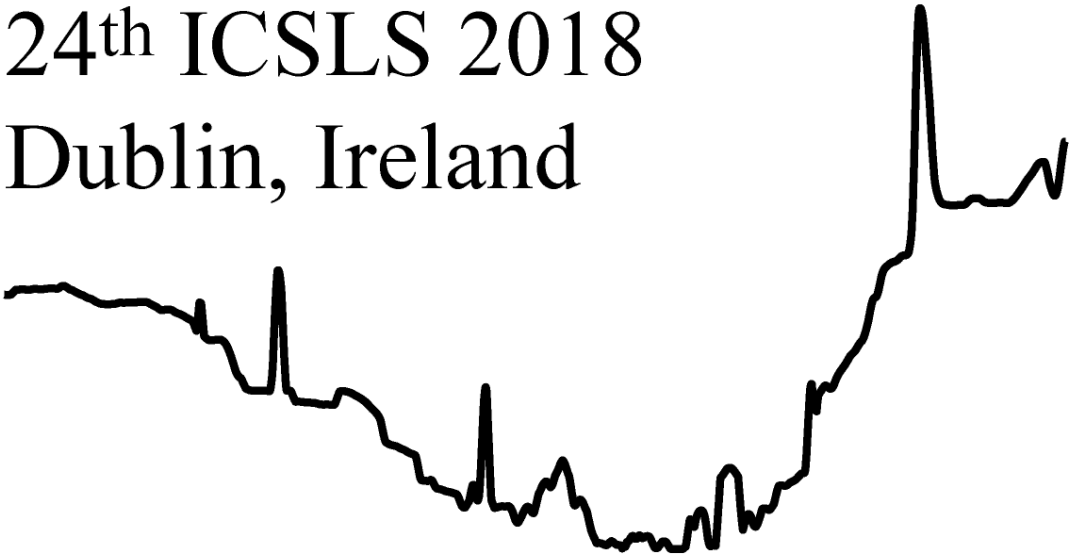

Thursday Oral Session 2
Th.O.2

Multiphoton Ionization of Chiral Molecules

Thomas Baumert

Universitaet Kassel, Institut fuer Physik, Heinrich-Plett-Str. 40, D-34132 Kassel, Germany
baumert@physik.uni-kassel.de

Molecular chirality is widely recognized for its relevance to the building blocks of life and its vital role for medicine and health. Chiral recognition in the gas phase using electromagnetic radiation is an emerging research field and promising for fundamental research as well as for applications due to the non-interacting nature of molecules in the gas phase.

Photoelectron angular distributions after one photon or multiphoton ionization turned out to be especially sensitive to that end and are usually measured by velocity map imaging (VMI) techniques. The corresponding circular dichroism is termed photoelectron circular dichroism (PECD) and reviewed in [1]. Based on electric dipole interaction, its magnitude of up to a few ten percent typically surpasses that of other chiroptical techniques and can be turned into a highly sensitive analytic tool with respect to investigation of enantiomeric excess.

Resonance-enhanced multi-photon ionization (REMPI) gives access to electronic intermediates and, with the help of femtosecond laser excitation and ionization, PECD has been demonstrated on bicyclic ketones. As more angular momentum can be transferred in a multiphoton process in comparison to single photon ionization, higher order nodal structures were observed. An exploration of the nuclear and electron dynamics of the intermediate resonance may stimulate the development of laser driven purification schemes.

In this talk I will present the field and our experiments. References also to related work are compiled for example in our latest publication [2].

References

[1] Nahon, L., Garcia, G. A. and Powis, I. 2015 J. Elec. Spectr. Relat. Phenom. **204**, 322–334.
[2] Kastner, A. et al. 2017 JCP **147** 013926 (9 pp).

Water vapor line-broadening coefficients for molecules in the HITRAN database

Yan Tan[a], I.E. Gordon[a], R.V. Kochanov[a,b], L.S. Rothman[a]

[a]*Harvard-Smithsonian Center for Astrophysics, Atomic and Molecular Physics Division, Cambridge MA, USA, Email: yan.tan@cfa.harvard.edu*
[b] *Tomsk State University, Laboratory of Quantum Mechanics of Molecules and Radiative Processes, Tomsk, RUSSIA.*

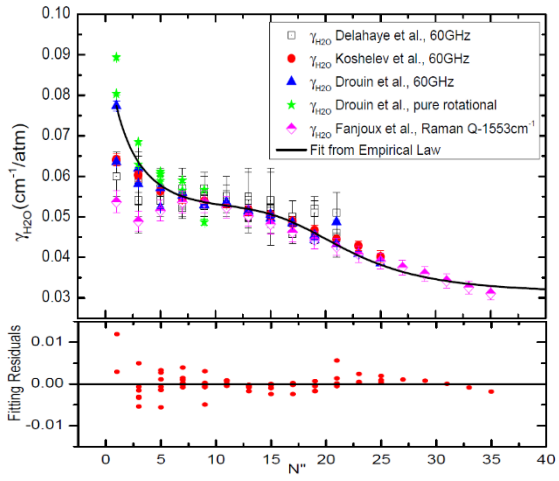

The new edition of HITRAN2016 has been officially released[1] and this edition has substantially increased the potential for the database to model radiative processes in the terrestrial and planetary atmospheres. Water vapor in earth's atmosphere is highly variable which causes water to represent a potentially significant cross-sensitivity source. Its concentration may be subject to large variations, especially in high-accuracy remote sensing of trace gas retrievals, such as O_2, CO_2 and CH_4. With that the water vapor is a very efficient broadened in comparison to nitrogen and oxygen. For purpose of characterizing and reducing uncertainties in modeling the spectra of atmospheres with significant amounts of water vapor, the line-shape parameters for the line-broadening coefficients and the temperature dependence exponents for molecules of terrestrial interest broadened by water vapor were investigated through both experimental and theoretical studies. As a first step, oxygen broadened by water vapor was successfully investigated as shown in the figure above. A clear rotational dependence of the O_2 broadening coefficients by H_2O was observed and then fitted by an empirical law[2]–[5].Empirical Law used for fitting:

$$\gamma_{H_2O} = A + B/(1 + c_1 x c_2 x^2 + c_3 x^3)$$

We also performed similar investigation for water vapor broadening coefficients of CO_2, CH_4, CO, NH_3, N_2O, OCS, CH_3CN and HCHO. As a final step, a complete data set for all these broadening parameters by water vapor will be implemented into the HITRAN database and will improve the accuracy of remote-sensing experiments in the future.

This work is supported by NASA AURA and PDART program grants *NNX14AI55G* and *NNX16AG51G.*

References

[1] I. E. Gordon *et al.*, *J. Quant. Spectrosc. Radiat. Transf.*, vol. 203, pp. 3–69, Dec. 2017.
[2] T. Delahaye, X. Landsheere, E. Pangui, F. Huet, J.-M. Hartmann, and H. Tran, *J. Quant. Spectrosc. Radiat. Transf.*, vol. 184, pp. 316–321, Nov. 2016.
[3] B. J. Drouin, V. Payne, F. Oyafuso, K. Sung, and E. Mlawer, *J. Quant. Spectrosc. Radiat. Transf.*, vol. 133, pp. 190–198, Jan. 2014.
[4] G. Fanjoux, G. Millot, R. Saint-Loup, R. Chaux, and L. Rosenmann, *J. Chem. Phys.*, vol. 101, no. 2, pp. 1061–1071, Jul. 1994.
[5] M. A. Koshelev, I. N. Vilkov, and M. Y. Tretyakov, *J. Quant. Spectrosc. Radiat. Transf.*, vol. 154, pp. 24–27, Mar. 2015.

Temperature dependent spectroscopic study of carbon monoxide in the fundamental band

Adriana Predoi-Cross[a,b], Nazrul Islam[a], Mary Ann Smith[c], Malathy Devi[d], Sergey Ivanov[e], Oleg Buzykin[f], Franck Thibault[g]

[a]*Department of Physics and Astronomy, University of Lethbridge, Lethbridge AB Canada T1K 3M4*
[b]*Present Address: 512 Silkstone Crescent West, Lethbridge AB Canada T1J 4C1*
[c]*Science Directorate, NASA Langley Research Center, Hampton, VA, USA*
[d]*Department of Physics, The College of William and Mary, Williamsburg, VA, USA*
[e]*Federal Scientific Research Centre "Crystallography and Photonics" of Russian Academy of Sciences,Leninsky pr. 59,Moscow, Russia*
[f]*Central Aerohydrodynamic Institute (TsAGI), Moscow, Russia*
[g]*Institut de Physique de Rennes, UMR CNRS 6251, Université de Rennes 1, Campus de Beaulieu, F-35042 Rennes, France*

We present the results from a spectroscopic study of 29 spectra of the fundamental band of pure carbon monoxide and carbon monoxide mixed with air, recorded at 0.005 cm^{-1} resolution over a range of temperatures (79 K to 296 K) using the Fourier Transform spectrometer formerly located at the National Solar Observatory on Kitt Peak, AZ. Two variable temperature gas cells made of copper were used to record the spectra. The spectra were calibrated using line positions of carbon dioxide and water vapor present in the spectra as impurities, taken from Ref. [1].

The spectra were analyzed using the multispectrum fitting software described in Ref. [2]. Voigt, speed-dependent Voigt and Rautian line shape models have been employed in the analysis. The narrowing parameters needed for analysis using the Rautian model had no rotational quantum number dependence. They were computed using diffusion constants for CO-CO, CO-O_2, and CO-N_2 obtained using the method described in Ref. [3].

Line intensities, air- and self-broadening coefficients, pressure induced air- and self-shift coefficients, Einstein A-coefficients and line-mixing parameters have been retrieved. The exponential power gap scaling law has been used to calculate line-mixing parameters.

The N_2-broadened carbon monoxide half-width coefficients have been calculated at different temperatures using a potential energy surface based on Tipping-Herman intermolecular interaction and taking the electrostatic interactions into account. This computational method ensures that the three dimensional motion of the molecule is accounted for. However, the calculations used vibrationally independent potentials. We have compared our measurement results with theoretical calculations obtained for CO-N_2 systems and with previous published measurements for the CO-air system.

References

[1] Gordon IE, Rothman LS, Hill C, Kochanov RV. Tan Y, Bernath PF, *et al.* 2017. The HITRAN2016 Molecular Spectroscopic Database. *J Quant Spectrosc Radiat Transf* **203** 3-69.

[2] Benner DC, Rinsland CP, Devi VM, Smith MAH, Atkins D 1995. A multispectrum nonlinear least squares fitting technique. *J. Quant. Spectrosc. Radiat. Transfer* **53(6)** 705-721.

[3] Hirschfelder JO, Curtiss CF, Bird RB 1954. Molecular theory of gases and liquids. *New York: Wiley and Sons*.

24th ICSLS 2018
Dublin, Ireland

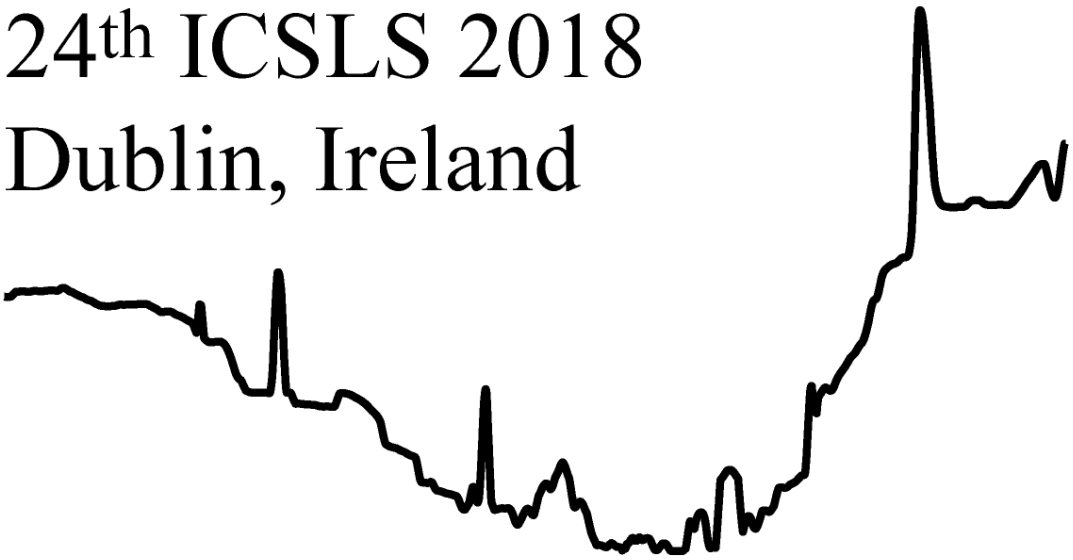

Friday Oral Session 1
Fr.O.1

The Impact of Line Mixing and Speed Dependence on Retrievals of Atmospheric CO_2 and CH_4 from Ground-Based Solar Absorption Spectra

K. Strong[a], J. Mendonca[a,b], D. Wunch[a], G.C. Toon[c], K. Sung[c], D.A. Long[d], J.T. Hodges[d], V.T. Sironneau[d], J.E. Franklin[e], V.M. Devi[f], N.M. Deutscher[g], and D.W.T. Griffith[g]

[a]*Department of Physics, University of Toronto, Toronto, ON, Canada (strong@atmosp.physics.utoronto.ca)*
[b]*Now at Environment and Climate Change Canada, Downsview, ON, Canada*
[c]*Jet Propulsion Laboratory, Pasadena, CA, USA*
[d]*National Institute of Standards and Technology, Gaithersburg, MD, USA*
[e]*Harvard John A. Paulson School of Engineering and Applied Sciences, Cambridge, MA, USA*
[f]*Department of Physics, The College of William and Mary, Williamsburg, VA, USA*
[g]*Center for Atmospheric Chemistry, University of Wollongong, Wollongong, NSW, Australia*

A quadratic speed-dependent Voigt (qSDV) line shape with line mixing (LM) has been implemented into the forward model of the spectral fitting software GFIT to improve the retrievals of total columns of CO_2, CH_4, and O_2 from high-resolution ground-based solar absorption spectra [1,2,3]. Absorption coefficients were calculated using the qSDV+LM spectral line shape with spectroscopic parameters for the strong CO_2 band centered at 4850 cm^{-1}, the weak CO_2 bands centered at 6220 cm^{-1} and 6340 cm^{-1}, and the $2\nu_3$ band of CH_4.

Absorption coefficient calculations were validated using laboratory spectra of CO_2 and CH_4. Laboratory spectra were modeled better with the qSDV+LM than with the Voigt line shape. The qSDV was used to fit air-broadened, room-temperature, cavity ring-down spectra of the $a^1\Delta_g \leftarrow X^3\Sigma_g^-$ O_2 band. It was shown that the Voigt line shape is inadequate to model the spectral lines of this O_2 band and that speed-dependent effects need to be taken into account. Spectroscopic parameters of the discrete spectral lines of the O_2 $a^1\Delta_g \leftarrow X^3\Sigma_g^-$ band were retrieved and implemented in GFIT.

A year of ground-based solar absorption spectra acquired at Eureka (Canada), Park Falls (USA), Lamont (USA), and Darwin (Australia) were processed using GFIT. Total columns of CO_2, CH_4, and O_2 were retrieved using absorption coefficients calculated assuming a Voigt spectral line shape and the qSDV+LM (with LM used when applicable). With the qSDV+LM, spectral fits of CO_2 and CH_4 improved as a function of solar zenith angle. The airmass dependence of the retrieved columns of CO_2, CH_4, and O_2, as well as the column-averaged dry-air mole-fraction of CO_2 (XCO_2) decreased while the accuracy of XCO_2 improved.

References

[1] Mendonca J, Strong K, Toon GC, Wunch D, Sung S, Deutscher NM, Griffith DWT, and Franklin JE, 2016 *J. Mol. Spec.*, **323**, 15-27.
[2] Mendonca J, Strong K, Sung K, Devi VM, Toon GC, Wunch D and Franklin JE, 2017 *J. Quant. Spectrosc. Rad. Transfer*, **190**, 48-59.
[3] Mendonca J, Strong K, Wunch D, Toon GC, Long DA, Hodges JT, Sironneau VT, and Franklin JE, 2018 *Atmos. Meas. Tech. Discuss.*, doi.org/10.5194/amt-2018-62, in review.

Line Shape Investigation of O_2 B-band Transitions: Simultaneous Observation of the Speed-Dependence and Dicke Narrowing

K. Bielska*, J. Domysławska, S. Wójtewicz, M. Słowiński, A. Cygan, R. Ciuryło, D. Lisak

Institute of Physics, Faculty of Physics, Astronomy and Informatics, Nicolaus Copernicus University in Toruń, Grudziadzka 5, Torun 87-100, Poland
**kasia@fizyka.umk.pl*

High signal-to-noise ratio (SNR) measurements of self-perturbed O_2 B-band transitions near 690 nm were performed with a cavity ring-down spectrometer (CRDS) referenced to an optical frequency comb (OFC). The OFC-assisted, Pound-Drever-Hall (PDH) locked, frequency stabilized CRD spectrometer (FS-CRDS) was used in a configuration similar to one described in Ref. [1]. We show two examples where both narrowing mechanisms, that is the speed dependence of the line width as well as the Dicke narrowing have to be included in the line shape analysis [2-4] in order to properly describe observed profiles. One of the strongest O_2 B-band transitions with intensity $S = 5.4 \cdot 10^{-25}$ cm/molecule (P9 P9 line) was investigated with SNR of about 40000. Simultaneous presence of the speed dependence of collisional width and the Dicke narrowing was observed in the pressure range as low as 8.5 Torr (1.1 kPa). It has not been detected previously for spectra characterized by lower SNR [5]. The other case is the three orders of magnitude weaker R35 Q36 transition of the intensity $S = 6.1 \cdot 10^{-28}$ cm/molecule measured at pressure of 100 Torr (13.3 kPa). Even for moderate SNR of about 2000 but much higher pressure range both narrowing effects need to be accounted for in order to properly describe the measured line shape as well.

Results of the present investigation are especially important in atmospheric applications requiring sub-percent accuracy. They enhance our previously determined set of O_2 B-band line shape parameters [6], where the speed-dependent Voigt profile was proposed for description of O_2 B-band transitions line shapes, to more advanced line profiles.

References

[1] Cygan A et. al. 2015 *Opt. Express* **23** 22.
[2] Lance B et. al. 1997 *J. Mol. Spectrosc.* **185** 262.
[3] Pine AS 1999 *J. Quant. Spectrosc. Radiat. T.* **62** 397.
[4] Ciurylo R, Szudy J 1997 *J. Quant. Spectrosc. Radiat. T.* **57** 411.
[5] Wójtewicz S et. al. 2014 *J. Quant. Spectrosc. Radiat. T.* **144** 36.
[6] Domysławska J et. al. 2016 *J. Quant. Spectrosc. Radiat. T.* **169** 111.

Advantages of Dispersion over Absorption Measurements in Cavity-Enhanced Spectroscopy

A. Cygan*, P. Wcisło, S. Wójtewicz, G. Kowzan, M. Zaborowski, D. Charczun, K. Bielska, R. Ciuryło, P. Masłowski, D. Lisak

Institute of Physics, Faculty of Physics, Astronomy and Informatics, Nicolaus Copernicus University in Toruń, Grudziadzka 5, Torun 87-100, Poland
**agata@fizyka.umk.pl*

Studies of exoplanetary atmospheres and Earth's global climate changes are an important challenges of high-resolution Doppler-broadened spectroscopy. Spectroscopic retrievals are typically modeled by the Voigt profile which is straightforward but not very accurate approach even in case of Doppler, low-pressure regime. To meet 0.1% accuracy requirements [1] of remote sensing the Hartmann-Tran profile [2,3] capturing most of the molecular collisions physics was recommended [4] to model both atmospheric as well as reference spectra at pressures ranging from Doppler up to collisional regime. Nevertheless, a consequence of greater unification of the line-shape model is its dependence on larger number of parameters with tendency to correlations between them. As a result multi-spectrum fitting technique [5] has to be used together with high-quality laboratory spectra recorded in the broad range of pressures to remove partial correlations between parameters [6].

High pressures expected in spectra modeling preclude the use of the most accurate cavity ring-down spectroscopy for comprehensive study of the strongest transitions of atmospheric importance. Here we demonstrate a cavity mode-dispersion spectroscopy (CMDS) [7] exhibiting an accuracy unattainable for other cavity-enhanced spectroscopies and exposed in a wide dynamic range of absorptions. We compare it with two other absorption methods on example of spectroscopy of a weak near-infrared CO transition up to near atmospheric pressures. Optical dispersive signal was acquired in radiofrequencies what greatly reduced systematic errors of detection common for absorption spectroscopy. The lowest uncertainty of CO line position found for CMDS in the Doppler-limited case is comparable with the best sub-Doppler frequency metrology in HD [8,9] what indicates potential of CMDS in a basic research of molecular hydrogen. CMDS can also be easily implemented into high-resolution broadband spectroscopic methods employing optical frequency combs [10].

References

[1] Miller C E, et al 2005 *C. R. Phys.* **6** 876.
[2] Pine A S 1999 *JQSRT* **62** 397.
[3] Ngo N H, et al 2013 *JQSRT* **129** 89. Ngo N H, et al 2014 *JQSRT* **134** 105.
[4] Tennyson J, et al 2014 *Pure Appl. Chem.* **86** 1931.
[5] Benner D C, et al 1995 *JQSRT* **53** 705.
[6] Pine A S, Ciuryło R 2001 *J. Mol. Spec.* **208** 180.
[7] Cygan A, et al 2015 *Opt. Express* **23** 14472. Cygan A, et al 2016 *J. Chem. Phys.* **144** 214202.
[8] Tao L-G, et al 2017 arXiv:1712.08705 [physics.atom-ph]
[9] Cozijn F M J, et al 2017 arXiv:1712.08438 [physics.atom-ph]
[10] Kowzan G, et al *Optical cavity mode measurements at Hz-level precision with a comb-based VIPA spectrometer*, CLEO 13-18.05.2018, San Jose, CA, USA

24th ICSLS 2018
Dublin, Ireland

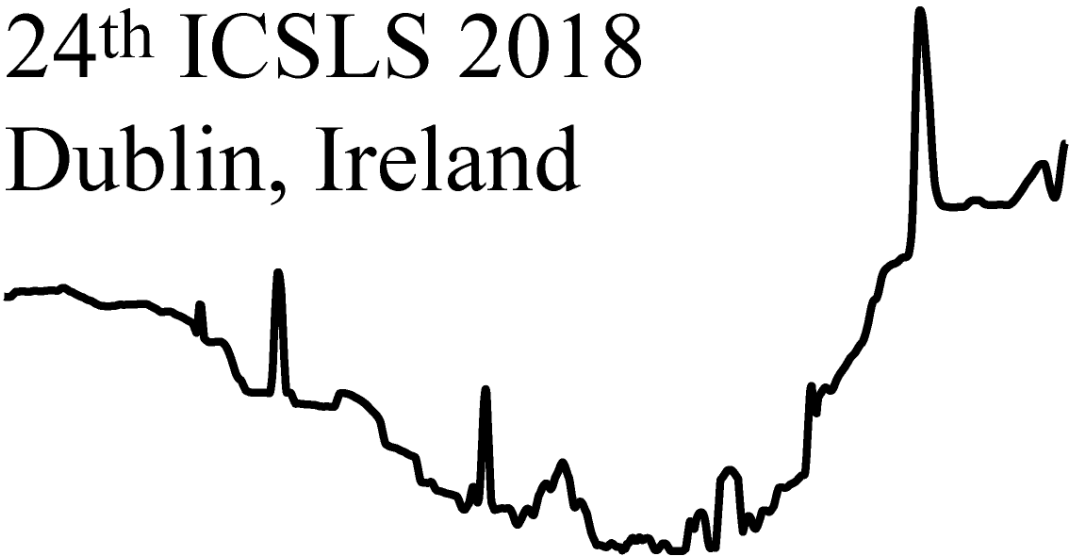

Friday Oral Session 2
Fr.O.2

Characteristics of High-density Cascade Arc Discharges for an Atmosphere-vacuum Interface

S. Namba[a], T. Shugyo[a], Y. Iwamoto[a], Y. Asano[a], K. Fukuyama[a], L. Matsuoka[a], N. Tamura[b], and T. Endo[a]

[a]*Graduate School of Engineering, Hiroshima University, 1-4-1 Kagamiyama Higashihiroshima, Hiroshima, Japan, namba@hiroshima-u.ac.jp*
[b]*National Institute for Fusion Science, 322-6 Oroshi-cyo, Toki, Gifu, Japan*

The concept of a cascade arc discharge (wall-stabilized arc plasma) that generates an atmospheric high-density plasma channel was proposed by Maecker [1]. In order to apply the cascade arc as a novel interface (*plasma window* [2]) to separate a vacuum chamber from the atmosphere without needing a large differential pumping system, two cascade arc plasma sources with channel diameters of 3 and 8 mm have been developed [3], and their plasma parameters were determined by visible and vacuum UV emission spectroscopy.

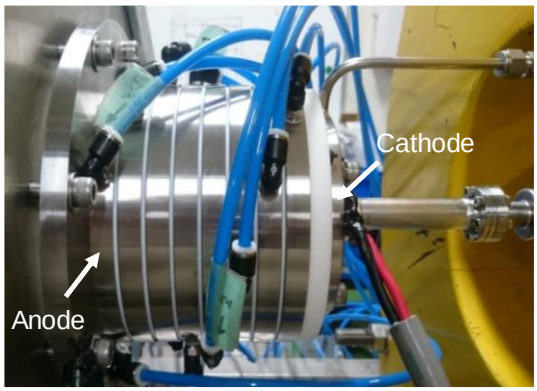

Figure 1. Cascade arc source of 3-mm plasma channel.

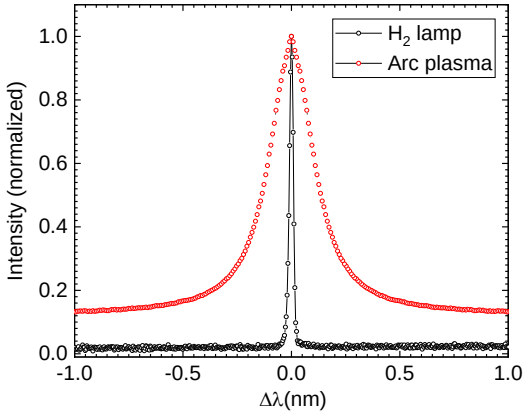

Figure 2. Hβ spectra of the 3-mm Ar cascade arc discharge and H_2 lamp.

Figure 1 shows a photograph of the cascade arc apparatus having 3-mm plasma diameter. The electrode housing had a 3.2mm-CeW cathode, eight intermediate electrodes, and a CuW anode. The Ar gas was fed into the discharge section with a constant flow rate up to 3.3 L/min. Spectral analysis of Ar I emission indicated that the plasma had an electron temperature of ~1 eV at 50 A at the anode exit. Electron density was evaluated from the Stark broadening of Hβ spectrum (impurity). Figure 2 shows the Hβ spectrum observed at 50-A Ar discharge. For reference, the spectrum of H_2 lamp with a low gas pressure is plotted. From the broadening width, the density at the anode was determined to be 2.4×10^{16} cm^{-3}. Absolute pressures in the discharge and expansion sections were also measured to examine the performance as the plasma window. At Ar discharge of 50 A, the gas pressure in the discharge section was 100 kPa, while the pressure in the expansion section was 0.1 kPa, showing the steep pressure gradient through the discharge channel. As for the arc plasma having 8-mm channel diameter, He plasmas were generated under low-gas flow rates, and electron temperature and density were measured.

References

[1] H. Maecker, Z. Naturforsch., An **11**, 457 (1956).
[2] A. Hershcovitch, J. Appl. Phys. **78**, 5283 (1995).
[3] S. Namba, T. Endo, S. Fujino, C. Suzuki and N. Tamura, *Rev. Sci. Instrum.* **87,** 083503 (2016).

Study of the Influence of the Cathode Material in the Behaviour of a Hollow-Cathode Glow-Discharge in Hydrogen

V. Gonzalez-Fernandez, K. Grützmacher, C. Pérez, M. I. de la Rosa
Dpto. de Física Teórica, Atómica y Óptica, Universidad de Valladolid, Paseo Belén 7, 47011, Valladolid, Spain
veronica.gonzalez.fernandez@alumnos.uva.es

Low pressures discharges have been object of study during many years due to its many applications in industry and research. Namely, *glow-discharges* are used in material processing, etching, thin-film deposition, spectroscopy, etc. Any of these applications require a deep knowledge of its behaviour, from theoretical and experimental point of view. The E-field present in the discharge is one of the most interesting parameters, due to the discharge dynamics is strongly conditioned by it. In the Plasma Laser Spectroscopy Laboratory (University of Valladolid, Spain) E-field measurements are performed with high spatial and temporal resolution. The measurements are done in the cathode fall region of a hollow cathode discharge (HCD) operated in pure hydrogen or deuterium. The technique is based in the Stark shifting and splitting of the 2S level of hydrogen, followed by optogalvanic detection. The E-field determination is done measuring the separation in GHz of the components $2P^{1/2}$ and $2P^{3/2}$. The measurements are carried out with pulsed 243 nm radiation (10 Hz), generated by an injection seeded Q-switched Nd:YAG laser, which pumps a second laser system based in non-linear crystals (OPO-OPA-SFG). This system provides single-longitudinal mode radiation up to 5 mJ, with a temporal duration of 2.5 ns and 300 MHz bandwidth. In the experimental set-up, the UV radiation is divided in two counter propagating laser beams, circularly polarized in opposite directions. The two beams are focalized in a 100 μm and 10 mm overlapping volume in the upper central part of the discharge and parallel to the cathode surface. Following the selection rules for two-photon absorption (ΔL=0), only one photon from each beam is absorbed, leading in Doppler-free measurements. The plasma source is a home-made HCD, with a cylindrical cathode placed between two peaked anodes. All pieces have an axial perforation to allow end-on spectroscopic measurements, which are taken at different distances from the cathode surface. The discharge can be operated in a wide range of pressures and currents; from 400 to 900 Pa, and from 50 to 300 mA. The main aim of the work presented here is to study the influence of the cathode material in the cathode fall characteristics. To do that, E-field measurement were performed with two cathodes, stainless steel and tungsten, both of them with 15 mm of inner diameter. Although both materials are widely used in this kind of discharges, the sputtering rate is 10^4 times bigger in stainless steel than in tungsten. This difference affects directly the E-field strength fall and other properties of the discharge, as can be the maintenance voltage, the maximum E-field reached and the length of the cathode dark space. The effect of the sputtering is also depending on the pressure and current applied to the discharge. A complete study will be presented at the Conference.

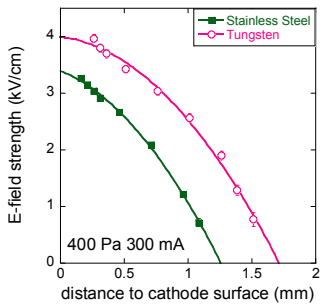

Figure 1. E-field fall strength vs the distance from the cathode surface for two cathodes of stainless steel and tungsten and an inner diameter of 15 mm.

H_2-He Interaction And Its Scattering States Observation With Highly Accurate Cavity-Enhanced Spectroscopy

M. Słowiński[a*], F. Thibault[b], Y. Tan[c], J. Wang[c], A.-W. Liu[c], S.-M. Hu[c], S. Kassi[d,e], A. Campargue[d,e], M. Konefał[a,d,e], H. Jóźwiak[a], K. Patkowski[f], P. Żuchowski[a], R. Ciuryło[a], D. Lisak[a], P. Wcisło[a]

[a]*Institute of Physics, Faculty of Physics, Astronomy and Informatics, Nicolaus Copernicus University in Toruń, Grudziadzka 5, 87-100 Torun, Poland*
[b]*Institut de Physique de Rennes, UMR CNRS 6251, Université de Rennes 1, Campus de Beaulieu, Bât. 11B, F-35042 Rennes, France*
[c]*Hefei National Laboratory for Physical Sciences at Microscale, iChEM, University of Science and Technology of China, Hefei, 230026 China*
[d]*University of Grenoble Alpes, LIPhy, F-38000 Grenoble, France*
[e]*CNRS, LIPhy, F-38000 Grenoble, France*
[f]*Department of Chemistry and Biochemistry, Auburn University, Auburn, AL 36849 USA*
[*]*suowik@fizyka.umk.pl*

We employ highly accurate cavity-enhanced molecular spectroscopy to study the H_2-He collisions and interactions [1]. Hydrogen molecule in its ground electronic state perturbed by the helium atom constitutes the simplest system of perturbed molecule (it contains only four electrons). This gives possibility to make a link between the experiment and the theory from first principles, allowing to use *ab initio* calculations to make the physical interpretation of the experimental spectra.

In contrast to most of the previous studies, we do not fit spectra with phenomenological line shapes, but directly [2] superimpose theoretical profiles (originating from our *ab initio* calculations) on the raw experimental spectra without fitting any of the line-shape parameters. Within this approach not only the shapes of experimental lines are reliably reproduced, but also the underlying physics of molecular collisions can be traced. Besides the analysis of the basic line-shape effects (such as relaxation or phase changes of the internal states of the molecule), we also analyse the more sophisticated ones such as speed-dependent effects or velocity-changing collisions (complex Dicke narrowing parameter) [3-4], which are particularly pronounced for the H_2-He system [1,5-7]. We achieved good agreement between raw experiment data and *ab initio* calculations reaching the differences at the 1% level.

According to our knowledge, this is the first comparison of highly accurate experimental spectra with advanced *ab initio* models which includes the speed-dependent effects and velocity-changing collisions. It allows us to study quantum scattering for molecules as well as to validate *ab initio* quantum potentials in ranges very challenging for quantum chemistry methods (for instance, for highly stretched molecules).

References

[1] Thibault F, Patkowski K et al. 2017 *J. Quant. Spectrosc. Radiat. T* **202** 308.
[2] May A D, Liu W-K et al. 2013 *Can. J. Phys.* **91** 879.
[3] Hess S 1972 *Physica* **61** 80.
[4] Ciuryło R, Shapiro D A et al. 2002 *Phys. Rev. A* **65** 012502.
[5] Wcisło P, Tran H et al., 2014 *J. Chem. Phys.* **141** 074301.
[6] Thibault F, Wcisło P et al. 2016 *Eur. Phys. J. D* **70** 236.
[7] Martínez R Z, Bermejo D et al. *J. Raman Spectrosc.* (accepted).

24th ICSLS 2018
Dublin, Ireland

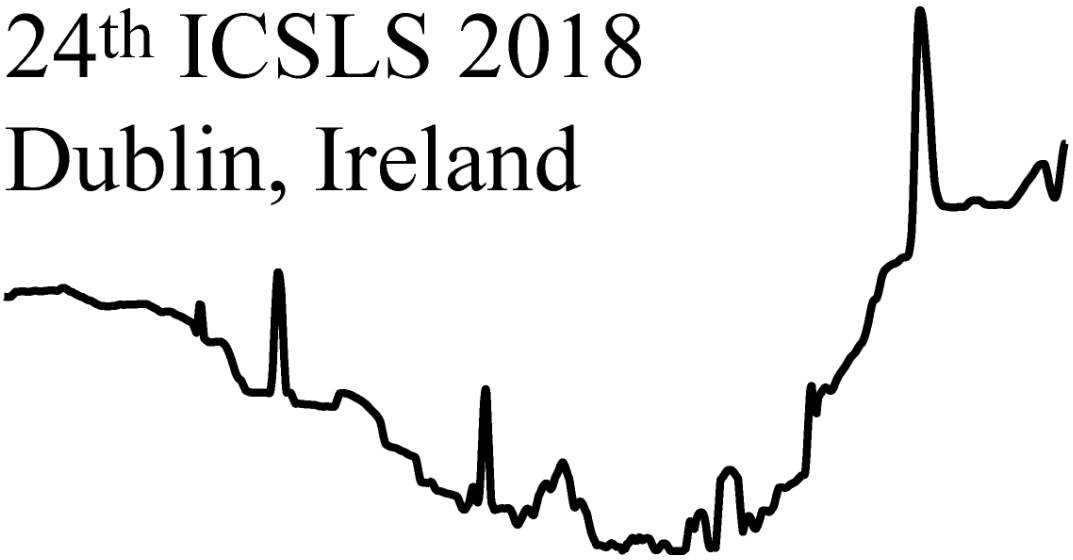

Tuesday Poster Session
Tu.P

Line-shape Parameters and Their Temperature Dependence for the ν_6 Band of CH_3D-N_2

Anna Dudaryonok[a], Nina Lavrentieva[a], Jeanna Buldyreva[b]

[a]*V.E. Zuev Institute of Atmospheric Optics, Siberian Branch of the Russian Academy of Sciences, 1 Akademishian Zuev square, 634021 Tomsk, Russia (lnn@iao.ru)*
[b]*Institut UTINAM, UMR 6213 CNRS, Université Bourgogne Franche-Comté, 16 Route de Gray, 25030 Besançon cedex, France (jeanna.buldyreva@univ-fcomte.fr)*

Theoretical estimates for line-shape parameters of CH_3D infrared absorption lines broadened and shifted by N_2 pressure are obtained by a semi-empirical approach [1] for the perpendicular ($\Delta K = \pm 1$) ν_6 band, completing the previous results on the parallel ($\Delta K = 0$) ν_3 band [2]. Calculations are based on the use of Anderson-type expressions corrected by a few-parameter factor to take account of various deviations from Anderson theory approximations. A mathematically convenient form consistent with the experimentally observed features of line-width J-dependences is chosen and its model parameters are fitted on some broadening coefficients measured at 296 K. For line-shift calculations, the unknown CH_3D polarizability in the excited vibrational state is considered as an additional fitting parameter and its value is deduced from fits on some room-temperature experimental line-shifts. After validation by comparison with experimental values available for various sub-branches of the band (Fig. 1), computations of line-broadening and line-shifting coefficients as well as their temperature-dependence characteristics are performed for wide ranges of rotational quantum numbers ($0 \le J \le 70$, $0 \le K \le 20$) requested by spectroscopic databases and in the temperature range 200-400 K recommended for HITRAN. These data can be useful for astrophysical and planetary-science applications.

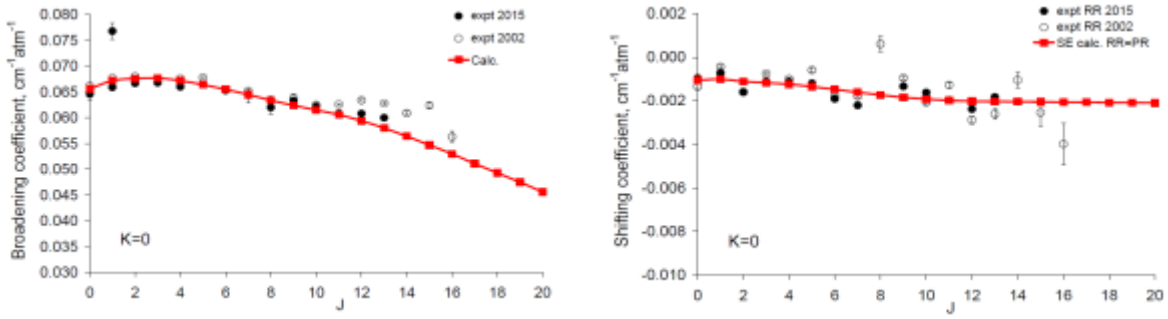

Figure 1. Computed room-temperature broadening coefficients (left panel) and shifting coefficients (right panel) for the ^{R}R-sub-branch lines with K=0 compared to the experimental values [3, 4].

References

[1] Bykov AD, Lavrentieva NN, Sinitsa LN 2004 *Mol. Phys.,* **102,** 1653-1658.
[2] Buldyreva J, Lavrentieva NN, Dudaroynok AS 2017 *JQSRT,* **203,** 355-366.
[3] Predoi-Cross A, Devi VM, Sung K, Sinyakova T, Buldyreva J, Benner DC, Smith MAH 2015 *JQSRT,* **163,** 120-141.
[4] Devi VM, Benner DC, Brown LR, Smith MAH, Rinsland CP, Sams RL, Sharpe SW 2002 *JQSRT,* **72,** 139-191.

Vacuum Ultraviolet Laser Induced Breakdown Spectroscopy (VUV-LIBS) With Machine Learning For Pharmaceutical Analysis

Muhammad Bilal Alli[a], Daniela Szwarcman[b], Daniel Salles Chevitarese[b], Patrick Hayden[a]

[a] *School of Physical Sciences and NCPST, Dublin City University, Glasnevin, Dublin 9, Ireland*
Corresponding author email address: muhammed.alli2@mail.dcu.ie
[b] *IBM Research – Rio de Janeiro, Brazil*

As an analytical technique, Laser Induced Breakdown Spectroscopy (LIBS) allows quick analysis to determine the elemental composition of the target material. Samples need little\no preparation, removing the risk of contamination or loss of analyte [1]. It is minimally ablative so negligible amounts of the sample is destroyed, while allowing quantitative and qualitative results [1]. VUV-LIBS [2,3], due to the abundance of transitions at shorter wavelengths [4], offers improvements over LIBS in the visible region, such as achieving lower limits of detection for trace elements and extends LIBS to elements\samples not suitable to visible LIBS. These qualities also make VUV-LIBS attractive for pharmaceutical analysis. Due to success in the pharmaceutical sector molecules representing the Active Pharmaceutical Ingredients (API) have become increasingly complex. These organic compounds reveal spectra densely populated with carbon and oxygen lines in the visible and infrared regions, making it increasingly difficult to identify an inorganic analyte. The vacuum ultraviolet region poses a solution as there is much better spacing between spectral lines. VUV-LIBS experiments were carried out on Pharmaceutical Samples and Chemometric techniques were applied to analyze the samples [5-7]. The motivation for the application of these Chemometric techniques is the classification of analytes, allowing us to distinguish pharmaceuticals from one another based on their spectra. Three machine learning techniques have been compared, Self-Organizing Maps [8-10], Support Vector Machines [11,12] and Convolutional Neural Networks [13].

References

[1] Noll R 2012 *Springer*.
[2] Jiang X, et al. 2013 *Spectrochim. Acta B* **86** 66.
[3] Jiang X, et al. 2014 *Spectrochim. Acta B* **101** 106.
[4] Kelly R L, et al. 1973 *NRL Report* 7599, USA
[5] Doucet F R, et al. 2008 *J Anal AtSpectrom* **23** 694.
[6] Gemperline P 2006 *Practical Guide to Chemometrics Taylor &Francis Group*
[7] Myakalwar A K, et al. 2011 *Talanta* **87** 53–9.
[8] Kohonen T 1998 *Neurocomputing*. **21** 1–6.
[9] Kohonen T 2013 *Neural Netw* **37** 52–65.
[10] Kangas J, Kohonen T 1996 *Math Comput Simulat* **41** 3–12.
[11] Lu S, Dong M, Huang J, Li W, Lu J, Li J 2018 *Spectrochim. Acta B* 140 35–43.
[12] Hsu CW, Lin CJ 2002 *IEEE Trans. Neural Netw. Learn. Syst* 13**(2)** 415–25.
[13] Li H, Xu B, Wang N, Liu J 2016 *ICANN* 128–35.

VUV Photoabsorption Spectra of Pb and Bi Ions Using Dual Laser Plasma Technique

Hu Lu[a,b], Patrick Hayden[a], Piergiorgio Nicolosi[b] and John Costello[a]

[a]*School of Physical Sciences, Dublin City University, Dublin, Ireland (hu.lu3@mail.dcu.ie)*
[b]*Department of Information Engineering, University of Padova, Padova, Italy*

A significant body of work exists on the study of photoionization processes in rare gas atoms where electron correlation has been revealed as a key physical mediator leading to the observation of giant photoionization resonances, single photon-multiple electron excitation and/or ionization, etc. In contrast metal atoms and ions have been much less studied. The current project centres on a study of vacuum ultraviolet (VUV) photoabsorption spectroscopy of metal atoms and ions using laser plasma generated continuum radiation at DCU [1]. Photoabsorption spectra have been measured using the well-established Dual Laser Plasma (DLP) photoaborption technique [1]. Using this technique, the absorption spectra of lowly charged ions of lead and bismuth have been obtained.

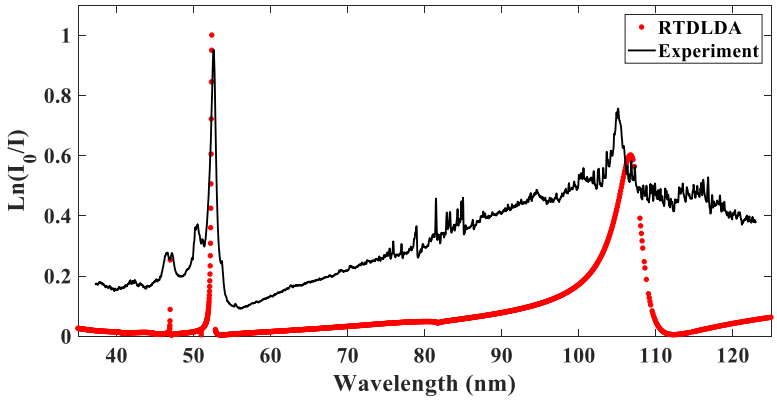

Figure 1. Comparison of experiment and RTDLDA calculation of Bi.

The main focus of the work presented will be on using the DLP technique to establish the conditions for which the population of a particular ion stage is maximised, as a function of time and space. While the RTDLDA code of Andy Zangwill [2] provides a good approximation to the overall spectral shape calculations (Figure 1), the Cowan suite of codes [3], with input parameters tuned by comparison with spectral lines already identified in the literature [4,5,6,7,8], are needed to identify unknown lines. This work is currently ongoing.

References

[1] Costello J T et al. 1991 *Physica Scripta* T**34**, 77
[2] Liberman D A and Zangwill A 1984 *Comput. Phys. Commun*. **32** 75
[3] Cowan R D 1981 Berkeley, "The Theory of Atomic Structure and Spectra" *CA: University of California Press*
[4] Connerade J P et al. 1977 *Proc. R. Soc. Lond. A*. **357** 499-512
[5] Mazzoni M et al. 1987 *J. Phys. B: At. Mol. Phys*. **20** 2193-2202
[6] Joshi Y N and Mazzoni M 1986 *Phys. Rev. A* **118** 237-8
[7] Yoo R K et al. 1995 *J. Phys. B: At. Mol. Opt. Phys*. **28** 1743-1759
[8] Andrzejewska M 2013 *J. Phys. B: At. Mol. Opt. Phys*. **46** 205003

Ion Energy Distribution from Colliding Laser Plasmas

C B Doherty[1], M Kelly[2], T Donnelly[3], J G Lunney[4], J T Costello[1]
[1] *Dublin City University, Glasnevin, Whitehall, Dublin 9*
[2] *University of Hull, HU6 7RX, Hull, UK*
[3] *University College Dublin, Belfield, Dublin 4, Ireland*
[4] *Trinity College Dublin, College Green, Dublin 2*
columb.doherty33@mail.dcu.ie

When two individual laser pulses are focussed onto a target side by side the plasmas produced have the potential to *interpenetrate* or *stagnate* upon collision, with the outcome determined by the collisionality parameter, ζ. [1]. Previous work on stagnation layers focussed mainly on their radiative emissions [2, 3] with less investigation of the particle emissions [4]. This work examines the characteristic energy and charge state distribution of the ions emitted from a colliding plasma system, with the intention of engineering an ion beam source for use in e.g., particle accelerators, biomedical and nanofabrication technologies.

By adjusting the target geometry, we can significantly increase the percentage of highly charged ions emitted (shown in figure 1). We used a 1064 nm, 73 mJ laser pulse of ~6ns pulse-width, split in 2 for the colliding plasmas. For ion signal analysis we used an ESA (Electrostatic Sector Analyzer) at the end of a time-of-flight tube, which was designed and built in-house. This enabled the discrimination of incoming charged particles based on their charge-to-mass ratio allowing us to separate and identify the various elements, ion stages and even isotopes of the charged particles.

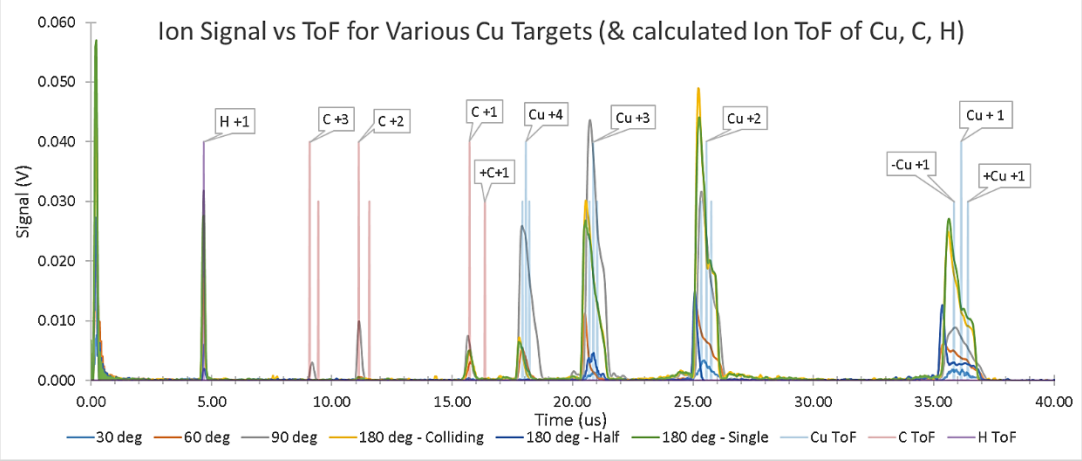

Figure 1 - ToF ion signals with a pass energy of $E_p=\frac{Z*(100V)}{\frac{r1}{r2}-\frac{r2}{r1}}$ eV (where symbols have the regular meaning) for both flat and wedged (30, 60, 90°) Cu targets

References

[1] Rumsby PT, Paul JWM, Masoud MM. Interactions Between Two Colliding Laser Produced Plasmas. Plasma Phys. 1974;16:969–75
[2] Kavanagh KD. Imaging and Spectroscopy of Laser-Produced Colliding Plasmas. Dublin City University; 2006
[3] Hough P. Laser, Optical and Electrical Diagnostics of Colliding Laser-Produced Plasmas. Dublin City University; 2010
[4] Yeates P, Fallon C, Kennedy ET, Costello JT. Charge Resolved Electrostatic Diagnostic of Colliding Copper Laser Plasma Plumes. Phys Plasmas. 2011;18(103104):1–11

Photoassociation spectroscopy in the RbHg system

M. Witkowski[a,b*], R. Muñoz-Rodriguez[a], M. Borkowski[a], P. S. Żuchowski[a], R. Ciuryło[a], M. Zawada[a]

[a]*Institute of Physics, Faculty of Physics, Astronomy and Informatics, Nicolaus Copernicus University in Toruń, Grudziądzka 5, 87-100 Toruń, Poland*
[b]*Institute of Physics, University of Opole, Oleska 48, PL-45-052 Opole, Poland*
[*]*mwitkowski@uni.opole.pl*

We present the detection of near-threshold bound states of excited heteronuclear Rb*Hg molecules through photoassociation spectroscopy [1] near the 795 nm Rb D1 line. The necessary ultracold mixture of Rb and Hg atomic gases was produced using a two-species magneto-optical trap (MOT) [2]. The interaction properties of the RbHg system as well as the prospects for photoassociation near Rb resonance lines and the production of RbHg molecules in their rovibrational ground state were recently analysed *ab initio* [3]. These theoretical predictions helped find and identify the photoassociation resonances.

Ground state molecules composed of an alkali-metal and a closed-shell atom, like RbYb [4] or RbHg, offer both permanent magnetic-dipole and electric-dipole moments thanks to their unpaired valence electron. Recently, magnetic Feshbach resonances were observed in such systems [5] providing a valuable tool for efficient control of atomic collisions. On the other hand, Hg is applicable in fundamental research with optical atomic clocks [6]. Dimers containing Hg were also proposed as good candidate species in the search for the electron electric dipole moment [7].

References

[1] K. M. Jones, E. Tiesinga, P. D. Lett, and P. S. Julienne 2006 *Rev. Mod. Phys.* **78** 483.
[2] M. Witkowski, B. Nagórny, R. Munoz-Rodriguez, R. Ciuryło, P. S. Żuchowski, S. Bilicki, M. Piotrowski, P. Morzyński, M. Zawada 2017 *Opt. Express* **91** 879.
[3] M. Borkowski, R. Munoz-Rodriguez, M. B. Kosicki, R. Ciuryło, P. S. Żuchowski 2017 *Phys. Rev. A* **96** 063411.
[4] N. Nemitz, F. Baumer, F. Münchow, S. Tassy, and A. Görlitz 2009 *Phys. Rev. A* **79** 061403(R).
[5] V. Barbe, A. Ciamei, B. Pasquiou, L. Reichsollner, F. Schreck, P. S. Żuchowski, J. M. Hutson 2017 *Nat. Phys.* (in press), arXiv:1710.03093
[6] K. Yamanaka, N. Ohmae, I. Ushijima, M. Takamoto, and H. Katori 2015 *Phys. Rev. Lett.* **114** 230801
[7] E. R. Meyer, J. L. Bohn 2009 *Phys. Rev. A* **80** 042508.

Accurate Line Shape Measurement of D_2-He and Comparison with *ab initio* Calculation

A. Nishiyama[a,b], F. Thibault[c], M. Słowiński[a*], M. Zaborowski[a], N. Stolarczyk[a], D. Charczun[a], A. Cygan[a], S. Wójtewicz[a], G. Kowzan[a], P. Masłowski[a], R. Ciuryło[a], D. Lisak[a], P. Wcisło[a]

[a]*Institute of Physics, Faculty of Physics, Astronomy and Informatics, Nicolaus Copernicus University in Toruń, Grudziadzka 5, 87-100 Torun, Poland*
[b]*Department of Engineering Science, Graduate School of Informatics, The University of Electro-Communications (UEC), 1-5-1 Chofugaoka, Chofu, Tokyo 182-8585, Japan*
[c]*Institut de Physique de Rennes, UMR CNRS 6251, Université de Rennes 1, Campus de Beaulieu, Bât. 11B, F-35042 Rennes, France.*
[*]*suowik@fizyka.umk.pl*

We measured helium-perturbed S(2) transition in the first overtone band of D_2 at several conditions with different pressures and temperatures. Accurate line shapes were obtained by the optical frequency comb (OFC) linked frequency-stabilized cavity-ring down spectroscopy (FS-CRDS) [1]. A probe laser was locked to a high-finesse ring-down cavity using Pound-Drever-Hall (PDH) method and the high-finesse cavity was locked to a I_2 stabilized Nd:YAG laser. The frequency axis of spectrum was precisely calibrated with OFC referenced to UTC(AOS) frequency standard (Coordinated Universal Time from the Astro-Geodynamic Observatory in Borowiec, Poland). We prepared D_2-He mixture with molecular deuterium concentration of 5%. We recorded 12 spectral line shapes at different temperatures (from 298 to 333K) and pressures (350 to 1400 Torr). The temperature of the cell was controlled with an accuracy of 50 mK [2]. We performed *ab initio* quantum scattering calculations for the D_2-He system and we used the resulting S-matrices to calculate the line-shape parameters [3]. We use the speed-dependent billiard-ball profile (SDBBP) [4,5] to simulate the shapes of the D_2 line. The calculation is following the method of line-shape calculations from the transport-relaxation equation [6,7], where also the description of the velocity-changing collisions originates from *ab initio* interaction potential. We will present a comparison of our experimental spectra with line-shape simulations.

References

[1] Cygan A, Wójtewicz S et al. *J. Chem. Phys.* **144** 214202.
[2] Zaborowski M, Wcisło P et al. 2017 *J. Phys. Conf. Ser.* **810** 012042-1.
[3] Thibault F, Patkowski K et al. 2017 *J. Quant. Spectrosc. Radiat. T* **202** 308.
[4] Wcisło P, Tran H et al. 2014 *J. Chem. Phys.* **141** 074301.
[5] Wcisło P, Thibault F et al. 2015 *Phys. Rev. A* **91** 052505.
[6] Ciuryło R, Shapiro D A et al. 2002 *Phys. Rev. A* **65** 012502.
[7] Wcisło P, Cygan A et al. 2013 *Phys Rev. A* **88** 012517.

Compact Gain Switched Optical Frequency Comb Generator for Sensing Applications

M. Hammad[a], E. P. Martin[a], M. Deseada Gutierrez[b], P. D. Lakshmijayasimh[a], G. Jainb, P. Landais[a], J. Braddell[b] and P. M. Anandarajah[a]

[a] *Radio and Optical Communications Laboratory, School of Electronic Engineering, Dublin City University, Glasnevin, Dublin 9, Ireland (Author e-mail address: mohab.hammad2@mail.dcu.ie)*

[b] *Pilot Photonics, Invent Centre, Dublin City University, Glasnevin, Dublin 9, Ireland*

An optical frequency comb (OFC) source is a type of laser that generates a large stable array of equally spaced, highly coherent, narrow-band spectral lines [1]. These features have resulted in them being considered for use in wide range of applications spanning over many disciplines such as millimeter wave and terahertz signal generation [2], efficient optical transceivers [3], and spectroscopy [4]. OFC generation by gain switching an externally injected semiconductor laser diode [5] has proven to be a simple, flexible, and cost-effective technique. Such an OFC avails from the tunability of both the free spectral range (FSR) and the central emission wavelength, which facilitates the matching of the OFC lines to the absorption spectra of the target gas. External optical injection also provides narrow linewidth, low relative intensity noise (RIN) and high optical gain. These parameters portrayed by this externally injected gain switched OFC source make it an excellent candidate for spectroscopy. In this paper, we present a complete characterisation of an InP photonic integrated optically injected device for the generation of a gain switched OFC. The device that will be discussed is composed of two lasers with different cavity lengths integrated in a master-slave configuration. The overall length of the device is ~1.5 mm, consisting of four electrically independent sections (master reflector, master gain, shared reflector and slave gain). The structure of the device is based on five strained AlGaInAs quantum wells in the active region on an n-doped InP substrate emitting at 1550 nm [6]. Optimum parameters required for the generation of an OFC for application in industrial sensing and spectroscopy applications are also discussed.

Acknowledgments: This work was supported in part by Science Federation of Ireland's (SFI) career development award (15/CDA/3640) and the Enterprise Ireland commercialisation fund (CF-2017-0683A-P).

References

[1] J. Ye, S.T. Cundiff (eds.), "Femtosecond Optical Frequency Comb: Principle, Operation, and Applications", Kluwer Academic Publishers/ Springer, Norwell MA, 2005.

[2] T. Shao, et al., "60 GHz Radio over Fiber System Based on Gain-Switched Laser", IEEE/OSA Journal of Lightwave Technology, vol. 32, issue 20, pp 3695-3703, Feb. 2014.

[3] V. Vujicic, et al., "Quantum dash mode-locked lasers for data centre applications" IEEE J. Sel. Top. Quantum Electron. vol. 21, no. 6, pp. 53-60, Nov./Dec.2015.

[4] B. Jerez, et Al., "Dual optical frequency comb architecture with capabilities from visible to mid-infrared", Opt. Express vol.24, 14986, Jun. 2016.

[5] P. M. Anandarajah, et al., "Generation of Coherent Multi-carrier Signals by Gain Switching of Discrete Mode Lasers", IEEE Phot. Journal, vol. 3, no. 1, pp 111 – 122, Feb. 2011.

[6] M. D. Gutierrez Pascual, et al., "InP photonic integrated externally injected gain switched optical frequency comb", OSA Opt. Lett. vol. 42, no. 3, Feb. 2017.

The Probabilities of the $\nu'1\left(^3P_1\right)-\nu''0^+\left(^1S_0\right)$ Transitions and the Radiative Lifetimes of the $\nu'1\left(^3P_1\right)$ States of the CdAr Molecules

O S Alekseeva[a], A Z Devdariani[b,c], M G Lednev[a], A L Zagrebin[a]

[a]*Baltic State Technical University «VOENMEH», Krasnoarmeiskaya St. 1, 190005, St.Petersburg, Russia*
[b]*snbrn2@yandex.ru, St. Petersburg State University, Peterhof , Ul'janovskaja St. 3, 198504, St.Petersburg, Russia*
[c]*The Herzen State Pedagogical University of Russia, nab. reki Moiki, 48, 191186, St.Petersburg, Russia*

We present the calculation of the probabilities of the radiative transitions $\nu'1\left(^3P_1\right)-\nu''0^+\left(^1S_0\right)$ and the radiative lifetimes of the resonance $\nu'1\left(^3P_1\right)$ states of the CdAr molecules as functions of the vibrational excitation degree. The calculations have been fulfilled in the framework of the effective Hamiltonian method [1] and the semi-empirical method of quasi-molecular term analysis [2] with the use of the new experimental potential energy curves which were obtained in [3]. The results are presented in the Table.

The probabilities $A\cdot10^{-4}$ (s^{-1}) of the $\nu'1\left(^3P_1\right)-\nu''0^+\left(^1S_0\right)$ transitions of the $\nu'1\left(^3P_1\right)$ states of CdAr molecules

ν' \ ν''	0	1	2	3	4	5
0	3.7	6.7	7.7	7.4	6.3	5.1
1	19.1	14.7	7.1	2.7	0.6	0.07
2	32.7	1.6	1.2	3.9	4.3	3.3
3	20.7	14.2	9.5	1.9	0.02	0.3
4	3.6	33.8	2.3	6.9	4.7	2.0
5	0.02	8.8	39.1	0.01	2.3	3.2

For all states considered the radiative lifetime is $\tau = 1.25\cdot10^{-6}$ s and is close to the atomic one.

REFERENCES

[1] Devdariani AZ, Zagrebin AL, Blagoev KB 1989 *Ann. Phys. Fr.* **14** (5) 467.

[2] Alekseeva OS, Devdariani AZ, Lednev MG, Zagrebin AL 2011 *Russian Journal of Physical Chemistry B* **5** 946.

[3] Koperski J, Urbańczyk T, Krośnicki M, Strojecki M 2014 *Chem. Phys.* **428** 43.

Determination of Radiation Characteristics of Molecular Transitions. Band HgXe(A^3O^+) – HgXe(X^1O^+)

A Z Devdariani[a,b], N A Kryukov[a], M G Lednev[c], A L Zagrebin[c], V V Olevskaia[a]

[a]snbrn2@yandex.ru,*St. Petersburg State University, Peterhof , Ul'janovskaja St. 3, 198504, St.Petersburg, Russia*
[b]*The Herzen State Pedagogical University of Russia, nab. reki Moiki, 48, 191186, St.Petersburg, Russia*
[c]*Baltic State Technical University «VOENMEH», Krasnoarmeiskaya St. 1, 190005, St.Petersburg, Russia*

Emission of excimers HgXe(A^30^+) forms molecular band in the red wing of the intercombination transition Hg(6^3P_1 – 6^1S_0). Observed spectrum contains information about quasi-molecular terms and dipole moments, population distribution by rovibrational states of excimer molecules, reaction rate constant of bound and quasi-bound molecule formation. The influence of buffer gas atom density on spectral line shape at T ≈ 300 K is described in [1]. Profile is shown to be asymmetric and decreases monotonically within the low-density limit. However, increasing of the Xe pressure leads to the formation of maximum near λ_{max}= 273 nm and dip near λ_{dip}= 257 nm. At pressure $P_{Xe}\geq$ 1 atm the spectral profiles unchange. We investigated the inverse spectroscopic problem taking into account the formation of quasi-bound molecules. In all cases potential energy curves determined in [2,3] were used. Assuming Franck-Condon transitions we isolated groups of vibrational states, emission from which forms discussed spectral peculiarities of excimer band HgXe(A^30^+) – HgXe(X^10^+) under the high densities of buffer gas (Figure 1). The dependence of the reduced radiation width $\gamma=\Gamma(R)/\Gamma_{at}$ was calculated (Figure 2). Comparison of obtained results (points) with calculations [4] (continuous curve) validates the radiation width behavior in the region of interatomic distances more than 3.5 Å where our theoretical procedure is justified.

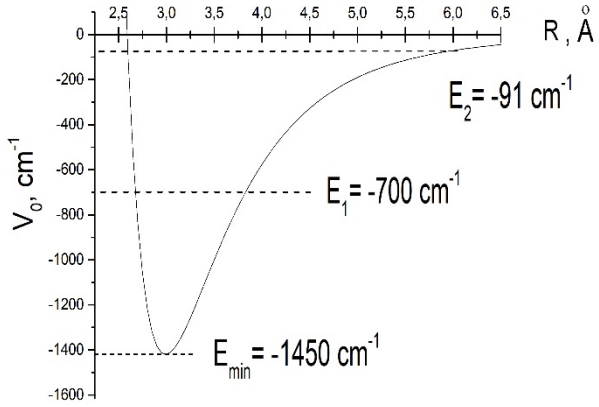

Figure 1

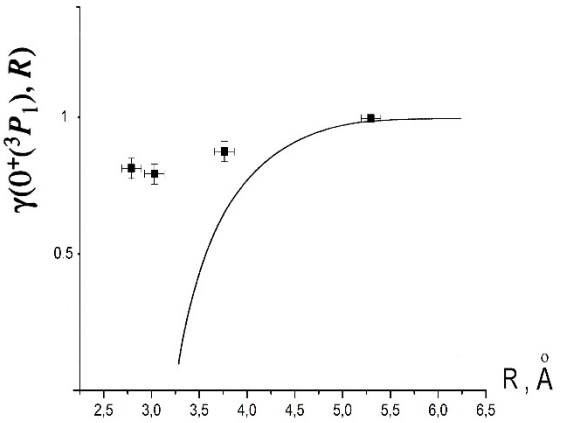

Figure 2 Reduced radiation widths of HgXe(A30+)

References:

[1] Devdariani AZ, Kryukov NA, Lednev MG, Zagrebin AL 2016 *23rd International Conference on Spectral Line Shapes (Torun, Poland), Book of abstracts* 120.
[2] Grycuk T, Findeisen M 1983 *J. Phys. B* **16** 975.
[3] Okunishi M, Nakazava H, Yamanouchi K, Tsuchiya S 1990 *J. Chem. Phys.* **93** 7526.
[4] Zagrebin AL, Lednev MG 1995 *Opt. Spectrosc.* **78** 681.

Fluorescence Spectrum Of Rydberg Atomic Hydrogen In The Dynamic Chaos Regime

Alaa Abo Zalam[a], V. A. Srećković[b], M. S. Dimitrijević[c,d], N. N. Bezuglov[a], and A. N. Klyucharev[a]

[a] *Saint Petersburg State University, 7/9 Universitetskaya nab., St. Petersburg 199034 Russia*
[b] *Institute of physics, University of Belgrade, P.O. Box 57 11001, Belgrade, Serbia*
[c] *Astronomical Observatory, Volgina 7 11060, Belgrade 74, Serbia, mdimitrijevic@aob.rs*
[d] *LERMA (Laboratoire d'Etudes du Rayonnement et de la Matière en Astrophysique et Atmosphères), Observatoire de Paris, PSL Research University, CNRS, Sorbonne Universities, UPMC Univ., Paris 06, 5 Place Jules Janssen, 92195 Meudon Cedex, France.*

In presence of a microwave electromagnetic field of frequency ω_L, Rydberg states of hydrogen atoms may undergo photoionization. At high field intensity F, the direct multi-photon ionization dominates, while at moderate intensities the diffusion ionization is the more probable mechanism [1,2]. Redistribution of population prior to ionization over a range of Rydberg states due to the dynamic chaos regime is described as stochastic diffusion of electrons in the Rydberg energy space using a Fokker-Planck type equation [1,2].

The spectrum of the fluorescence emitted by Rydberg atoms in the process of the diffusion ionization is investigated in this contribution. Previous studies [2,3] have demonstrated that onset of the global chaos exhibits a threshold, which depends on the field intensity F. For a given initial value n_0 of the Rydberg electron principal quantum number the threshold field value F_c satisfies the relation $F_c n_0^5 = n_0/(49 n_0 \omega_L^{1/3})$ provided $n_0^3 \omega_L >> 1$. If $F > F_c$, there exists a well-defined boundary $n_b < n_0$ that separates the region $n > n_b$ of chaotic motion of RE from the region $n < n_b$ of regular motion.

We have solved analytically the Fokker-Planck equation and obtained the average time $\langle d\tau \rangle = \tau(n)dn$ during which the RE is located in the vicinity dn of the quantum number n: if one determines the reduced temporal distribution $\tau'(n) \equiv 0.65 F^2/\omega_L^{4/3}\ \tau(n)$, then $\tau'(n) = 1/(2n_0^2)$ when $n_b < n < n_0$ and $\tau'(n) = 1/(2n^2)$ when $n_0 < n$. This allowed us to find the fluorescence spectrum having taken into account that (i) the main contribution to the spectrum is from the optical transition between the state nl and the most low-lying state n_g of the left-hand adjacent (l-1)-atomic series [4], and (ii) the corresponding number dN of photons emitted during the time interval $\langle d\tau \rangle$ is $dN = A_l n^{-3} \langle d\tau \rangle$ [4]. The obtained fluorescence line shape $I(\omega)$ appears to have a strongly asymmetric exotic form. It is constant on the red side ($\omega < \omega_c$) from the central line frequency $\omega_c = 1/(2n_0^2) - 1/(2n_g^2)$ and drops as $[1/(2n_g^2) - \omega]$ on the blue side ($\omega_c < \omega < 1/(2n_g^2)$).

The authors are thankful to the Ministry of Education, Science and Technological Development of the Republic of Serbia for the support of this work within the projects 176002 and III44002.

References

[1] *Zaslavsky G.M.* 2002 *Physics Reports* **371**, 461–580.
[2] Krainov V. P. 2010 *Zh. Eksp. Teor. Fiz*. **138**, 196.
[3] Gnedin Yu.N., Mihajlov A.A., et al. 2009 *New Astron. Rev.* **53**, 259.
[4] Bezuglov N.N., Borisov E.N. and Verolaĭnen Ya.F. 1991 *Sov. Phys. Usp.* **34** (1), 3-29.

Gain Switched Frequency Comb lasers for Atmospheric Trace Pollutant Monitoring

S. Chandran[1], A. A. Ruth[1*], E. P. Martin[2], F. Peters[3], P. M. Anandarajah[2]
[1] *Physics Department and Environmental Research Institute, University College Cork, Cork, Ireland*
[2] *Photonic Sensing Laboratory, School of Electronic Engineering, Dublin City University, Glasnevin, Dublin 9, Ireland*
[3] *Physics Department and Tyndall National Institute, University College Cork, Cork, Ireland*
[*] *Albert A. Ruth (a.ruth@ucc.ie)*

In this study, we report the use of a gain switched frequency comb (GSFC) laser [1,2] as a light source for cavity enhanced absorption spectroscopy. We used a GSFC laser in the near IR, to investigate whether an application to a medium finesse cavity ($F = 450$) is feasible, without the need for cavity mode matching. Even though the sensitivity improvement is expectedly modest, the advantages are the experimental simplicity, the fibre coupling feature, the cost efficiency and potential compactness. The gain-switched frequency comb laser had ~20 spectrally equally spaced comb lines with full-width-half-maximum (FWHM) of ~300 kHz of whom three lines were tuned to overlap with appropriate "fingerprint"-like absorption features of a target gas. The intensities of the comb lines that overlap an absorption resonance of the target gas decrease. In our proof-of-principal static gas experiments we demonstrated that the absorption of hydrogen sulfide (H_2S) in the range from 6347 – 6354 cm^{-1} can be measured with this simple approach. A Fourier transform spectrometer was used for signal detection. The lower detection limit or sensitivity of this simple approach is ~700 ppmv [3]. This sensitivity is well below the lower explosion limit of H2S of 4%. In the presentation the experimental parameters such as spectral resolution, integration time and duty cycle, operational pressure, experimental advantages and drawbacks, will be discussed. Furthermore, the feasibility and advantages of GSFC lasers operating with free spectral ranges (FSRs) within the ranges of 100 MHz to 2.5 GHz for trace pollutant monitoring will be discussed with the help of proof of principle measurements carried out using suitable target gases in a single-pass gas cell. Similarly, the possibility of compact gas sensing instrumentation using custom-designed integrated GSFCs will be also discussed.

Acknowledgments: This work was supported in part by Science Federation of Ireland's (SFI) TIDA programme (14/TIDA/2415) and the Enterprise Ireland commercialization fund (CF-2017-0683A-P).

References

[1] P.M. Anandarajah, R. Maher, Y. Xu, S. Latkowski, J. O'Carroll, S.G. Murdoch, R. Phelan, J. O'Gorman, L.P. Barry, Generation of coherent multicarrier signals by gain switching of discrete mode lasers. IEEE Photonics J. 3, 112 (2011)
[2] P. Anandarajah, R. Zhou, R. Maher, M.D. Guitérrez-Pascual, F. Smyth, V. Vujicic, L.P. Barry, Flexible optical comb source for super channel systems. Optical Fiber Communication Conference, Proceedings Paper# OTh3I.8, Anaheim CA, USA, 2013
[3] S. Chandran, S. Mahon, A. A. Ruth, J. Braddell, M. D. Gutiérrez. Cavity-enhanced absorption detection of H2S in the near-infrared using a gain-switched frequency comb laser. Applied Physics B,124, 63 (2018)

Radial Distribution Of Cyanide in Laser-Induced Plasma

Christopher M Helstern, Christian G Parigger

University of Tennessee, University of Tennessee Space Institute, Center for Laser Applications, 411 B.H. Goethert Parkway, Tullahoma, TN 37355, U.S.A.
e-mail: cparigge@tennessee.edu

This work presents molecular CN spectra measured after initiation of optical breakdown plasma in gaseous mixtures. Q-switched, 150 mJ, 6 ns pulsed Nd:YAG laser radiation at the fundamental wavelength of 1064 nm generates micro-plasma in ultra-high purity nitrogen and research grade carbon dioxide. The CO_2 and N_2 ratio is 1 to 1 at atmospheric pressure inside a chamber. A 0.64 m Czerny-Turner spectrometer disperses optical emissions and an intensified charge-coupled device records the data along the wavelength and slit dimensions [1].

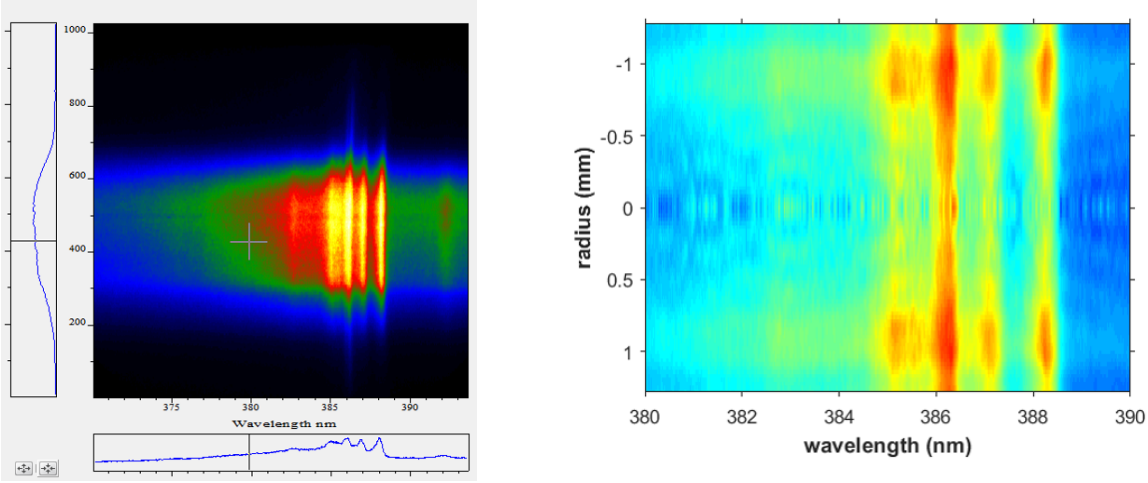

Figure 1. Recorded raw spectra 450 ns after optical breakdown in a 1:1 CO_2:N_2 atmospheric gas mixture (left) and Abel inverted spectra versus radius for a time delay of 450 ns (right)

The raw spectra show well-developed CN band heads of the $\Delta v = 0$ sequence and additionally it shows an atomic line near 386.2 nm, i.e., the carbon C I 193.09 nm atomic line recorded in second order. The data are Abel inverted to determine the radial distribution of the plasma, but symmetric profiles are necessary for Abel inverse transformations. Therefore, the analysis of CN spectra uses symmetrization methods previously applied for analysis of atomic hydrogen spectra [2]. Application of Chebyshev polynomials accomplishes direct inversion of the integral equation describing the line-of-sight measurements. The polynomial method includes implicitly digital filtering that causes broadening of the obtained radial spectra [3]. Further investigation employs algorithms routinely utilized in the analysis of diatomic molecular spectra following laser-plasma generation. At the center, the CN signals are weaker than at 1 mm, and there is spectral interference from the atomic carbon line. Stark widths of the atomic line that overlaps with the 2-2 CN band head indicate smaller electron density in the central region than at the periphery.

References

[1] Parigger CG, Helstern CM, Gautam G 2017 *Int. Rev. At. Mol. Phys.* **8** 25.
[2] Parigger CG, Surmick DM, Gautam G 2017 *J. Phys.: Conf. Ser.* **810** 012012.
[3] Pretzler G, Jäger H, Neger T, Philipp H, Woisetschläger J 1992 *Z. Naturforsch.* **47a** 955.

Contribution of the dimers on the collision induced absorption spectra in a Ar-Kr gas mixture – Benchmark for a new Ar-Kr potential

Wissam Fakhardji[a], Magnus Gustafsson[a], M.S.A El-Kader[b,c], Anastasios Haskpoulos[d], George Maroulis[d]

[a]*Applied Physics, Department of Engineering Science and Mathematics, Luleå University of Technology, SE-97187 Luleå, Sweden,* wissam.fakhardji@ltu.se
[b]*Department of Engineering Mathematics and Physics, Faculty of Engineering, Cairo University, Giza 12211, Egypt*
[c]*Department of Physics, Faculty of Sciences and Humanity Studies, Huraimla, Shaqra University, Shaqra, Saudi Arabia*
[d]*Department of Chemistry, University of Patras, Patras GR-26500, Greece*

Quantum simulations are able to provide collision induced absorption (CIA) spectra for two colliding particles but describing more than two-body interactions remain impossible in the frame of the quantum dynamical formalism. However, it has been shown that molecular dynamics (MD) is a useful tool to compute accurate collision induced absorption spectra for different gaseous systems [1]. This technique allows to compute CIA spectra at various temperatures and densities and therefore permits to explore purely two-body as well as three or more body interactions. In this study we investigated the contributions of the dimers to the absorption spectrum for the Ar-Kr system. By comparing the MD calculation with the dimer-free absorption computed with the free-to-free quantum dynamical formalism, we are able to quantify the proportion of the absorption due to the dimers. Considering that at low density only the free-to-free absorption should remain we attempt the determine the density for which the low density limit is valid, in other words where the three-body effects are negligible. The spectral moments, computed thanks to some formulas, provide insight in this analysis.
In parallel, we also investigate the accuracy of an empirical Barker-fisher-Watts potential for the argon-krypton pairs. This is done by comparing the MD absorption coefficient with one computed with the empirical potential from Aziz et al. [2] and experimental data from Buontempo et al. [3]

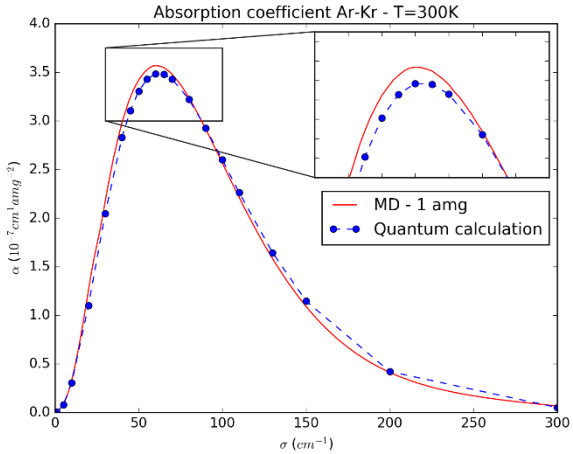

Figure 1. Comparison between the absorption spectra for the the Ar-Kr mixture at T=300K computed with the MD (at 1 amg) and quantum methods. The difference is due to the dimers contribution. In addition to the free-to-free absorption, The MD approach includes the bound-to-bound and the bound-to-free contributions.

References

[1] J.-M. Hartmann et al. 2010, *The Journal of Chemical Physics* **113**, 1276
[2] R.A. Aziz and A. van Dalen 1983, *The Journal of Chemical Physics* **78**, 2413
[3] U. Buontempo et al. 1977, *The Journal of Chemical Physics* **66**, 1278

Vibrational Dependence And Prediction Of Line Shape Parameters For The H_2O-H_2 Collisional System

Robert R. Gamache[a], Bastien Vispoel[a]

[a] *Department of Environmental, Earth, and Atmospheric Sciences, University of Massachusetts Lowell, Lowell, MA 01854, USA, Robert_Gamache@uml.edu*

The Modified Complex Robert-Bonamy (MCRB) formalism was used to calculate the half-width, γ, and line shift, δ, for the H_2O-H_2 collision system at 14 temperatures between 200 and 3000 K for over 7 thousand rotational transitions for the rotation band, the (301)-(000) band and bands for ν_1, ν_2, and ν_3 with 1-4 vibrational quanta exchanged. The calculations include all complex terms, explicit velocity integration, and a potential composed of electrostatic, induction, London dispersion, and atom-atom (expanded to 20th *order* and *rank* 4) terms using the parameters of Renaud *et al.* [1]. These data were used to study the vibrational dependence of the half-width and line shift. It is shown that the H_2O-H_2 collision system is strongly off-resonance. The results demonstrate strong and unusual vibrational dependence.

The half-width and line shift data for different vibrational bands were used to determine if a prediction routine for γ and δ could be developed. Following the work of Jacquemart *et al*. [2] and Gamache and Lamouroux [3], the expressions

$$\gamma\left[\left(v_1',v_2',v_3'\right)f\leftarrow\left(v_1'',v_2'',v_3''\right)i\right]=I^{\gamma}_{f\leftarrow i}+A_{f\leftarrow i}\left(c_1\left|\Delta v_1\right|+c_2\left|\Delta v_2\right|+c_3\left|\Delta v_3\right|\right)^{p_\gamma}$$

and

$$\delta\left[\left(v_1',v_2',v_3'\right)f\leftarrow\left(v_1'',v_2'',v_3''\right)i\right]=I^{\delta}_{f\leftarrow i}+B_{f\leftarrow i}\left(c_1\left|\Delta v_1\right|+c_2\left|\Delta v_2\right|+c_3\left|\Delta v_3\right|\right)^{p_\delta}$$

were used to predict the half-width and line shift where the powers p_γ, p_δ, and coefficients $I^{\gamma}_{f\leftarrow i}$, $A_{f\leftarrow i}$, $I^{\delta}_{f\leftarrow i}$, and $A_{f\leftarrow i}$ were determined by non-linear least-squares techniques. In addition, a normal mode prediction technique was also studied.

The results of the fits are discussed in the context of this unusual collision system.

References

[1] Renaud C. L., Cleghorn K., Hartmann L., Vispoel B., Gamache R. R., 2018, Icarus, **306**, 275-384.
[2] Jacquemart D., Gamache R. R., Rothman L. S., 2005, J. Quant. Spectrosc. Radiat. Transfer **96**, 205-239.
[3] Gamache R. R., Lamouroux J., 2013 J. Quant. Spectrosc. Radiat. Transfer, **130**, 158-171.

Asymmetric Photoelectron Emission From Chiral Molecules Using A High Repetition Rate Laser

Jason B. Greenwood, Caoimhe Bond

Centre for Plasma Physics, School of Maths and Physics, Queen's University Belfast, BT7 1NN, UK

j.greenwood@qub.ac.uk

The use of polarized light to identify the handedness of chiral chemicals has been employed for more than 200 years, but recently a completely new chiro-optical phenomenon has been discovered. Known as photoelectron circular dichroism, the angular distribution of electrons ionized from chiral molecules by circularly polarized light pulses has been found to be anti-symmetric with respect to the direction of the light propagation [1,2].

To study this phenomenon, chiral molecules were multiphoton ionized with a femtosecond laser in our laboratory. Using a magnetic field to confine electrons along the laser direction, the electrons emitted in the forward and backward hemispheres were separated and directed onto two detectors. This simple stereo-detection setup allows direct measurements of the asymmetry and demonstrates that the instrument can be used to measure the relative proportion of left-handed to right-handed chiral molecules in samples [3].

Using 260 nm pulses produced at a rate of 1 MHz to efficiently ionize the exemplar aromatic chiral molecule 1-phenylethanol, Figure 1 shows how the photoelectron asymmetry value G changes as the proportion of the circular polarisation in the pulse (the Stokes S_3 parameter) is varied. The linear dependence indicates that the photoelectron circular dichroism originates due to a single photon process from the excited state of the molecule. This is in contrast to previous results for camphor where a more complex dependence on S_3 suggested that selective excitation of molecules with certain orientations was influential [3].

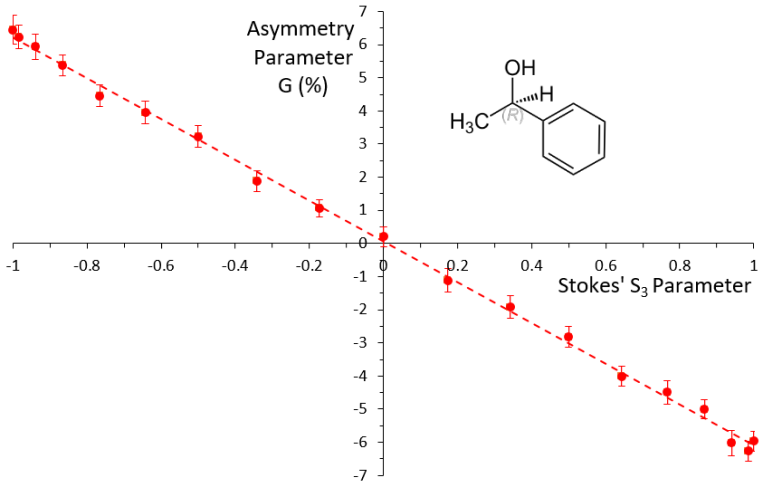

Figure 1. Photoelectron circular dichroism asymmetry parameter G of 1R-Phenylehanol as a function circularly polarised fraction of the pulse (the S_3 Stokes parameter). The ionising laser pulses were 300 fs long, at a wavelength of 260nm and an intensity of approximately 5 x 10^9 Wcm^{-2}.

References

[1] L. Nahon et al., J. Elect. Spect. Rel. Phen. **204**, 322 (2015)
[2] C. Lux et al, Angew. Chem. Int. Ed., **51**, 1(2012)
[3] J. Miles et al., Anal. Chim. Acta, 984, 134 (2017)

Effect of Wave Collapse on Lyman and Balmer lines

Hannachi[a,b] I., Meireni[a] M., Rosato[a] J., Stamm[a] R., Marandet[a] Y.

[a] *Physique des Interactions Ioniques et Moléculaires, UMR 7345, AMU-CNRS, Marseille, France (ibtissam.hannachi@univ-batna.dz)*
[b] *PRIMALAB, Faculty of Material Sciences, University of Batna, Batna, Algeria*

If a strong external source of energy is coupled to a plasma, like an energetic beam of electrons, it is possible to observe the nonlinear coupling of Langmuir waves with ion sound and electromagnetic waves. We examine conditions were the ratio W of the wave energy density to the plasma thermal energy density is of the order of one, allowing the development of a modulational instability. This instability modulates an initially uniform plane wave, and can separate it into wave packets [1]. The evolution of such wave packets may be described by a non-linear Schrödinger equation (NLSE) in the limit of small density fluctuations. Wave packets undergo a wave collapse during a cycle were the electric field magnitude grows, collapses, dissipates and reforms.

We have recently developed a model for calculating hydrogen line shapes emitted in a plasma subjected to wave collapse [2]. The electric field experienced by an emitter in wave collapse conditions is modeled by a sequence of envelope solitons. A stochastic renewal model is used for creating a large number of histories of the electric field, and a numerical integration of the Schrödinger equation allows the calculation of the dipole autocorrelation function (DAF) and its Fourier transform, the line shape. We present new calculations of Lyman and Balmer lines since they are of interest for a diagnostic of astrophysical and laboratory plasmas [3]. We calculate the DAF and profiles of these lines for conditions found in edge plasmas of fusion devices, and discuss how the DAF is modified by a change of the oscillation frequency.

The line profile can be calculated for the effect of solitons alone, or by taking account of the simultaneous effects of solitons and Stark broadening of the background plasma. The differences between such profiles may be used as a diagnostic of wave collapse conditions.

References

[1] Robinson P 1997 *Rev. Mod. Phys*., **69**, 507.
[2] Hannachi I, Stamm R; Rosato J; Marandet Y 2016 *EPL* **114**, 23002.
[3] Rosato J, Bufferand H, Koubiti M, Marandet Y, Stamm R 2015 *J. Quant. Spectrosc. Radiat. Transfer* **165**, 102-107.

Measurements and calculations of H_2- broadening and shift parameters of water vapor transitions in a wide spectral region

T.M. Petrova[a], A.M. Solodov[a], A.A. Solodov[a], V. M.Deichuli[a,b] , V.I. Starikov[c,d]

V.E. Zuev Institute of Atmospheric Optics, Siberian Branch, Russian Academy of Sciences, 1, Academician Zuev Square, 634021 Tomsk, Russia ,tanja@iao.ru;

[b] National Research Tomsk State University, Lenina Av. 36, 634050, Tomsk Russia;

[c]Tomsk State University of Control System and Radio Electronics, Lenina Av. 40, 634050,Tomsk, Russia;

[d] National Research Tomsk Polytechnic University, Lenina Av. 30, 634050, Tomsk Russia

Hydrogen pressure induced broadening and shift coefficients for water vapor absorption lines in the 6700–9000 cm^{-1} region have been measured and calculated. The spectra were recorded using Bruker IFS 125 HR spectrometer at room temperature, at the spectral resolution of 0.01 cm^{-1} and in a wide pressure range of H_2. The multispectrum fittings with the quadratic speed dependent Voigt profile were performed to retrieve the broadening parameters for H_2O spectral lines of 11 vibrational bands ($2\nu_1$, $2\nu_3$, $\nu_1+\nu_3$, $2\nu_2+\nu_3$, $\nu_1+2\nu_2$, $\nu_2+2\nu_3$, $2\nu_1+\nu_2$, $3\nu_2+\nu_3$, $\nu_1+3\nu_2$, $\nu_1+\nu2+\nu_3$ and $6\nu_2$).

The calculations of the broadening coefficients were performed in the framework of the semi-classical method with use of an effective vibrationally depended interaction potential [1]. The optimal sets of potential parameters that give the best agreement with the measured broadening coefficients for the each vibrational band separately were found. Then, the obtained broadening coefficients and literature data [2, 3] were used to determine the analytical dependence of some potential parameters on vibrational quantum numbers. The analytical expressions that reproduce the broadening coefficients for different vibrational bands are proposed. Figure presents the example of measured and calculated broadening coefficients for H_2O molecule lines broadened by H_2.

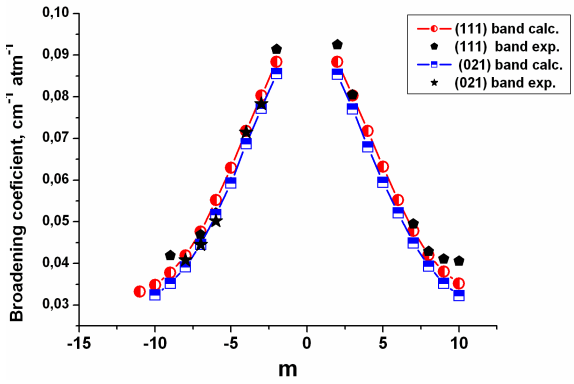

Figure. Experimental and calculated values of H_2O broadening coefficients as a function of rotational quantum number m, m = J" + 1 for R branch and m = –J" for P-branch (J" is the rotational quantum number of lower vibrational state)– for sub-branch (J 1 J)↔(J–1 1 J–1).

The authors acknowledge support from the Russian Foundation for Basic Research (RFBR, grants 17-52-16022)

References

[1] V.I. Starikov V.I. 2015 J. Quant. Spectrosc. Radiat. Transfer. **155**, 49.
[2] Brown L.B., C. Plymate C., 1996 J. Quant. Spectrosc. Radiate. Transfer. **56,** 263.
[3] Lucchesini A., Gozzini S. and Gabbanini C. 2000 Eur. Phys. J.D. **8,** 223.

Stark Broadening Analysis of Balmer Lines in Tokamak Edge Plasmas

M. Meireni[a] , I. Hannachi[a,b], J. Rosato[a], M. Koubiti[a] , Y. Marandet[a] , R. Stamm[a]

[a] *PIIM, Aix-Marseille Université / CNRS, 13397 Marseille Cedex 20, France*
[b] *PRIMALAB, Faculty of Material Sciences, University of Batna, Batna, Algeria*

Atomic processes and plasma surface interactions play a key role in the physics of the edge, divertor and X-point plasmas. Passive spectroscopy is one of the best methods helping to characterize tokamak edge plasmas [1]. A spectroscopic database for the interpretation of hydrogen Balmer lines in conditions of high-density recombining divertor plasma has been developed [2]. The spectra in the database have been obtained by a computer simulation for calculating the dynamic ion field combined to a numerical integration of the Schrödinger for the emitter evolution operator. The model uses an impact collision operator for the electrons, and includes the Zeeman effect created by the magnetic field of the tokamak. The 5 first Balmer lines have been calculated for densities N = 1, 2.15, 4.64 x (10^{13}, 10^{14}, 10^{15}), and 10^{16} cm^{-3}, temperatures $T_e = T_i = T_{at}$ = 0.316, 1, 3.16, 10, and 31.6 eV, and magnetic fields B = 0, 1, 2, 2.5, 3, and 5 T. A fitting procedure can be used for a comparison with measured spectra from current tokamaks. We present new fitting results enabling a diagnostic of the plasma parameters at the edge.

References

[1] M. Koubiti, et al. 2002. *Plasma Phys. Control. Fusion* **44** 261.
[2] J. Rosato, et al. 2017. *Journal of Quantitative Spectroscopy & Radiative Transfer* **187** 333–337

Analysis of Wavelength Modulation Spectra for Determination of OH Radical Concentration in an Atmospheric Pressure Laminar Premixed Flames

Václav Nevrlý[a], Petr Bitala[a], Vít Klečka[a], Michal Vašinek[a], Zdeněk Zelinger[b], Jan Suchánek[b], Michal Dostál[a,b], Václav Válek[a]

[a]*Faculty of Safety Engineering, VŠB-Technical University of Ostrava, Lumírova 13/630, 700 30 Ostrava – Výškovice, Czech Republic, vaclav.nevrly@vsb.cz*
[b]*J. Heyrovský Institute of Physical Chemistry, Academy of Sciences of the Czech Republic, Dolejškova 3 182 23 Prague 8, Czech Republic*

Quantification of hydroxyl radical concentration in harsh environment of flame is of significant importance for practical combustion diagnostics as well as for validation of chemical kinetic models. This work is aimed at application of wavelength modulation spectroscopy with second harmonic detection (i.e. 2*f*-WMS technique) for the given purpose consistently with previous studies [1-3] dealing with determination of OH radical concentration and temperature profiles in laminar premixed flames of methane-air mixtures.

Our recent analysis is focused on relatively narrow wavelength region (see Figure 1) which we investigated experimentally employing conventional 2*f*-WMS experimental setup. Spectral line parameters of several H_2O and OH transition were tentatively adjusted within the range of their uncertainties in order to obtain satisfactory best-fit simulation of experimental spectrum.

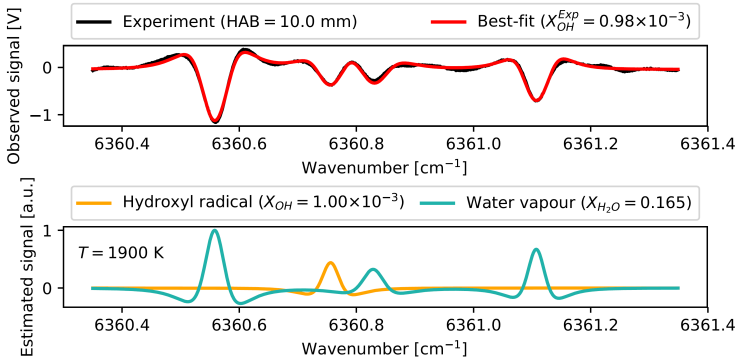

Figure 1. Experimental second-harmonic spectrum depicted with the result of nonlinear least-square fitting procedure (upper trace) and initial guess of 2*f*-WMS signal contributions assuming mole fraction of water vapour and hydroxyl radical as reported in [2] and [3] respectively (lower trace).

Finally, local mole fraction of OH radical in post-flame region was determined assuming water vapour concentration, which was measured previously [2] using identical flat-flame burner setup and experimental conditions (same stoichiometry and flow rate of reactants).

REFERENCES

[1] Aizawa T 2001 *Appl. Opt.* **40** 4894
[2] Qu Z, Ghorbani R, Valiev D and Schmidt F M 2015 *Opt. Expr.*, **23**, 16492
[3] Rutkowski L, Johansson A C, Valiev D, Khodabakhsh A, Tkacz A, Schmidt F M and Foltynowicz A 2016 *Photonics Lett. Pol.* **8** 110

Line Shapes of Raman and Plasmon-Enhanced Raman Spectroscopy for Probing Molecules in Solutions and on Noble Metals of Nanostructures

De-Yin Wu[a], Jingdong Zhang[b], Zhong-Qun Tian[a], Jens Ulstrup[b]

[a] *State Key Laboratory of Physical Chemistry of Solid Surfaces and Department of Chemistry, College of Chemistry and Chemical Engineering, Xiamen University, Xiamen 361005, China, Email: dywu@xmu.edu.cn*
[b] *Department of Chemistry, Technical University of Denmark, DK-2800 Kgs. Lyngby, Denmark*

Surface plasmon resonance (SPR) not only extremely enhances giant spectral signals but also induces chemical reactions of molecules adsorbed on noble metals of nanostructures. The former belongs to the radiation process while the latter is a radiationless process. Recently, the SPR effects can be thought as three kinds of the SPR effect (the field enhancement, the hot carrier, and the photothermal effect) [1]. Among the three mechanisms, the photophysics and photochemistry strongly depend on the environment factors of molecules adsorbed on metal nanostructures, for example, a probing molecule approaching to an isolated metal sphere or embodied into a nanogap. The latter can form the SERS hot spot, with the stronger local optical fields [2,3].

To consider the different SPR effects on the Raman spectral lineshapes, we investigate the Raman and surface-enhanced Raman spectra of probing molecules in solution and adsorbed on metal nanostructures. First, we built up the molecule-metal cluster model and carried out the density functional theoretical calculations [4]. On the basis of these DFT theoretical calculations, we further obtain the energy level alignment and the low-lying states. They will be matched to the light scattering processes due to the SPR effect. Meanwhile, we also calculated the vibrational frequencies and Raman intensities of the probing molecules in the metal-molecule-metal nanogaps. These properties were used to analyze the surface-enhanced Raman spectra of the probing molecules. Second, we further constructed the metal-molecule-metal nanogap to calculate the field enhancement and light absorption in the configurations. We considered the SPR effect of the nanogap on the optical absorption and the SPR induced chemical reactions. Finally, we do further comparison of the line shape of Raman peaks of molecules in gas, solution, and adsorption states on the surfaces of metallic nanostructures. Our calculated results indicates that the environment effect significantly influence on the Raman lineshapes of probing molecules. A very interesting theoretical result was observed in the Raman lineshape due to the solute-solvent and adsorption interaction as well as the coupling interaction in the nanostructures.

References

[1] Chen X J, Cabello G, Wu D Y, Tian Z Q, 2014 *J. Photochem. Photobiol. C*, **21(SI)**, 54.
[2] Aravind P K, Nitzan A, Metiu H, 1981, *Surf. Sci.*, **110**, 189.
[3] Gao Y, Galperin M, Nitzan A, 2016 *J. Chem. Phys.*, **144**, 244114.
[4] Wu D Y, Zhao L B, Liu X M, Huang R, Ren B, Tian Z Q, 2011 *Chem. Commun.*, **47**, 2520.

Collisional contribution to line profiles in plasmas in presence of an external magnetic field

K. Touati [(*)], M.T. Meftah [(**)]K. Chinini[(**)] et S. Douis[(**)]
[(*)] *L*P. Jean Lurçat, Boulevard des Rayettes, 13500 Martigues, France.
[(**)] Département de physique, LRPPS, Université de Ouargla 30000, Algérie
[(*)] E-mail: ktouati@yahoo.com

In the presence of a magnetic field, the light emitted by an atom or an ion immersed in a plasma is polarized and the line profiles then depend on the one hand, on the direction of observation and, on the geometry of the system on the other hand: (observation direction), (magnetic field), (electric field), (polarization). This dependency, considerably complicates the calculation, because the hypothesis of a free plasma, therefore isotropic, is a simplification which is no longer valid in the presence of a magnetic field [1]. Based on [2-4], we have formulated the basic formalism necessary for the modeling of line profiles in the presence of a magnetic field. We have seen that this part makes use of general notions, like the fact that the spectral profile is given by the Fourier transform of the autocorrelation function of the dipole. The calculation of this function is reduced to that of the average of the evolution operator which takes into account the average effect of all the perturbers of the thermal bath. The determination of this operator requires the resolution of the stochastic equation. In the case, where this equation involves the perturbed electric dipole, the action of the electrons and the ions is treated separately, the action of the electrons in the stochastic equation is described by the collision operator. But this effect of anisotropy is not the only possible manifestation of the field. Indeed, each component of the profile is also disturbed. From a theoretical point of view, it is difficult to obtain a complete formula of the spectral profile. To obtain a realistic expression of the profile, it is first necessary to diagonalize the Hamiltonian in the presence of electric and magnetic fields, and then to determine the real trajectory of the perturbers in these fields. In this work we propose to focus on the effect of the magnetic field on collisions in a plasma. From a theoretical point of view, the collisional contribution to the profile is also modified by the presence of the magnetic field. In the case of electronic perturbers, the resolution of the stochastic equation is usually based on the theory of impact of the interaction [5]. In the standard model, the emitter is subjected to a succession of independent collisions carried out by the electrons. The collective aspect of interactions with electrons is generally introduced by a screened potential of Debye. The solution of the stochastic equation is given in the impact regime, corresponding to the long interest time in front of the average duration of a collision. The collision operator must in certain cases take into account the influence of the magnetic field on the collision: the trajectory of the perturbers can be modified in the presence of the magnetic field, as well as the function of distribution of the velocity of the latter. The electron trajectories in the presence of the magnetic field are hellicoidal with axis parallel to the magnetic field and radius of curvature (radius of Larmor). We then studied, the collisional contribution to the line profile in the presence of the magnetic field, in order to obtain a detailed description of the competition that exists between the different effects responsible for the structure of the lines: the orders of magnitude will be specified as well as the relative importance of the different effects. It is also demonstrated that in the presence of the magnetic field and under some plasma conditions, the influence of the curvature of the trajectories is not negligible and must be taken into account. As application, we will do on the Lyman alpha line by introducing the effects of the internal structure of the emitter, the effects due to the Lorentz field and the effects due to the movement of the emitter, to give a " picture " more realistic line profiles. The advantage of Lyman alpha line is that it allows analytical calculations for all these effects. These calculations will provide a useful reference for testing the developed digital for arbitrary spectral lines. This study also makes it possible to specify the domains of validity of the different theories.

References

[1] K. Touati, M. T. Meftah, Journal of Modern Physics Vol.3, 943 (2012)
[2] K. Touati, « Analyse spectroscopique des plasmas en présence d'un champ magnétique »
Université de Provence Marseille (2003).
[3] Koubiti M., Godbert-Mouret L., Marandet Y., Stamm R., Touati K., Escarguel A., Capes H., Guirlet R., De Michelis C., Spectroscopic analysis of the Plasma-Neutral Relaxation near to the plasma boundary, JQSRT 71 (2001) 455-463
[4] Godbert-Mouret L., Koubiti M., Stamm R., Touati K., Felts B., Capes H., Corre Y., Guirlet R., De Michelis C.., Spectroscopy of magnetized plasmas, JQSRT 71 (2001) 365-372
[5] H. R. Griem, A. C. Kolb and K. Y. Shen, Phys. Rev. 116,4 (1956).

Radiative and Collisional Spectroscopy of Multicharged Ions: Advanced Quantum Approach

Vasily V. Buyadzhi

Odessa State Environmental University, Lvovskaya str. 15, Odessa,65016, Ukraine
e-mail: buyadzhivv@gmail.com

The properties of laboratory and astrophysical plasmas have drawn considerable attention over the last decades. It is known that multicharged ions play an important role in the diagnostics of a wide variety of plasmas [1,2]. Similar interest is also stimulated by importance of this information for correct determination of the characteristics for plasma in thermonuclear (tokamak) reactors, searching new mediums for X-ray range lasers [3]. The electron-ion collisions as well as different radiative and radiative-collisional processes play a major role in the energy balance of plasmas [1-4]. For this reason, modelers and diagnosticians require absolute cross sections for these processes. The paper is devoted to development of an advanced relativistic quantum approach to computing the important radiative and collisional characteristics of the multicharged ions in the Debye plasmas. The approach is based on the relativistic energy formalism (the Gell-Mann and Low formalism) [3-5] and relativistic many-body perturbation theory (PT) with the Debye shielding model Hamiltonian for electron-nuclear and electron-electron systems [6,7]. The optimized one-electron representation in the PT zeroth approximation is constructed by means of the correct treating the gauge dependent multielectron contribution of the lowest PT corrections to atomic radiation widths. The results for the oscillator strengths and energy shifts due to the plasmas environment effect, the effective collision strengths for the Be- and Ne-like ions of Fe, Zn and Kr embedded to different types of plasmas environment (with temperature kT=0.02-2 keV; electron density n_e =10^{16}-10^{24} cm^{-3}) are listed, analyzed and compared with available literatue data (in particular, data by Li etal [2]). As illustration in table below we list our results of computing oscillator strengths gf for $2s^2$-$[2s_{1/2}2p_{1/2,3/3}]_1$ transitions of Be-like Fe ions at different plasmas parameters n_e, T (gf_0 –the gf value for free ion).

Table. Values gf for $2s^2$-$[2s_{1/2}2p_{3/2}]_1$ transition of Be-like Fe for different plasmas parameters

Be-like Fe	n_e (см$^{-3}$)	10^{22}	10^{23}	10^{24}
kT (in eV)	gf_o: our data	gf: our data	gf: our data	gf: our data
500	0.15403	0.15406	0.15431	0.15513
1000		0.15406	0.15428	0.15488
2000		0.15404	0.15426	0.15467

References:

[1] Oks E 2010 *Int. J. Spectr*. **1** 852581
[2] Yongqiang Li, JianhuaWu, Yong Hou, Jianmin Yuan 2008 *J. Phys. B* **41** 145002
[3] Ivanov L N, Ivanova E P and Knight L 1993 *Phys. Rev. A* **48** 4365
[4] Glushkov A V, Ivanov L N 1992 *Phys.Lett.A*. **170** 33
[5] Glushkov A V 2012 *Progress in Theoretical Chemistry and Physics* (Springer) **26** 231-254
[6] Malinovskaya S V, Glushkov A V, Khetselius O Yu 2011 *Int.J.Quant.Chem*. **111** 288
[7] Buyadzhi V V 2013 *Photoelectronics* **21** 57

Spectroscopy of Rydberg atoms in a Black-Body Radiation Field: Relativistic Theory of Excitation and Ionization

Valentin B. Ternovsky, Vasily V. Buyadzhi, Anna A. Kuznetsova, Andrey A. Svinarenko, Pavel A. Zaichko

Odessa State Environmental University, Lvovskaya str. 15, Odessa,65016, Ukraine
e-mail: ternovskyvb@gmail.com

In this paper we present an advanced relativistic quantum defect and model potential method to calculation of the spectra, radiation amplitudes for the Rydberg Na, K, Rb, Cs atoms, their ionization rates of states with n = 10-100 in the field of blackbody radiation (BBR). The starting master method is the combined energy approach and relativistic many-body perturbation theory with the zeroth model potential and quantum defect approximation [1,2]. It provides sufficiently correct and simultaneously simplified numerical procedure to determination of the corresponding radiative transition and ionization properties. Interaction of the Rydberg atom A(*nL*) with the BBR induces transitions to the bound states and states of continuum: $A(nL) + \hbar\omega_{BBR} \rightarrow A^+ + e^-$, where $\hbar\omega_{BBR}$- an energy of the BBR photon; , A^+ is the corresponding atomic ion and e^- is a free electron,which is emitted during the Rydberg atom ionization. Probability of induced BBR transition between the *nlj* and *n'l'j'* states is determined by the standard radiative matrix element and number of photons for $\omega_{nn'}$, $W(nl \rightarrow n'L') = \Gamma(nL \rightarrow n'L')/[\exp(\omega_{nn'}/kT) - 1]$. A rate of ionization in the initial bound Rydberg state *nl* is determined by an intergral (integration is carrying out on the BBR frequency) of the kind: $\int_{|E_{nl}|}^{\infty} \sigma_{nl}(\omega)\rho(\omega,T)d\omega, \sigma_{nl}(\omega) \sim \omega[lM^2_{nl\rightarrow El-1} + (l+1)M^2_{nl\rightarrow El+1}]$, where E_{nL} –is the threshold frequency of ionization of the atom in the Rydberg state nL with the corresponding quantum defect. The calculated data (as example in table 1 there are our data on the BBR rates for Na) on the energy parameters, radiation amplitudes for RA Na, K, Rb, Cs, their ionization rates of states with n = 10-100 in the BBR field (T=300-600K) are presented and compared with available experimental data (Kleppner et al; Burkhardt et al) and some results of the alternative theories (Glukhov-Ovsiannikov; Lehman; Dyachkov-Pankratov, Beterov etal) [3].

Table 1. Rates (s^{-1}) of BBR ionization for Na (T=300K; see text)

state/n	10	20	30	40	state/n	50	70	100
Na S	2.86	169	187	448	Na S	106	61.4	29.5
Na P	49	1207	1147	2610	Na P	576	311	141
Na D	124	1205	1038	2365	Na D	496	268	122

References

[1] Glushkov A V 2012 *Progress in Theoretical Chemistry and Physics* (Springer) **26** 231-252
[2] Svinarenko A, Ignatenko A, Ternovsky V etal 2014 *J. Phys: Conf. Ser.* **548** 012047
[3] Kleppner D et al 1982 *Phys. Rev.A* **26** 1490; Lehman L 1983 *J. Phys.B* **16** 2145; Glukhov V, Ovsiannikov D 2009 *J. Phys.B* **42** 075001; Beterov I et al 2009 *New J. Phys*. **11** 013052

Computing Collisional Shift and Broadening of Heavy Atom Hyperfine Lines in an Atmosphere of the Buffer Inert Gas

Eugeny V. Ternovsky, Alexander V. Glushkov, Anna V Ignatenko, Olga Yu. Khetselius, Valery Mansarliysky

Odessa State Environmental University, Lvovskaya str. 15, Odessa, 65016, Ukraine
e-mail: ternovskyev@gmail.com

Studying collisional shifts and broadening the hyperfine lines for heavy elements (alkali, alkali-earth, lanthanides and others) in an atmosphere of inert gases is one of the important and actual topics of collision theory and spectral lines theory. Especial interest attracts the corresponding phenomenon for alkali and lanthanides atom [1,2]. To calculate the hyperfine spectral lines collision shift one should use the expression from kinetical theory of the spectral lines [2,3]:

$$f_p = \frac{D}{p} = \frac{4\pi w_0}{kT}\int_0^\infty dw(R)\exp\left(-U(R)/kT\right)R^2 dR$$

where *U(R)* is an effective potential of the inter atomic interaction, which has a central symmetry in a case of the pairs A-B (for example, A=Rb; B=He); *T* is temperature, w_0 is a frequency of the hyperfine transition in the isolated active atom; $d\omega(R)=Dw(R)/w_0$ is the relative local shift of the hyperfine lines, which is arisen due to the disposition of atoms of the A and B on a distance *R*. The relativistic many-body perturbation theory [4-6] is used to determine the relativistic Dirac functions for studied atoms.

We present new data on the local and observed collisional f_p shifts and widths Γ_a for pairs: A-B *(*A=alkali atom, Tl,Yb; B=He,Ar, Kr,Xe) in dependence on temperature T. Our results are compared with the available experimental data and other theoretical results (see Refs. in [1,7]), which are obtained within a perturbation theory with the Hartree-Fock or Dirac-Fock zeroth approximation. The feature of our scheme is a precise accounting for the correlation effects with using effective potentials [5]. Analysis shows that our data for studied systems are in the reasonable agreement with available experimental data (at least for available T). Very interesting features are found for the collisional broadening Γ_a parameter, namely, violation of the known Folly law ($\Gamma_a \sim f_p$) for lines in optical part of a spectrum. Our data are as follows: $\Gamma_a/f_p \sim 1/53$ for the pair Tl–He; $\Gamma_a/f_p \sim 1/47$ for Tl–Ne, $\Gamma_a/f_p \sim 1/63$ for Tl–Ar, $\Gamma_a/f_p \sim 1/72$ for Tl – Kr, $\Gamma_a/f_p \sim 1/59$ for Tl- Xe.

References

[1] Chorou B, Scheps R, Galagher J, 1976 *J. Chem. Phys.* **65** 326
[2] Batygin V and Sokolov I 1983 *Opt. Spectr.* **55** 30
[3] Malinovskaya S V, Glushkov A V, Khetselius O Yu et al 2009 *Int. J. Quant. Chem.* **109** 3325
[4] Khetselius O Yu, Florko T A, Svinarenko A A, Tkach T B 2013 *Phys. Scr.* **T153** 014037
[5] Glushkov A V et al, 1998 *Opt. Spectr.* **84** 670; 1998 *J. Str. Chem.* **39** 220
[6] Glushkov A V 2012 *Progress in Theoretical Chemistry and Physics* (Springer) **26** 231-252
[7] Khetselius O Yu 2015 *Progress in Theoretical Chemistry and Physics* (Springer) **29** 54-76

Spectroscopy of Heavy Atoms and Nuclei in a Strong Laser Field: Stark effect, Autoionization and Multiphoton Resonances

Alexander V. Glushkov, Anna A. Kuznetsova, Anna A Buyadzhi, Alexandra Makarova

Odessa State Environmental University, Lvovskaya str. 15, Odessa, 65016, Ukraine
e-mail: glushkovav@gmail.com

An advanced combined relativistic energy approach and relativistic operator perturbation theory (PT) [1-3] have been applied to studying interaction of the finite Fermi systems (heavy atoms, nuclei, molecules) with a strong (superstrong) external (DC electric and laser) field. The energy approach is based on the Gell-Mann and Low adiabatic formalism and method of the relativistic Green's function for the Dirac equation with complex energy. The operator perturbation theory formalism includes a new quantization procedures of the Dirac (Schrödinger) equation states of the finite Fermi-systems in a strong field.

Results of the computing energies and widths of the DC, AC strong field Stark resonances, multi-photon and autoionization resonances, ionization profiles for a few heavy atoms (Eu, Tm, Gd, U) are presented. Some unusual spectral features have been found. It has been studied a giant broadening effect of the autoionization resonance width in a sufficiently weak electric (laser) field for lanthanide atoms and discovered for uranium atom. It is declared that probably this effect is universal for optics and quantum chemistry of lanthanides and actinides and superheavy elements.

We present the results of studying a direct interaction of super intense laser field ($I \sim 10^{25}$-10^{35} W/cm^2) with nuclei. We present the results of AC Stark shifts of single proton states in the nuclei ^{16}O, ^{168}Er and compared these data with available data [5,6]. New data are also listed for the ^{57}Fe and ^{171}Yb nuclei. Shifts of several keV are reached at intensities of roughly 10^{34} W/cm^2 for ^{16}O, ^{57}Fe and 10^{32} W/cm^2 for heavier nuclei.

It is firstly presented a consistent relativistic theory of multiphoton-resonances in nuclei and first data for the energies and widths of multiphoton resonances and other spectral parameters are presented for ^{57}Fe and ^{171}Yb nuclei.

References

[1] Glushkov A V 2012 *Progress in Theoretical Chemistry and Physics* (Springer) **26** 231-252
[2] Glushkov A V 2012 *J. Phys.:Conf. Series* **397** 012011
[3] Glushkov A V 2014 *J. Phys.:Conf. Series* **548** 012020
[4] Lisitsa V S 1977 *Phys. Uspekhi* **153**, 379
[5] Glushkov A V, Ivanov L N, Letokhov V S Nuclear quantum optics 1991 *Preprint of Institute of Spectroscopy, USSR Academy of Sciences, Troitsk,* N4
[6] Bürvenich T**,** Evers J and Keitel C 2006 *Phys. Rev.C* **74** 044601

Spectral Parameters for Hyperfine and Electroweak Interaction and Parity Nonconservation Effect in Heavy Atoms and Nuclei

Olga Yu. Khetselius, Yuliya V. Dubrovskaya, Larisa A. Vitavetskaya, Valentin B. Ternovsky

Odessa State Environmental University, Lvovskaya str. 15, Odessa, 65016, Ukraine
e-mail: okhetsel@gmail.com

Now days the parity non-conservation (PNC) effect in heavy atomic, nuclear and molecular systems has a potential to probe a new physics beyond the Standard Model [1,2]. In our paper we systematically apply the formalism of the nuclear-QED many-body perturbation theory [3-6] to precise studying a parity violation effect in heavy atoms with account for the relativistic, nuclear and radiation QED corrections. The nuclear block of theory is presented by the relativistic mean field model (the Dirac-Woods-Saxon model) [7,8]. The results of computing the energy levels, hyperfine structure intervals, E1,M1 radiation transitions amplitudes in the heavy atoms such as ^{133}Cs, ^{173}Yb, ^{205}Tl are presented and compared with available data. Further we have computed the parity violation radiative amplitudes for a number of the atomic and nuclear systems, namely: ^{133}Cs, ^{173}Yb, ^{205}Tl (atomic parity violation) and ^{119,121}Sn (nuclear parity violation). Accuracy of accounting for the inter electron exchange-correlation corrections, the Breit and weak e-e interactions, radiation & nuclear (magnetic moment distribution, finite size, neutron "skin") effects, nuclear spin dependent corrections due to an anapole moment, Z-boson [(A_nV_e) current] exchange, the hyperfine-Z boson exchange [(V_nA_e) current] have been analysed. Besides, the weak charge has been calculated for the ^{133}Cs, ^{205}Tl atoms and firstly ^{173}Yb and comparison of the theoretical results with the Standard Model data has been done. Using the experimental parity non-conservation parameter value $\Delta E_1^{PNC}/\beta$==39mV/cm (Berkeley, 2009; Tsigutkin et al) and our value $9.707\cdot10^{-10}ea_B$, it is easily to determine the weak charge value Q_W=-92.31 for ^{173}Yb (Z=70, N=103) that should be compared with the Standard Model value Q_W=-95.44. In quantum many-body systems with dense spectra of excited states weak perturbation can be significantly enhanced. The PNC enhancement is studied too and new possibilities are examined.

References

[1] Johnson W R, Sapistein J, Blundell S A 1993 *Phys. Scr*. **T46** 184
[2] Tsigutkin K et al 2009 *Phys. Rev. Lett*. **103** 071601
[3] Glushkov A V 2012 *Progress in Theoretical Chemistry and Physics* (Springer) **26** 231-252
[4] Khetselius O Yu 2009 Phys. Scr. **T13**5 014023
[5] Khetselius O Yu 2009 *Int. J. Quant.Chem*. **109** 3330
[6] Glushkov A V, Khetselius O Yu and Lovett L 2010 *Progress in Theoretical Chemistry and Physics* (Springer) **20** 127-152
[7] Khetselius O Yu 2013 *Progress in Theoretical Chemistry and Physics* (Springer) **26** 217-230
[8] Khetselius O Yu 2015 *Progress in Theoretical Chemistry and Physics* (Springer) **29** 54-76

24th ICSLS 2018
Dublin, Ireland

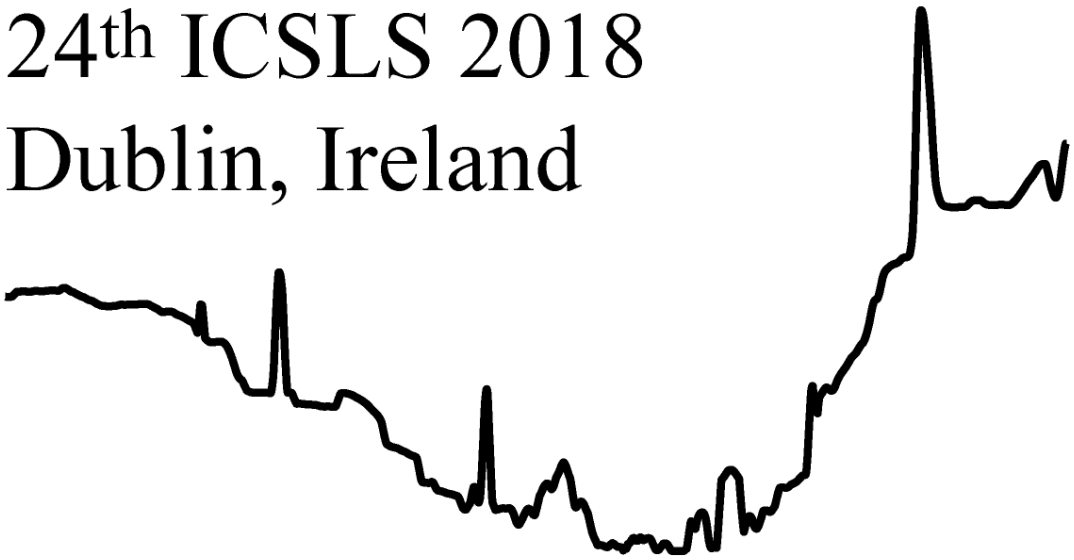

Wednesday Poster Session
We.P

Measurement of Line Emission Polarization for a Study of Anisotropy in the Electron Velocity Distribution Function at LHD

N. Nimavat[a], M. Goto[a,b] and T. Oishi[a,b]

[a]*Department of Fusion Science, SOKENDAI, Toki 509-5292, Japan (e-mail: nilam.nimavat@nifs.ac.jp)*
[b]*National Institute for Fusion Science, Toki 509-5292, Japan*

Emission lines due to excitation by anisotropic collisions are generally polarized because such collisions create an inhomogeneous population distribution over magnetic sublevels of ions [1]. Therefore, plasma polarization measurements provide a possibility to study anisotropy of the electron velocity distribution function, which is important in understanding the plasma confinement.

In the Large Helical Device (LHD), a measurement of polarization in the Lyman-α line at 121.56 nm has been started. The same optical components as those used for CLASP (Chromospheric Lyman-Alpha Spectro-Polarimeter) [2] have been incorporated into an existing 3m normal incidence spectrometer so that a high sensitivity polarization measurement is realized.

In the spectrometer, the light diffracted by a grating is reflected by a polarization analyzer so that a fixed vertical linear polarization component is only guided to a CCD detector, where Brewster's angle reflection is utilized. On the other hand, a half wave plate placed just after the entrance slit is continuously rotated so that linear polarization components at different angles in the plasma are serially obtained.

The observed line intensity shows a sinusoidal behavior even during a steady phase of a discharge, namely, the intensity of linear polarization component depends on its angle. This result obviously indicates that the line is polarized.

The details of the measurement and some initial results of analysis regarding the dependence of the polarization degree on plasma conditions such as the electron density will be presented at the conference.

References

[1] T. Fujimoto and A. Iwamae, *Plasma Polarization Spectroscopy* 2008 (Springer).
[2] R. Kano *et al.* The Astrophysical Journal Letters **839** (2017) L10.

Calculation of SO_2 and NO_2 Linebroadening Induced by Carbon Dioxide

Nina Lavrentieva, Anna Dudaryonok

V.E. Zuev Institute of Atmospheric Optics, Siberian Branch of the Russian Academy of Sciences, 1 Akademishian Zuev square, 634021 Tomsk, Russia (lnn@iao.ru)

Carbon dioxide-broadened line widths of SO_2 and NO_2 molecules are obtained at the room temperature. In the case of nitrogen dioxide calculations were performed for ~400 000 lines, rotational quantum numbers vary in the range: J to 70 и K_a to 20. The temperature exponents for every line were calculated. The data have been evaluated theoretically in the frame of two methods: semi-empirical approach [1] and averaged energy differences method [2]. Semi-empirical method is based on the straight-line trajectory approximation within the framework of semi-classical impact theory and including a few-parameter correction to account for the real curved trajectories. The averaged energy difference method is based on matching the so called coupled energy state difference with a line broadening value. The averaged energy differences for lines with experimentally-determined collision-induced widths are then used to match averaged state energy differences to line broadening values using a fitting formula. The main contribution to the line-broadening coefficients is given by the quadrupole-quadrupole interaction. We also take into account the dipole-quadrupole and polarization (both induction and dispersion) terms of intermolecular potential. The vibrational dependence of the line-broadening coefficients was found to be small (less than 5%). Being validated by comparison with measurements, these approaches were used to compute extensive line list which could be useful for atmospheric, astrophysical applications and spectroscopic databases.

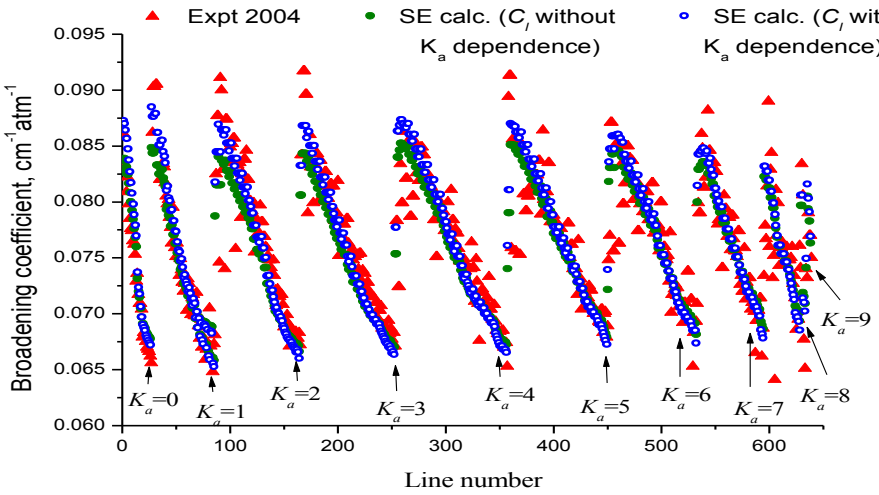

Figure 1. Measured [3] and theoretical air-broadening coefficients of NO_2 lines up to N = 35 at T = 296 K.

References

[1] Bykov AD, Lavrentieva NN, Sinitsa LN 2004 *Mol. Phys*., 102, 1653-1658.
[2] Dudaryonok AS, Lavrentieva NN, Ma Q 2015 *Atm. and oceanic optics* 28(6) 403-409.
[3] Benner DC, Blake TA, Brown LR, Devi VM, Smith MAH, Toth RA 2004 *J. Mol. Spectrosc.* **228** 593-619.

Radiative Decay of the Metastable State Hg(6^3P_2) in the Atmosphere of the Ar Atoms

A Z Devdariani[a,b], N A Kryukov[a], M G Lednev[c], A L Zagrebin[c]

[a]snbrn2@yandex.ru, *St. Petersburg State University, Peterhof , Ul'janovskaja St. 3, 198504, St.Petersburg, Russia*
[b]*The Herzen State Pedagogical University of Russia, nab. reki Moiki, 48, 191186, St.Petersburg, Russia*
[c]*Baltic State Technical University «VOENMEH», Krasnoarmeiskaya St. 1, 190005, St.Petersburg, Russia*

We studied the dependences of the absolute values of intencities and the spectral profiles produced by optical transitions in the Hg(6^3P_2) –Ar quasi-molecules under pressures P_{Ar}= (1- 60) Torr, temperatures T=(290-375) K. We also estimated the concentration of quasi-molecules. As an example Figure 1 shows the comparison of the experimental profile under P_{Ar}= 25 Torr and T=293 K, curve 1, and the calculated [1-3], curve 2. The experimental profile is a continuous band in the range 2230 - 2275 Å with a maximum at about 2255 Å. The profile is asymmetric with half-width 25 Å. The total intensity of the band decreases with increasing temperature.

The calculations were based on semiempirical analysis in the frame of the effective Hamiltonian approach [4]. The experimental results are in a reasonable agreement with calculations.

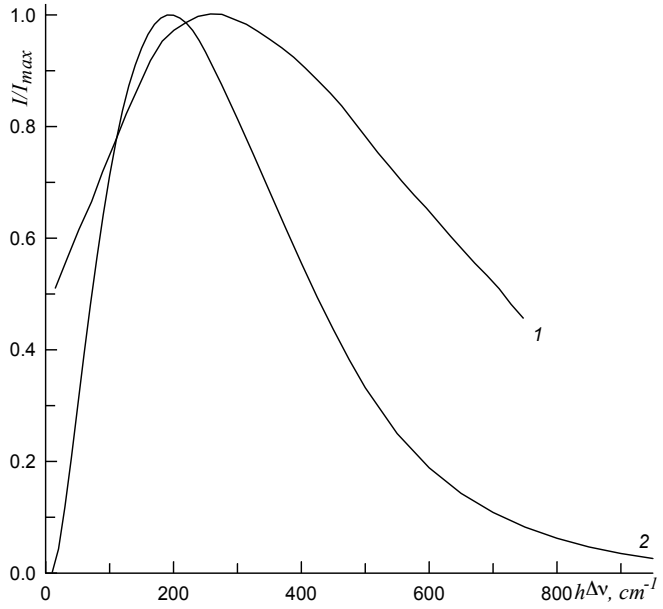

Figure 1

References:

[1] Zagrebin AL, Lednev MG 1995 *Opt. Spectrosc.* **78** (2) 159 .
[2] Zagrebin AL, Lednev MG 1995 *Opt. Spectrosc.* **78** (5) 681.
[3] Zagrebin AL, Lednev MG 1998 *Opt. Spectrosc.* **85** (2) 181.
[4] Devdariani AZ, Zagrebin AL, Blagoev KB 1989 *Ann. Phys. Fr.* **14** (5) 467.

Bound-To-Bound and Bound-To-Continuum Optical Transitions In Negative Quasi-Molecules

A Devdariani

[a]St. Petersburg State University, Peterhof , Ul'janovskaja St. 3, 198504, St.Petersburg, Russia
[b]The Herzen State Pedagogical University of Russia, nab. reki Moiki, 48, 191186, St.Petersburg, Russia
snbrn2@yandex.ru

This study develops the theory of optical transitions formed in collisions of atoms and negative ions

$$A + A^- \rightarrow A^- + A + \hbar\omega, A_2^- + \hbar\omega \quad (1)$$
$$A^- + A + \hbar\omega \rightarrow A + A + e, A_2 + e \quad (2)$$

The processes can be interesting for the problem of the molecular hydrogen formation in the early Universe [1], for the problem of the formation and stability of molecular ions H_2^- [2], and for the study of oscillations which appear in the photoionization cross section of a diatomic molecule [3]. The calculation of spectral profiles produced in the reaction (1) is reduced to the determination of oscillator strengths of optical transitions between two bound quasi-molecular states that are brought about due to resonant charge exchange. As for the reaction (2) one needs to find the density of oscillator strengths for the transition from an even or odd bound quasi-molecular state to the proper state of continuum [4]. Both reactions are considered within the framework of the zero-range potential approach [5], which simplifies calculations.

The results obtained demonstrate the formation of the H_2^- molecules in high rotational states to be possible as a consequence of the bound-to-bound transitions. In the case of photo-detachment of quasi-molecules, i.e. reaction (2), the bound-to-continuum transitions are found to lead to the formation of oscillating structures in the density of oscillator strengths. The structures are connected not only with the interference due to two possible ways of electron detachment. Another source of oscillations are resonances produced in scattering by two potential wells.

References

[1] Millar T J, Walsh C and Field T A 2017 *Chemical Reviews* **117** 1765.
[2] Kreckel H, Bruhns H, Čížek M, Glover S C O, Miller K A, Urbain X and Savin D W 2010 *Science* **329** 69.
[3] Afaq A and Du M L 2009 *J. Phys. B: At. Mol. Opt. Phys.* ***42*** *105101.*
[4] Devdariani A, Dadonova A and Shevtsova J 2014 *J. Phys.:Conf. Series* **548** 012018.
[5] *Demkov Yu N and Ostrovsky V N 1988 Zero-Range Potentials and Their Application in Atomic Physics* (New York: *Plenum Press*).

Ab-initio Studies of Few Photon Ionisation of Helium

K.N.R. Tejaswi
School of Physical Sciences, Dublin City University, Dublin, Ireland.

In this work, an ab-initio method is used to study few-photon ionization of atomic helium in a linearly and circularly polarized light. The method involves (a) a configuration interaction (CI) calculation of the helium eigenenergies and dipole transition matrix elements followed followed by (b) the propagation of the time-dependent wavefunction using the TDSE and (c) the calculation of photoionization cross sections employing non-vanishing lowest-order perturbation theory (LOPT) [1,2].

The photoionization cross sections estimated from the (TDSE) calculated yields are compared with those obtained from the LOPT. As expected, for low intensities the cross sections are in good agreement while for higher intensities, the corresponding values deviate . We also show the effects of the resonant ionization (e.g. 3-photon) which results to differences between the TDSE and LOPT approaches even for low intensities.

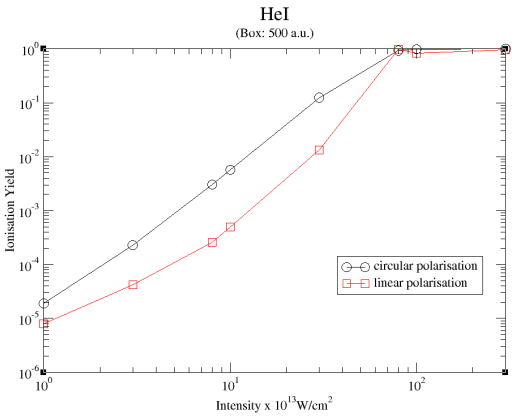

Moreover, the ionization yields obtained from the two type of polarizations (circular, linear) are compared with each other in the case of the three-photon ionization. For low intensities, circular polarization ion yields are higher than that of linear polarization.

This is due to the strongest two-electron transition matrix element of the circularly polarized light relative to the linearly polarized [3]. Note, that towards higher-order absorptions (corresponding to higher intensities) the situation is reversed due to overwhelming number of ionization channels for linearly polarized light. These observations are in agreement with similar calculations performed in Mg [4].

Acknowledgements:
This work is under supervision of Dr. L. Nikolopoulos, School of Phys. Sciences, DCU.

References

[1] L. A.A. Nikolopoulos , Comp. Phys. Communications, 150,140–165, (2003).
[2] L. A.A. Nikolopoulos and P. Lambropoulos Phys. Rev. Lett., 82(19), 3771-3774, (1999)
[3] Unpublished notes, LAAN.
[4] Takashi Nakajima and Gabriela Buica, Phys. Rev. A, 74, 023411, (2006).

Vacuum-UV Ionization of Kr

Lazaros Varvarezos*, John T Costello*, Stefan Duesterer†, Cedric Bomme†, Benjamin Erk†, Gregor Hartmann†^, Bastian Manschwetus†, Dimitrios Rompotis†, Evgeny Savelyev†, Alberto De Fanis‡, Tommaso Mazza‡, Michael Meyer‡, Nikolay Kabachnik§, Per Johnsson ¶, Andrey Kazansky& and Mossy Kelly#

* Dublin City University, School of Physical Sciences and NCPST, Glasnevin Campus, Dublin 9,Ireland
† Deutsches Elektronen-Synchrotron (DESY), Notkestrasse 85, D-22603 Hamburg, Germany
‡European XFEL GmbH, Albert-Einstein-Ring 19, D-22761 Hamburg, Germany
§Skobeltsyn Institute of Nuclear Physics, Lomonosov Moscow State University, Moscow 119991,Russia
¶Lund University, PO Box 118, SE-221 00 Lund, Sweden
&Departamento de Fisica de Materiales, University of the Basque Country, E-20018 San Sebastian/Donostia, Spain
#School of Mathematics and Physical Sciences, University of Hull, Hull HU6 7RX, United Kingdom
^Institute of Physics, University of Kassel, Heinrich-Plett-Strasse 40, 34132 Kassel, Germany

The advent of Free electron lasers (FELs) paved the way for studying few-photon inner-shell ionization of atoms in the VUV region. More specifically, electron [1,2] and ion [3] TOF spectroscopy has been applied to study the two-photon ionization of atoms. It was only recently that a study involving the angular distribution of the electrons was reported [4]. Thus, we investigated the two-photon double-ionization TPDI process in Kr. The photon energy was set at 25.2 eV, slightly above the 4p ionization threshold for Kr^+, leading to a small number of open channels as can be seen in figure 1 below.

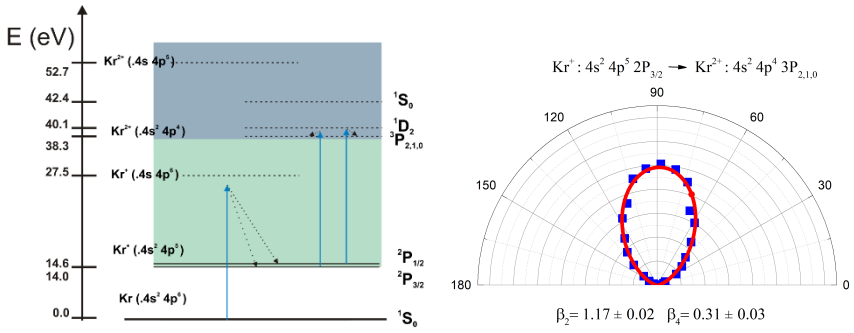

Figure 1. Energy level diagram (left) and angular distribution together with the fitted curve (right)

The angular distribution of the emitted electron was measured and the anisotropy parameters were extracted for all the open channels. The DESY-FLASH [5] FEL pulse duration was estimated to be 80 fs, with pulse-to-pulse fluctuations between 60 fs and 100 fs. The pulse energy at focus position, varied between 3 μJ and 10 μJ. Assuming a focal spot of 50 μm the intensity ranged between $2*10^{12}$ and $5*10^{12}$ W.cm^{-2}. Furthermore, the FWHM bandwidth of the photon energy was approximately 0.4 eV.

In order to investigate the dependence of the asymmetry parameters on the intensity, we divided the raw VMI images according to FEL pulse energy into 5 equal intervals ranging from the lowest 20% to the highest 20%. A representative angular distribution is shown in Figure 1 (right) together with the fitted curves (red lines) and the extracted anisotropy parameters. The full results for all 5 FLASH energy bins will be presented.

References

[1] V. Richardson *et al.*, *Phys. Rev. Lett.*, **105** (2010)
[2] M. Meyer *et al.*, *Phys. Rev. Lett.*, **104** (2010)
[3] R. Moshammer *et al.*, *Phys. Rev. Lett.*, **98** (2007)
[4] M. Braune *et al.*, *J. Mod. Opt.*, **1**, pp 1–10 (2015)
[5] W. Ackermann *et al.*, *Nat. Photon.* **1** pp336–342 (2007)

LIBS for thin films depth profiling- A comparison of Time Integrated and Time resolved methods

Syedah Sadaf Zehra [a], Muhammad Bilal Alli [a], Piergiorgio Nicolosi[b], John Costello[a], Paddy Hayden[a]

[a] *Dublin City University, Dublin 9 (syedah.zehra2@mail.dcu.ie)*
[b] *University of Padova,Italy .*

Laser Induced Breakdown Spectroscopy (LIBS) is an analytical technique used to classify and potentially quantify elements in complex hosts (or matrices). Vacuum Ultraviolet Laser Induced breakdown Spectroscopy (VUV LIBS) [1, 2] can offer potential improvements over traditional LIBS [3, 4] in the visible region, due to the abundance of resonance transitions at these shorter wavelengths. This extends the ability to discriminate between the emissions from different elements, particularly light elements such as carbon, sulfur, lithium, and beryllium etc. In this study, silicon based aluminium thin films are developed to study the depth profile and ablation rate of the material in time integrated and time resolved domain at two different laser energies. Time resolved LIBS (50 ns delay and 130 ns width) is used to record spectra for the higher power density (1.3×10^{10} Wcm^{-2}) to prevent saturation whereas Time integrated LIBS is used to record spectra for the lower power density (1.6×10^{9} Wcm^{-2}).5 films with different thicknesses from 1 mm to 1.5 micron are used in both methods. The experimental setup consists of single pulse system with Nd:YAG laser (1064 nm, up to 450 mJ, pulse duration 6 ns) used to irradiate the samples, optic fiber spectrometer is used to detect the spectrum. The results show higher ablation rate for time resolved method in comparison to time-integrated method.

References

[1] X. Jiang, et al., Spectrochim. Acta B **86** (2013) 66
[2] X. Jiang, et al., Spectrochim. Acta B **101** (2014) 106
[3] D. A. Cremers, and L. Radziemski *Handbook of Laser-Induced Breakdown Spectroscopy* Wiley (2006)
[4] R. Noll, *Laser Induced Breakdown Spectroscopy Fundamentals and Applications* Springer (2012)
[5] L. Dudragne, Ph. Adam, J. Amouroux, Appl. Spectrosc. **52** (1998) 132

Doppler Profile Diagnostics On VUV Spectra For Emission Intensity, Ion Temperature And Flow Velocity Of Impurity Ions In Edge Plasmas Of Large Helical Device

Tetsutarou Oishi[a,b], Shigeru Morita[a,b], Yang Liu[b], Motoshi Goto[a,b] and the LHD Experiment Group[a]

[a]*National Institute for Fusion Science, National Institutes of Natural Sciences, 322-6, Oroshi-cho, Toki, Gifu 509-5292, Japan, oishi@nifs.ac.jp*
[b]*Department of Fusion Science, SOKENDAI (Graduate University for Advanced Studies), 322-6, Oroshi-cho, Toki, Gifu 509-5292, Japan*

In the study of the impurity behavior in the edge region of magnetically-confined torus plasmas for fusion research, the vacuum ultraviolet (VUV) line of impurity ions is attractive for the impurity diagnostics because the emission from the correct charge states is located in the edge plasmas with a considerably low electron temperature. Therefore, VUV spectroscopy plays a significant role in investigating the impurity behavior and the impurity transport. The impurity species and its concentration can be examined through the identification of impurity lines and the line intensity, respectively. In addition, the spectral shape of impurity lines can also provide information on the ion temperature and the plasma flow based on Doppler-broadening and Doppler-shift measurements, respectively. The VUV spectroscopy with high spatial and spectral resolutions is thus required to observe the spatial distribution of spectral intensity and the shape of impurity lines.

Space-resolved VUV spectroscopy using a 3 m normal incidence spectrometer has been developed to measure the radial distribution of VUV lines in wavelength range of 300 - 3200 Å in the edge plasmas of the Large Helical Device (LHD) of which the major/minor radii are 3.6/0.64 m in the standard configuration with maximum plasma volume of 30 m^3 and toroidal magnetic field of 3 T [1,2]. The high spectral resolution of the spectroscopic system with the wavelength dispersion of 0.037 Å/CCD-pixel enables us to measure the Doppler profiles of impurity line spectra precisely. The edge plasma of LHD consists of stochastic magnetic fields with three-dimensional structure intrinsically formed by helical coils called “ergodic layer,” while well-defined magnetic surfaces exist inside the last closed flux surface. The VUV spectroscopy is appropriate for the edge impurity study because the emissions are only located inside the ergodic layer with electron temperatures distributing in ranges of 10 to 500 eV.

In this paper, observations of the emission intensity, the ion temperature, the impurity ion flow, and their vertical profiles derived by measuring the Doppler profile of impurity line spectra are summarized and its dependence on the experimental parameters, such as the electron density, position of the magnetic axis, and direction of the toroidal field, is discussed. The main target of the analysis is the second order of CIV 1548.20 Å (2s-2p) line emission from intrinsic carbon impurity ions sputtered from the carbon divertor plates, which are the most abundant impurity in LHD.

References

[1] Oishi T, Morita S, Dong C F *et al.* 2014 *App. Opt.* **53** 6900.
[2] Oishi T, Morita S, Dai S Y *et al.* 2018 *Nucl. Fusion* **58** 016040.

Effect of the macro bending and the signal line shapes on the spectral performance of fiber Bragg grating

Roston[1] G D, Mahran[1] O , Ellsaid[2] N and Nagham[2]
1 Physics Department, Faculty of Science, Alexandria University , Egypt
dr.gamal_daniel@yahoo.com
2 Physics Department, Faculty of Education, Alexandria University , Egypt

Abstract

This research is a theoretical study in the effect of macro bending and the signal line shapes on the spectral performance of fiber Bragg grating (FBG). Firstly, the effect of the bend radius and the signal wavelength in the bend loss were studied. Firstly, for the sine signal profile, the reflectivity power in the case normal case gives a peak at the FBG wavelength λ=155 μm, Secondly, for the Gaussian signal profile, the reflectivity powers are the same for both cases. It is found that the reflected power for Sine profile has a higher value than the of Gaussian profile under the same conditions and the bending of fiber will act to decrease the reflected power.

Results

Fig. (1,2) shows the effect of the signal wavelength and FBG length on the reflectivity power of the fiber Bragg grating at signal profiles (sine and Gaussian) for normal and macro binding cases

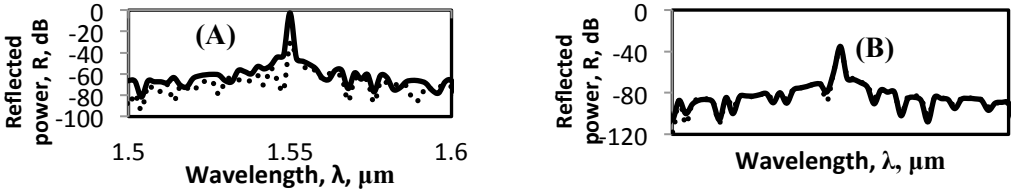

Fig. 1. (A) The reflectivity power of FBG for the sine **(A)** and Gaussian **(B)** profiles versus the wavelength of the signal at FBG length (L = 10) for the normal case (line) and macro bending(dishes)

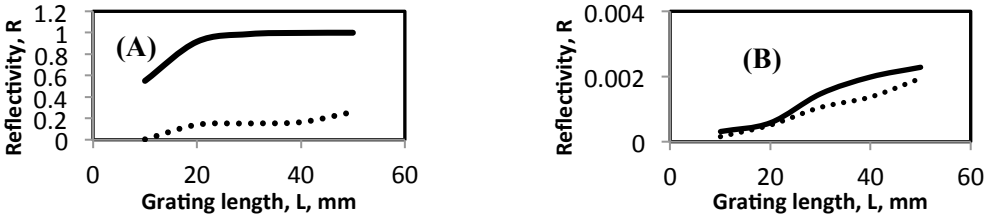

Fig. 2 The reflectivity with the length of the FBG in cases of normal (line) and macro bending (dishes) for sine (A) and Gaussian (B) profiles, at λ = 1550 nm and radius of the macro bending 3 mm **.**

REFERENCES

[1] Tawfik, N. I., Eldeeb, W. S., Mashade, M. B., & Abdelnaiem, A. E. Optimization of Uniform Fiber Bragg Grating Reflection Spectra for Maximum Reflectivity and Narrow Bandwidth. International Journal of Computational Engineering Research (IJCER), ISSN (e), 2250-3005

[2]Senior,John M.,and M. Yousif Jamro.(2009). Optical fiber communications: principles and practice.

[3] Lee, B. 2003. Review of the present status of optical fiber sensors. Optical fiber technology, 9, 57.

[4] Potyrailo, Radislav A., Steven E. Hobbs, and Gary M. Hieftje. Optical waveguide sensors in analytical chemistry: today's instrumentation, applications and trends for future development. Fresenius' journal of analytical chemistry 362.4 (1998): 349-373.

[5] Khalid, K. S., Zafrullah, M., Bilal, S. M., & Mirza, M. A. (2012). Simulation and analysis of Gaussian apodized fiber Bragg grating strain sensor. Journal of Optical Technology, 79(10), 667-673.

[6] Marcuse, D. (1976). Curvature loss formula for optical fibers. JOSA, 66(3), 216-220.

[7] Harris, A., & Castle, P. (1986). Bend loss measurements on high numerical aperture single-mode fibers as a function of wavelength and bend radius. Journal of Light wave technology, 4(1), 34-40.

[8] Lim, K. S., Yang, H. Z., Becir, A., Lai, M. H., Ali, M. M., Qiao, X., & Ahmad, H. (2013). Spectral analysis of bent fiber Bragg gratings: theory and experiment. Optics letters, 38(21), 4409-4412.

[9] Wade, S. A., Robertson, D. F., Thompson, A. C., & Stoddart, P. R. (2011). Changes in spectral properties of fiber Bragg gratings owing to bending. Electronics Letters, 47(9), 558-559.

[10] Lam, D. K. W., & Garside, B. K. (1981). Characterization of single-mode optical fiber filters. Applied Optics, 20(3), 440-445.

Spatial Characterization of Plasma Parameters inside Ablation Clouds in LHD

G. Seguineaud[a] and M. Goto[b]

[a]*Department of Fusion Science, Sokendai, Toki 509-5292, Japan (email: guillaume.seguineaud@nifs.ac.jp)*
[b]*National Institute for Fusion Science, Toki 509-5292, Japan*

Low-*n* Balmer series spectra emitted from slices of hydrogen ablation clouds are recorded using a spectrometer that has a vertical band-shaped line-of-sight. A spectral model that combines isolated emission lines and continuum radiations is used to fit the spectra in an attempt to extract the plasma parameters inside the ablation cloud.

The principal source of line broadening is found to be the Stark broadening while the Doppler broadening, Zeeman splittings and instrumental broadening are negligibly small. The line intensity ratios are calculated with the collisional-radiative model implying that the present model assumes no LTE condition. This is distinctive from the previous analysis [1] because, following the results in Ref. [2], the complete LTE assumption has been suspected to be incorrect in the edge region of the ablation cloud. Contributions of continuum radiation mainly come from the recombination and attachment processes [1]. The least squares fitting method is conducted on the experimental data in the wavelength range approximately from 400 nm to 550 nm where initial parameters are taken from the previous study [1].

Figure 1 shows the one-dimensional distributions of the electron density n_e and the electron temperature T_e along the axis of the ablation cloud elongation. The order of magnitude for both parameters is in agreement with those derived in the previous studies [1, 2] and they now show profiles consistent with our understanding of the ablation cloud structure.

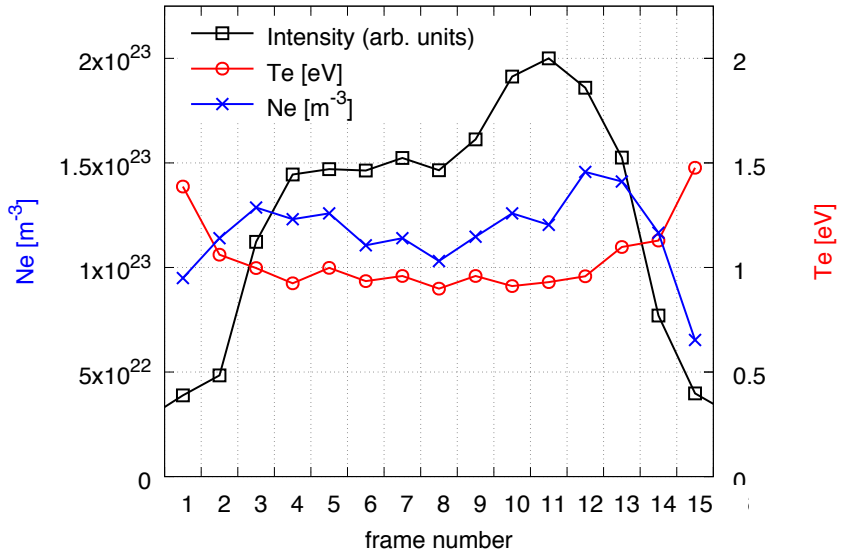

Figure 1. Spatial profiles of n_e (crosses) and T_e (circles) along the ablation cloud elongation axis obtained by the spectra fittings. The intensity summed up in the wavelength range used for the fitting is also shown by squares.

References

[1] Goto M *et al.* 2007 *Plasma Phys. Control. Fusion* **49** 1163
[2] Motojima G *et al.* 2012 *Rev. Sci. Instrum.* **83** 093506

Line Selection For Nuclear Debris Analysis In Laser-Induced Plasmas

Michael B Shattan[a,b], Christian G Parigger[c]

[a]*Department of Engineering Physics, The Air Force Institute of Technology, Wright Patterson Air Force Base, Ohio, 45433, USA*
[b]*Department of Nuclear Engineering, The University of Tennessee, Knoxville, Tennessee 37996, USA*
[c]*Department of Physics and Astronomy, University of Tennessee, University of Tennessee Space Institute, Center for Laser Applications, Tullahoma, Tennessee 37388, USA*
e-mail: cparigge@tennessee.edu

This work identifies analytical lines in laser-induced plasma for chemical analyses of major elements of interest found in surrogate nuclear debris. The line selection focuses on potential interferences and signal strength to insure they would be useful to measure relative concentrations, even in areas of the substrate with diminished presence of the analyte. Compact, portable instruments were used that can be included as part of a mobile nuclear forensics laboratory for field screening of nuclear debris and contamination [1].

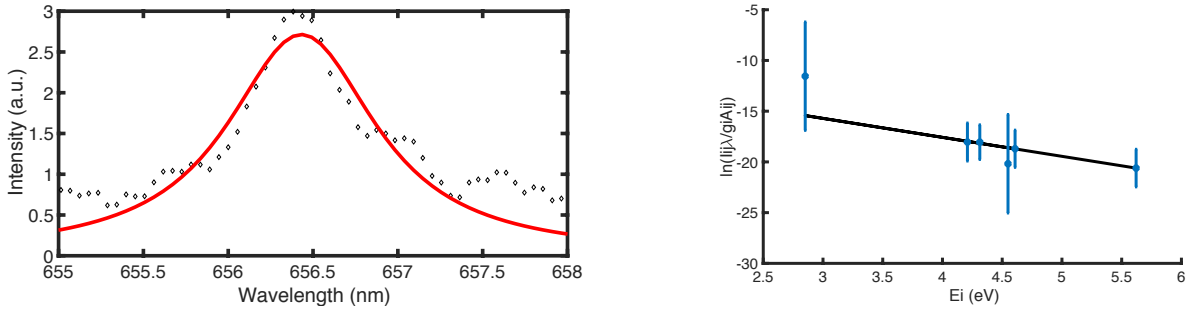

Figure 1. Hydrogen alpha line (left) and Boltzmann plot (right) used for electron density and temperature determinations, respectively

The average plasma temperature is inferred using the well-established Boltzmann plot technique [2], and the plasma's average electron density is determined using empirical formulae based on Stark broadening of the H-alpha line [3]. The measurements pose challenges given the complexity of the sample matrix, the laser device parameters of 50-mJ energy per 6-ns pulse at 266-nm excitation wavelength, and spectrometer resolving power or ratio of measurement wavelength and spectral resolution, $\lambda/\delta\lambda$, of 4000. Nonetheless, the average temperature for a temporal window of 2 to 12 μs after initiation of ablation is 6200 ± 800 K, and the electron density amounts to $0.76 \pm 0.1 \times 10^{17}$ cm^{-3}. The line-of-sight measurements suggest validity of partial local thermodynamic equilibrium. Therefore, quantitative measurements may be justified for the experimental arrangement and sample matrix.

References

[1] Shattan MB, Miller DJ, Cook MT, Stowe AC, Auxier JD, Parigger CG, Hall HL 2017 *Appl. Opt.* **56** 9868.
[2] Zhang S, Wang X, He M, Jiang Y, Zhang B, Hang W, Huang B 2014 *Spectrochim. Acta Part B: At. Spectrosc.* **97** 13.
[3] Surmick DM, Parigger CG 2014 *Int. Rev. At. Mol. Phys.* **5** 73.

Titanium Monoxide Diagnostic Of Pulsed Ablation

Todd A Van Woerkom[a], Glen P Perram[a], Christian G Parigger[b]

[a]*Air Force Institute of Technology, Department of Engineering Physics, 2950 Hobson Way, Wright-Patterson AFB, OH 45433, U.S.A.*
[b]*University of Tennessee, University of Tennessee Space Institute, Center for Laser Applications, 411 B.H. Goethert Parkway, Tullahoma, TN 37355, U.S.A.*
e-mail: cparigge@tennessee.edu

This work presents pulsed laser-ablation characterization using diatomic titanium-monoxide emission spectroscopy. An Er:YAG laser operated at the wavelength, λ, of 2.94 μm generates 50 μs pulses with an energy up to 1 J per pulse at a repetition rate of 10 Hz. A 100 mm CaF_2 lens focuses the radiation from the laser device to a spot size of typically 300 μm on a titanium wafer sample in air at standard ambient temperature and pressure. The optical spectrometer, model Ocean Optics HR4000 Custom, records data at a resolving power of the order of 600 for the reported line-of-sight overview spectra. Figure 1 illustrates the experimental arrangement and appearances of typical titanium monoxide (TiO) bands from primarily three electronic transitions.

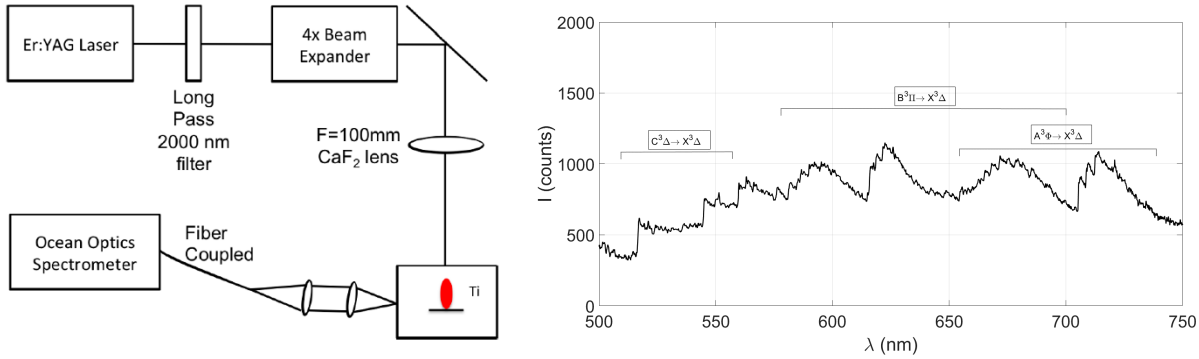

Figure 1. Experimental arrangement (left), and TiO bands of primarily C – X α, B – X γ', and A – X γ (right)

A 4 × beam expander enlarges the beam diameter of the radiation from the Er:YAG device, and the positioning of the focusing lens achieves a spot size of 307 ± 23 μm. Collection optics and an optical fiber relay the emitted light to the compact spectrometer. The recorded titanium monoxide (TiO) spectra in the wavelength range of 500 nm to 750 nm include primarily the C $^3\Delta$ – X $^3\Delta$ α, B $^3\Pi$ – X $^3\Delta$ γ', and A $^3\Phi$ – X $^3\Delta$ γ bands [1, 2]. The analysis utilizes line strength data [3] for fitting of measured and computed TiO bands. The work also discusses reaction kinetics and plume phenomena.

References

[1] Davis SP, Littleton JE, Phillips JG 1986 *Astrophys. J.* **309** 449.
[2] Parigger CG, Woods AC 2012 *Am. Inst. Phys. (AIP) Conf. Proc.* **1464** 628.
[3] Parigger CG, Woods AC, Surmick DM, Gautam G, Witte MJ, Hornkohl JO 2015 *Spectrochim. Acta Part B: At. Spectrosc.* **107** 132.

Modeling of line and continuum spectral emission of hydrogen for recombining plasma conditions

R.R. Sheeba, M. Koubiti, S. Ferri, Y. Marandet, T. Qbaich, J. Rosato, R. Stamm

Aix Marseille Univ, CNRS, PIIM, Marseille, France; e-mail: roshin-raj.sheeba@univ-amu.fr

The magnetic fusion community must tackle the major challenges facing it in order to ensure the success of future fusion-based power-plants. One of them concerns the exhaust of power, i.e., the handling of the huge heat and particle loads which escape from the confined plasma and hit the plasma facing components (PFCs). To avoid any damage, the power load should not exceed 20 MW/m^2 even for the most advanced materials. The most promising scenario to fulfill this requirement is the creation of a radiative mantle in the divertor region leading to the plasma detachment thanks to volume recombination. Therefore, a big effort is being devoted to the study of plasma detachment in both L- and H-modes especially in the framework of EUROfusion MST1 [1] and JET1 workplans [2] as this scenario is foreseen for future large scale fusion devices like ITER. Impurities like nitrogen, neon or other noble gases are injected to reach plasma detachment. In support of such studies, we propose the modelling of line and continuum emission of hydrogen for conditions relevant to detached plasma divertors in the aim of their characterization, i.e, providing their main plasma parameters (n_e, T_e and T_i).

In fact, under detachment conditions (n_e~10^{20}-10^{21} m^{-3}, T_e~1 eV) hydrogen spectra consisting of discrete *high-n* lines of the Balmer series and continuum emission can be observed. Due to a density effect, the continuum is shifted towards higher wavelengths $\lambda_c > \lambda_B^{lim}$, where λ_B^{lim} =364 nm is the theoretical Balmer series limit of hydrogen [3]. Under such conditions, *high-n* Balmer lines are mainly broadened by Stark effect with a significant contribution from Zeeman effect for the lowest values of *n* depending on the B-field value. Such lines are useful to infer the electron density of divertor plasmas along each viewing spectroscopic chord. The electron temperature can be inferred from the Boltzmann plot assuming a statistical equilibrium of the atomic populations over the excited levels but also from the slope of the continuum. For that purpose, the discrete to continuum radiation transition will be modeled using a dissolution factor approach [4] which leads to a smooth merging of the lines into the continuum and resulting eventually in the lowering of the continuum below the theoretical limit λ_B^{lim}. When possible, modeling results will be confronted to experimental data.

References

[1] Meyer H et al. 2017 Nucl. Fusion, **57,** 102014
[2] Litaudon X et al. 2017 Nucl. Fusion, **57,** 102001
[3] M. Koubiti et al. 2003 JQSRT, **81** 265.
[4] Pigarov A Yu et al. Plasma Phys. Control. Fusion **40**, 2055 (1998)

Analytical Extension Of Hard-Collision Model Of Velocity-Changing Collisions In The Hartmann-Tran Profile

M. Konefał[a,b,c], M. Słowiński[a*], M. Zaborowski[a], D. Lisak[a], P. Wcisło[a]

[a]*Institute of Physics, Faculty of Physics, Astronomy and Informatics, Nicolaus Copernicus University in Toruń, Grudziadzka 5, 87-100 Torun, Poland*
[b]*University of Grenoble Alpes, LIPhy, F-38000 Grenoble, France*
[c]*CNRS, LIPhy, F-38000 Grenoble, France*
[*]*suowik@fizyka.umk.pl*

Recently recommended line-shape profile - the Hartmann-Tran profile (HTP) [1] includes all significant effects used in line-shape modelling nowadays [2]. Nevertheless, it gives unsatisfactory results in the analysis of high-resolution spectra with a prominent effect of the Dicke narrowing [3], such as molecular hydrogen. Wcisło et al. [3] proposed a correction to the frequency of the velocity-changing collisions parameter in HTP corresponding to the Dicke narrowing effect. Although the correction works, it was applicable to the absorber to perturber mass ratio equals 1 and has efficiency only for the high ratio of frequency of velocity-changing collisions to the Doppler half width.

We propose the extension to this correction, making it useful not only in some specific cases, but for most of atmospheric and planetary spectroscopic applications. The correction enables to reproduce the molecular spectra with the percentage agreement to the more physically justified, but numerically complicated Speed Dependent Billiard Ball line-shape profile originated in the transport-relaxation equation [4] as shown in Figure 1.

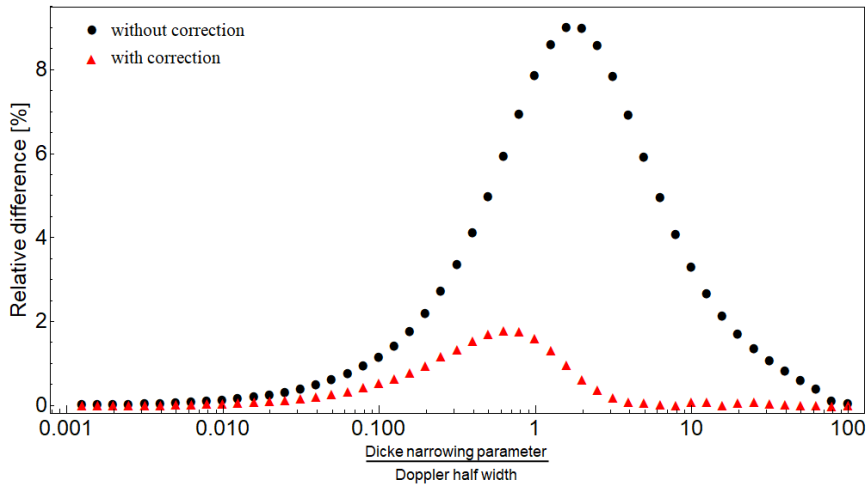

Figure 1. The relative difference between HTP without and with applied correction and the more advanced line-shape profile [3], dots and triangles respectively.

References

[1] NH Ngo et al 2013 *J. Quant. Spectrosc. Radiat. Transf.* **129** 89-100
[2] J Tennyson et al 2014 *Pure Appl. Chem.* **86** 1931-1943
[3] P Wcisło et al 2016 *J. Quant. Spectrosc. Radiat. Transf.* **177** 75-91
[4] R Ciuryło et al 2002 *Phys. Rev. A* **65** 012502

Atom-Rydberg Atom Collisions In Hydrogen Plasmas: Cross Sections And Rate Coefficients

V. A. Srećković[a], M. S. Dimitrijević[b,c], Lj. M. Ignjatović[a], N. N. Bezuglov[d] and A. N. Klyucharev[d]

[a] *Institute of physics, University of Belgrade, P.O. Box 57 11001, Belgrade, Serbia, vlada@ipb.ac.rs*
[b] *Astronomical Observatory, Volgina 7 11060, Belgrade 74, Serbia, mdimitrijevic@aob.rs*
[c] *LERMA (Laboratoire d'Etudes du Rayonnement et de la Matière en Astrophysique et Atmosphères), Observatoire de Paris, PSL Research University, CNRS, Sorbonne Universities, UPMC Univ., Paris 06, 5 Place Jules Janssen, 92195 Meudon Cedex, France.*
[d] *Saint Petersburg State University, St. Petersburg State University, 7/9 Universitetskaya nab., St. Petersburg 199034 Russia*

In order to improve the modeling of the solar photosphere, as well as to model atmospheres of other similar and cooler stars where the main constituent is also hydrogen, it is necessary to take into account the influence of all the relevant collisional processes on the excited-atom populations in weakly ionized hydrogen plasmas.

The ionization processes in atom-Rydberg atom collisions are investigated in this contribution. The method [1,2] is applied to the cases of H collisions for the principal quantum numbers $2 \leq n \leq 20$ and temperatures 4 000 K $\leq T \leq$ 20 000 K. The ionization processes in collisions of excited hydrogen atoms with atoms in ground states were considered, with a particular accent to the applications for astrophysical and laboratory hydrogen plasma research and its non-local thermodynamic equilibrium modeling [3,4].

In this work we:

- Present the results of calculation of the cross sections and rate coefficients of the corresponding ionization processes in the tabulated form easy for further use;
- Review the existing relevant literature;
- Present some examples of astrophysical importance.

The authors are thankful to the Ministry of Education, Science and Technological Development of the Republic of Serbia for the support of this work within the projects 176002 and III44002.

References

[1] Mihajlov A.A, Ignjatović Lj.M, Srećković V.A and Dimitrijević M.S. 2011 *The Astrophysical Journal Supplement Series,* **193,** 2(7pp).
[2] Mihajlov A.A, Ignjatović Lj.M, Srećković V.A. and Dimitrijević M.S 2011 *Open Astronomy,* **20,** 566-571.
[3] Mihajlov A.A., Srećković V.A., Ignjatović Lj.M., Simić, Z., & Dimitrijević M.S., *J. Phys.:Conf. Series* 2017 **810**(1), 012058.
[4] Gnedin Yu.N., Mihajlov A.A., Ignjatovic Lj.M., Sakan N.M., Sreckovic V.A., Zakharov M.Yu., Bezuglov N. N. and Klycharev A. N. 2009 *New Astron. Rev.* **53**, 259.

The *Ab Initio* Calculations Of The Line-Shape Parameters For The CO-N_2 Complex

H. Cybulski[a], H. Jóźwiak[a], N. Stolarczyk[a*], P. Wcisło[a], F. Thibault[b]

[a] *Institute of Physics, Faculty of Physics, Astronomy and Informatics, Nicolaus Copernicus University, Grudziadzka 5, 87-100 Torun, Poland (*Corresponding author: 280301@stud.umk.pl)*
[b] *Institut de Physique de Rennes, UMR CNRS 6251, Université de Rennes 1, Campus de Beaulieu, Bât. 11B, Rennes F-35042, France*

Collisional line-shape effects play an important role in optical spectroscopy. Molecular collisions manifest as a perturbation of the optical line shapes. Proper treatment of these effects is important to reach high accuracy in spectroscopy-based optical metrology [1,2]. The CO-N_2 system is of particular importance for terrestrial atmospheric measurements. Here we report the first line-shape calculations for this system based on quantum scattering theory and using an accurate *ab initio* potential energy surface (PES).

A four-dimensional PES, with the interatomic distances in N_2 and CO set to the experimental values (1.09768 and 1.128323 Å, respectively [3]) is used [4]. The interaction energies are calculated with the coupled-cluster CCSD(T) method and Dunning's aug-cc-pVQZ basis set extended further with midbond functions for more than 10 100 *ab initio* points, corresponding to 12 values of θ_{N2}, 13 values of θ_{CO} in range 0-180°, 5 values of φ in range 0-90° and 14 values of R in range 4-40 a_0.

The calculated PES is expanded over bispherical harmonics [5] leading to 206 radial coupling terms. The close-coupling equations are solved for a wide range of kinetic energies using the MOLSCAT code [6]. The calculations of generalized spectroscopic cross sections are performed for several purely rotational lines from R branch (from j = 0 up to 7). Finally, the standard pressure broadening and shifting coefficients are obtained. The data provided through this investigation can be used for upgrading the HITRAN database [7] and the HITRAN Application Programming Interface (HAPI) [8].

References

[1] Moretti L et al. 2013, Phys. Rev. Lett. **111**, 060803.
[2] Wcisło P et al. 2016, Phys. Rev. A **93**, 022501.
[3] Huber K P and Herzberg G, "*Molecular Spectra and Molecular Structure: IV Constants of Diatomic Molecules*", Springer Berlin Heidelberg, 1979.
[4] Cybulski H et al., Phys. Chem. Chem. Phys., submitted
[5] Hutson J M and Green S, MOLSCAT version 14, Collaborative Computational Project 6 of the UK Science and Engineering Research Council, Daresbury Laboratory, UK, 1995
[6] Green S 1979, J. Chem Phys. **62**, 2271.
[7] Gordon I E et al. 2017, J Quant. Spectrosc. Radiat. Transf. **203**, 3
[8] Kochanov R V et al. 2016, J Quant. Spectrosc. Radiat. Transf. **177**, 15

Line-Shape Parameters For Pure Rotational Raman Lines Of D_2 In He

Raúl Z. Martínez[a], Dionisio Bermejo[a], Franck Thibault[b], Piotr Wcisło[c]

[a]*Instituto de Estructura de la Materia, IEM-CSIC, Serrano, 123, 28006, Madrid, Spain*
[b]*Institut de Physique de Rennes, UMR CNRS 6251, Université de Rennes1, Campus de Beaulieu, Bât.11B, F-35042 Rennes, France (Franck.Thibault@univ-rennes1.fr)*
[c]*Institute of Physics, Faculty of Physics, Astronomy and Informatics, Nicolaus Copernicus University, Grudziadzka 5, 87-100 Torun, Poland*

We present a comparison between experimental and calculated values for the collisional line broadenings and shifts of the $S_0(0)$, $S_0(1)$ and $S_0(2)$ lines of the rotational Raman spectrum of D_2 in helium baths at 77, 195 and 300 K [1]. These Stokes lines were obtained by means of a stimulated Raman spectroscopy (SRS) experimental setup. Close coupling dynamical calculations were performed on the most recent ab initio H_2-He potential energy surface [2]. The resulting scattering matrix elements implemented in the general Hess method [3-5] allow us to provide pressure -broadening, -shifting and Dicke coefficients from 10 K to 400 K. When comparable, experimental and calculated values show good agreement.

Our analysis of the experimental profiles supported by our calculations take into account effects originating from the internal changes and effects due to the velocity changing collisions through the speed dependence of the pressure –broadening and –shifting parameters as well as the real and imaginary parts of the Dicke parameters.

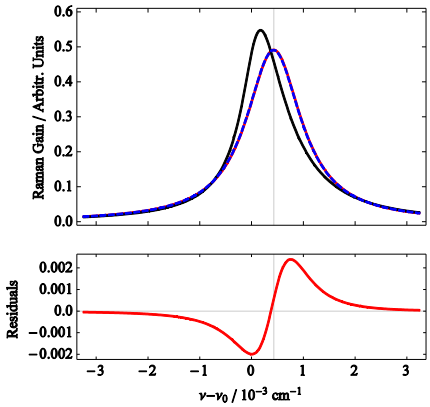

Figure 1. Simulations of the D_2 $S_0(0)$ line at 77 K and 1 atm. The red solid line is the simple Lorentz Profile shifted by δ_0 and whose HWHM is γ_0. The black solid line is the weighted sum of Lorentzians. The dashed blue line is the Speed-Dependent Hard-Collision Profile. The bottom panel shows the difference between the SDHCP and LP. Thus the Doppler width and the speed-dependent effects are almost completely killed and the profile converges to a simple Lorentz profile. At lower pressures considered in this study the shape is still Lorentzian, but its width has to be corrected for the residual Dicke-narrowed Doppler component.

References

[1] Martínez R.Z., Bermejo D., Thibault F., Wcisło P., 2018 *J. Raman Spectrosc.*, in press
[2] Thibault F., Patkowski K, Żuchowski P.S., Jóźwiak H., Ciuryło R., Wcisło P., 2017 *J. Quant. Radiat. Transfer*, **202**, 308-320.
[3] Hess S., 1972 *Physica*; **61**, 80.
[4] Corey G.C., McCourt F.R.W., 1984 *J. Chem. Phys.*, **81**, 2318.
[5] Monchick L., Hunter L.W., 1986 *J. Chem. Phys.*, **85**, 713.

H_2, He and CO_2 line-broadening coefficients for molecules in the HITRAN database. Part II: H_2CO, HCN, CO_2, H_2S, N_2O

Yan Tan[a], Shanelle Samuels[b], I.E. Gordon[a], R.V. Kochanov[a,c], L.S. Rothman[a]

[a]*Harvard-Smithsonian Center for Astrophysics, Atomic and Molecular Physics Division, Cambridge MA, USA, Email: yan.tan@cfa.harvard.edu*
[b]*University of Massachusetts Lowell, MA, USA*
[c] *Tomsk State University, Laboratory of Quantum Mechanics of Molecules and Radiative Processes, Tomsk, RUSSIA.*

The new HITRAN molecular absorption compilation has been released[1] and the broadening and shift parameters due to the perturbing gases such as H_2, He and CO_2 have been added into the database for the first time, see Wilzewski et al.[2]. In order to increase the potential for the database to model the spectra of atmospheres dominated by gases different from nitrogen and oxygen, especially in planets beyond the earth like Venus and Mars[3], [4] and gas giants, the previous work accomplished by Wilzewski et al.[2], which includes molecules for SO_2, NH_3, HF, HCl, OCS and C_2H_2, needed to be expanded further. In this work, the line-shape parameters for the line-broadening coefficients and the temperature dependence exponents for molecules including CO_2, N_2O, H_2CO, HCN and H_2S broadened by H_2, He, and CO_2 have been assembled from available peer-reviewed experimental and theoretical results. A set of semi-empirical models was developed based on the collected data, and then has been populated into the database so that every HITRAN line of the studied molecules has its corresponding parameters as well as its uncertainties and source information.

This work is supported by NASA PDART program grant and *NNX16AG51G.*

References

[1] I. E. Gordon *et al.*, "The HITRAN2016 molecular spectroscopic database," *J. Quant. Spectrosc. Radiat. Transf.*, vol. 203, pp. 3–69, Dec. 2017.

[2] J. S. Wilzewski, I. E. Gordon, R. V. Kochanov, C. Hill, and L. S. Rothman, "H_2, He, and CO_2 line-broadening coefficients, pressure shifts and temperature-dependence exponents for the HITRAN database. Part 1: SO_2, NH_3, HF, HCl, OCS and C_2H_2," *J. Quant. Spectrosc. Radiat. Transf.*, vol. 168, pp. 193–206, Jan. 2016.

[3] "Exploration of Venus [Special Issue]," *Planet. Space Sci.*, vol. 113–114, pp. 1–394, 2015.

[4] "Dynamic Mars [Special Issue]," *Icarus*, vol. 251, no. 1–338, 2015.

Studies of Thallium Line Spectra in Thallium – Mercury Discharge

Gita Revalde[a], Atis Skudra[b], Natalja Zorina[b], Anda Abola[b]

[a] *Institute of Technical Physics, Department of Materials Sciences and Applied Chemistry, Riga Technical University, Azenes str. 3/7, Riga, Latvia, e-mail: gitar@latnet.lv*
[b] *Institute of Atomic Physics and Spectroscopy, University of Latvia, Skunu str 4, Riga, LV 1050, Latvia.*

In this work, thallium and mercury discharge is studied. In our precious work we have observed extraordinary broadening above Doppler broadening for some spectral lines of thallium, for example 351.9 nm line [1]. We supposed that the additional broadening could be due to energy transfer in collisions of mercury and thallium atoms.

In this paper, we present further study of broadening of thallium emission spectral line shapes in the Tl-Hg discharge. The spectral lines were emitted from high frequency electrodeless lamps (HFEDLs) containing Tl, Hg, Ar mixtures and measured by means of Fourier transform spectrometer. The deconvolution procedure, by means of ill posed inverse task solution [2] was performed to obtain the real (without instrumental function) profiles for further analyze. The solution was implemented using Tikhonov regularization algorithm. The Tl 276.8 nm, 291.8nm, 292.1nm, 323.0 nm spectral lines were analyzed in detail in dependence on the discharge power. An example of spectral line deconvolution is given in Fig.1. For accuracy increasing the regularization parameter was obtained by two independent methods.

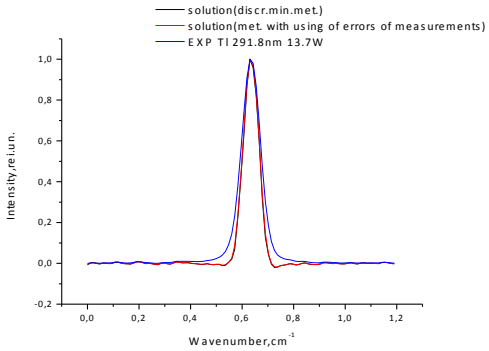

Figure 1. The comparison of 291.8nm ofTl^{205} experimental spectral line with deconvoluted ones.

Acknowledgements

The research was partly supported by project „Atomic physics, optical technology and medical physics (LU IAPS) ”

References

[1] A.Skudra, G.Revalde, A.Svagere, Z.Gavare, Studies of spectral line broadening in thallium containing high-frequency electrodeless lamps, ICSLS-21 International Conference on Spectral Line Shapes, Saint-Peterburg, Russia, June 3-9, 2012, p 94.

[2] N. Zorina, G. Revalde, R. Disch, Deconvolution of the mercury 253.7 nm spectral line shape for the use in absorption spectroscopy, AOMD-6 special issue of SPIE Proceedings, 2008,**7142**, 71420J-01- 71420J-09.

Validity Of Deconvolution Method For Multicomponent Spectral Line Shapes

Natalja Zorina[a], Gita Revalde [b], Atis Skudra[a],

[a] *Institute of Atomic Physics and Spectroscopy, University of Latvia, Skunu str 4, Riga, LV 1050, Latvia, e-mail: natalja.zorina@lu.lv*
[b] *Institute of Technical Physics, Department of Materials Sciences and Applied Chemistry, Riga Technical University, Azenes str. 3/7, Riga, Latvia*

The neglecting the instrumental function, in the case of low –pressure or cold plasma when instrument function is on the same order as experimental profile gives huge error [1] for the FWHM estimation and consequently for discharge temperature estimation. The instrumental function can conceal detailed structure of the spectral line, like the dip in the line centre caused by the self-absorption (self-reversal).

We present our study of deconvolution of multicomponent spectral line profiles in this paper. The study consists of deconvolution of theoretically modeled profiles as well as 323nm of Tl^{205} profiles, emitted from high frequency electrodeless lamps (HFEDLs). The solution of ill posed inverse task was implemented using Tikhonov regularization algorithm. The regularization parameter was obtained by two independent methods.

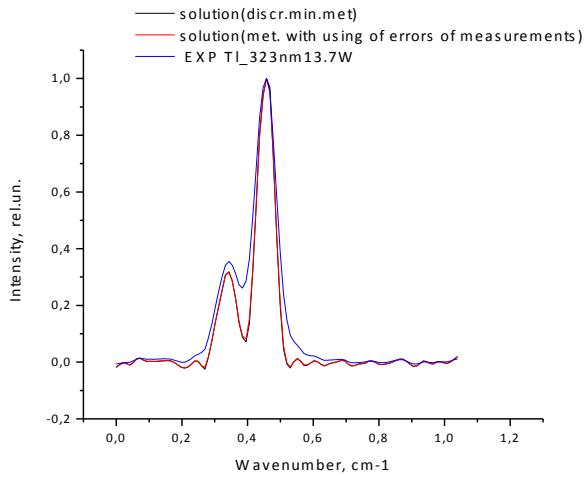

Figure 1. The comparison of 323nm ofTl^{205} experimental spectral line with deconvoluted ones .

Acknowledgements

The research was partly supported by project „Atomic physics, optical technology and medical physics (LU IAPS) ”

References

[1] N. Zorina, Deconvolution of the spectral line profiles for the plasma temperature estimation, Nuclear Inst. and Methods in Physics Research A,2010, **623** , 763-765

Choosing a Functional for Computing Absorption Transition Positions, Intensities and Shapes of Organic Semiconductors with TD-DFT

Muhammad Hassan Sayyad[a,*], Ramshah Ahmad Toor[a], Syed Afaq Ali Shah[a,] Nazia Nasr[a], Fatima Ijaz[b] and Munawar Ali Munawar[b]

[a]*Faculty of Engineering Sciences, Ghulam Ishaq Khan Institute of Engineering Sciences and Technology, Topi, District Swabi, Khyber Pakhtunkhwa 23640, Pakistan*
[b]*Institute of Chemistry, University of Punjab, Lahore 54000, Pakistan*

**Corresponding Author: hsayyad62@gmail.com, sayyad@giki.edu.pk*

The absorption maxima energy positions, intensities and shapes are simulated of the organic semiconductors with the simplified time dependent density functional theory (sTDDFT) at the B3LYP/TZP level of theory in gas phase. In the calculations carried out the ten lowest singlet-singlet excited transitions were taken into account. The optimized structure of the molecules and charge density distribution of their frontier orbitals are obtained. The computed absorption wavelengths (λ), absorption energy (E_g), oscillator strengths (f) and nature of the transitions are compared with the measured spectra. The computed absorption wavelengths and intensities of the conjugated molecules at the sTDDFT/B3LYP/TZP level of theory in gas phase are found in good agreement with the experiment.

Multi-photon Spectroscopy of Many-electron Atoms and Ions in the Debye Plasmas

Vasily V. Buyadzhi, Eugeny V. Ternovsky, Tatyana B. Tkach, Yuliya G. Chernyakova

Odessa State Environmental University, Lvovskaya str. 15, Odessa,65016, Ukraine
e-mail: buyadzhivv@gmail.com

The interaction of a high intensity laser field with an atomic system results in multi-photon excitation, ionization and shifts of the energy levels [1]. A great number of physically different effects occur in atomic systems (ensembles) in dependence upon a intensity, frequency, multi-colority of laser field, energy spectrum structure of an atomic system etc. In the last decade a considerable interest has attracted studying of the elementary atomic processes in plasma environments because of the plasma screening effect on the plasma-embedded atomic systems.

In this paper one-and two-color multi-photon spectroscopy of a number of transitions in a hydrogen, lithium, caesium and francium atoms and ions (free and immersed in a Debye plasmas) is studied theoretically. The theoretical approach is based on the relativistic operator perturbation theory (PT) and relativistic energy approach [2-4]. The energy shift and width of the multiphoton resonances are calculated within an energy approach, which is based on the Gell-Mann and Low adiabatic formalism and formalism of the relativistic Green function for the Dirac equation [3]. The plasmas medium effects are taken into account by introducing the Yukawa-type electron-nuclear attraction and electron-electron repulsion potentials into the electronic Hamiltonian for N-electron atom (ion) in a plasmas [5,6]. There is studied a plasmas with typical corresponding parameters: the Debye lengths λ_D=5a.u. (solar core: temperature T=10^7K; density 10^{32} m^{-3}) and 25 a.u. (inertial confinement: temperature T=10^4K; density 10^{28} m^{-3}) . It has been quantitatively determined a variation of the multi-photon resonance enhancement frequencies in dependence upon the plasmas parameters (the Debye length). For example, the corresponding values for the resonance enhancement frequencies ω_{r1}, ω_{r2} and ω_{r3} for the 1s–4f transition in the hydrogen for different Debye lengths (λ_D=5-50 a.u.) are between 0.009 and 0.023a.u. The obtained results reveal the plasma effects on the multi-photon transition amplitudes for the plasma-imbedded atoms (ions). The hydrogen plasma results are compared with the similar data, presented in [7].

References:

[1] Delone N B, Fedorov M V 1989 *Phys. Uspekhi*. **158** 215-248
[2] Glushkov A V, Ivanov L N 1992 *Phys.Lett.A*. **170** 33
[3] Glushkov A V, Ivanov L N 1993 *J. Phys. B: At. Mol. Opt. Phys*. **26** L379
[4] Glushkov A V 2012 *Progress in Theoretical Chemistry and Physics* (Springer) **26** 231-254
[5] Malinovskaya S V, Glushkov A V, Khetselius O Yu 2011 *Int.J.Quant.Chem*. **111** 288
[6] Buyadzhi V V 2013 Photoelectronics **21** 57
[7] Paul S and Ho Y K 2010 *J. Phys. B: At. Mol. Opt. Phys*. **43** 065701

Energy and Radiative Parameters and Spectral Line Shape for Hadronic Atomic Systems

Yuliya V. Dubrovskaya, Olga Yu. Khetselius, Larisa A. Vitavetskaya, Eugeny V. Ternovsky, Inga N. Serga

Odessa State Environmental University, Lvovskaya str. 15, Odessa, 65016, Ukraine
e-mail: ternovskyev@gmail.com

Sstudying the energy, spectral, radiation parameters, including the spectral lines hyperfine structure, for heavy exotic (hadronic, kaonic, pionic) atomic systems is of a great interest for the further development of a classical atomic and nuclear spectroscopy as quantum theory and spectroscopy of strongly interacted fermionic systems [1-6]. This paper is devoted to studying and computing the energy and radiative parameters, spectral line shape for hadronic (pionic) atomic systems. It has been applied a consistent relativistic theory of spectra of the exotic hadronic (pionic) atomic systems on the basis of the Klein-Gordon-Fock equation approach and relativistic many-body perturbation theory (electron subsystem) [6-10]. The key feature of the theory is simultaneous accounting for the electromagnetic and strong pion-nuclear interactions by means of using the generalized radiation and strong pion-nuclear optical potentials. The nuclear and radiative corrections are effectively taken into account. The modified Uehling-Serber approximation is used to take into account for the Lamb shift polarization part. In order to take into account the contribution of the lamb shift self-energy part we have used the generalized non-perturbative procedure, which generalizes the Mohr procedure and radiation model potential method by Flambaum-Ginges. There are presented data of calculation of the energy and spectral parameters for pionic atoms of the ^{93}Nb, ^{173}Yb, ^{181}Ta , ^{197}Au, with accounting for the radiation (vacuum polarization), nuclear (finite size of a nucleus) and the strong pion-nuclear interaction corrections. The measured values of the Berkley, Cern and Virginia laboratories and alternative data based on other versions of the Klein-Gordon-Fock theories with taking into account for a finite size of the nucleus in the model uniformly charged sphere and the standard Uehling-Serber radiation correction are listed too.

References

[1] Deloff A 2003 *Fundamentals in Hadronic Atom Theory* (Singapore, World Sci)
[2] Santos J, Parente F, Boucard S, Indelicato P and Desclaux J 2005 *Phys. Rev.A*. **71** 032501
[3] Taal A, David P , Hanscheid H, Koch J H, de Laat C T et al 1990 *Nucl.Phys.A*. **51**1 573
[4] de Laat C T, Taal A, Konijn J, et al 1991 *Nucl.Phys. A*. **523** 453
[5] Khetselius O Yu, Florko T A, Nikola L V et al 2010 *Quantum Theory: Reconsideration of Foundations* (AIP). **1232** 243
[6] Serga I N, Dubrovskaya Yu V, Kvasikova A S, Shakhman A N, Sukharev D E 2012 *J. Phys.: Conf. Ser.* **397** 012013
[7] Glushkov A V 2012 *Progress in Theoretical Chemistry and Physics* (Springer) **26** 231-252
[8] Khetselius O Yu 2009 *Phys. Scr.* **T13**5 014023
[9] Khetselius O Yu 2009 *Int. J. Quant.Chem*. **109** 3330
[10] Khetselius O Yu 2015 *Progress in Theoretical Chemistry and Physics* (Springer) **29** 54-76

Radiation Transition Probabilities for Heavy Rydberg Atoms within Advanced Relativistic Energy Approach

Valentin B. Ternovsky, Dmitry A Mironenko, Alexander V Glushkov, Eugeny V Ternovsky, Andrey A. Svinarenko

Odessa State Environmental University, Lvovskaya str. 15, Odessa,65016, Ukraine
e-mail: ternovskyvb@gmail.com

In this present work we present and advanced version of the relativistic energy approach [1] to computing the radiation transition probabilities (oscillator strengths) in spectra of heavy Rydberg neutral atoms and multicharged ions. The approach is based on the energy approach (S-matrix Gell-Mann and Low formalism) and relativistic many-body perturbation theory with optimized model potential zeroth approximation [1-6]. The key feature of the presented basis theory is an implementation of the optimized one-particle representation [6] into the frames of the S-matrix energy formalism. It provides a consistent method to minimization of the gauge-non-invariant contributions to the radiation transition (radiation decay width) probability and thus it makes our approach significantly more advantagable in comparison with standard methods to calculating radiative transition parameters. The important exchange-correlation effects are accounted with using relativistic Kohn-Sham –like density functionals.

We present the results of computing energies, radiation transition probabilities, oscillator strengths in spectra of the heavy Li-like multicharged ions (Z>55), neutral tantalum and thulium (in particular, transitions to the $4f^{13}_{7/2,5/2}6s_{1/2}[3/2]ns,np$ and $4f^{13}_{5/2}6s_{1/2}(2)nsp_{1/2}[3/2]$ states, n=15-40). We have compared the obtained results with the experimental results and other theoretical data, obtained on the basis of the Coulomb approximation with the Coulomb gauge of the photon propagator, the multiconfiguration Hartree-Fock and Dirac-Fock methods (see [6] and refs. therein). We have checked that the results for oscillator strengths, obtained within our approach in different photon propagator gauges (Coulomb, Babushkin, Landau), are practically equal (difference ~ 0.1-0.3%).

References

[1] Driker M, Ivanova E P, Ivanov L N, Shestakov A F 1982 *J.Quant.Spectr. Rad. Transf*er. **28** 531
[2] Ivanov L N and Letokhov V S 1985 *Com.Mod.Phys.D.:At.Mol.Phys*. **4** 169
[3] Glushkov A V, Ivanov L N 1992 *Phys.Lett.A*. **170** 33
[4] Ivanov L N, Ivanova E P and Knight L 1993 *Phys. Rev. A* **48** 4365
[5] Glushkov A V 2012 *Progress in Theoretical Chemistry and Physics* (Springer) **26** 231-252
[6] Svinarenko A, Ignatenko A, Ternovsky V etal 2014 *J. Phys: Conf. Ser.* **548** 012047

New Spectroscopy of Cooperative Laser Electron-γ-Nuclear Processes in Diatomic and Multiatomic Cryogenic Molecules

Alexander Glushkov, Anna V. Ignatenko

Odessa State Environmental University, Lvovskaya str. 15, Odessa, 65016, Ukraine
e-mail: glushkovav@gmail.com

In the modern molecular spectroscopy a great interest attracts studying a new class of phenomena, connected with modelling the cooperative laser-electron-γ-nuclear processes. It includes calculation of the probabilities of the mixed γ-optical transitions in molecules, intensities of the complicated γ-transitions due to the changing of the molecular excited state population due to a laser field effect. The first qualitative estimates of the cooperative effects parameters have been earlier presented (e.g. [1-3] and refs. therein). We develop an advanced computational approach to calculation of laser-electron-γ-transition spectra (electron-vibrational-rotational satellites) of nucleus in diatomic and multiatomic molecules, based on density functional (one version) and model potential (second version) methods and energy approach [4-6]. Decay and excitation probability are linked with imaginary part of the "nuclei - electron shells – laser field" system.

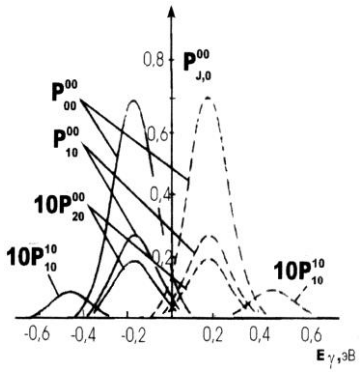

Fig.1 Emission and absorption spectrum of ^{127}I nucleus in $H^{127}I$ (ν_a=0, J_a=0)

New data on the electron-nuclear γ-transition spectra of a nucleus in some molecules are presented, namely, for diatomics, 3-atomic XY_2 ($D_{\infty h}$), 5-atomic XY_4(T_d), 7-atomic XY_6(O_h) ones (HI, Hbr, OsO_4, UF_6, alkali dimers). As example, in fig.1 the theoretical emission (solid curve) and absorption spectrum of nucleus ^{127}I in $H^{127}I$ is presented.

It is shown that studying cooperative electron-gamma-nuclear processes in the cryogenic Rydberg molecules (such as ^{133}Cs nucleus; $E^{(0)}_{\gamma}$=81 keB; $^{85}Rb^{133}Cs$ and others) allows to discover the cooperative effects experimentally for the first time.

References

[1] Letokhov V S, Moore C 1979 *Chemical and Biochemical Applications of Lasers* (Acad. Press, N-Y); Gol'dansky V I, Letokhov V S 1974 *JETP* **67** 213
[2] Letokhov V S, Minogin V 1976 *JETP* **70** 794; Ivanov L N, Letokhov V S 1987 *JETP* **93** 396
[3] Glushkov A V, Ivanov L N, Letokhov V S 1992 *Preprint ISAN* N-AS4 (Moscow)
[4] Glushkov A V, Ivanov L N 1992 *Phys.Lett.A.* **170** 33
[5] Glushkov A V, Khetselius O Yu, Malinovskaya S V 2008 *Molec.Phys.* **108** 1257
[6] Glushkov A V, Khetselius OYu, Malinovskaya S V 2008 *Progress in Theoretical Chemistry and Physics*(Springer) **18** 505-524
[7] Glushkov A V, Buyadzhi V, Ignatenko A et al 2017 *Progress in Theoretical Chemistry and Physics* (Springer) **30** 169-180

"Shake-Up" and NEET Effects in Laser Electron-Gamma-Nuclear Spectroscopy of Atoms and Multicharged Ions

Olga Yu. Khetselius, Alexander V. Glushkov Anna A. Kuznetsova, Vasily V. Buyadzhi

Odessa State Environmental University, Lvovskaya str. 15, Odessa, 65016, Ukraine
e-mail: okhetsel@gmail.com

A new class of problems has been arisen and connected with modelling the cooperative laser-electron-nuclear phenomena such as the electron shell shake-up and NEET or NEEC (nuclear excitation by electron transition or capture) effects in heavy neutral atomic/nuclear systems [1-5]. Though the shake-up effects in the neutral atoms (molecules) are quite weak (because of the weak coupling of the electron and nuclear degrees of freedom), the possibilities of their realization significantly change in a case of the multicharged ions (MCI). We present consistent, relativistic computational approach to calculation of the probabilities of the different cooperative laser electron-gamma-nuclear processes in the MCI (including the characteristics of the electron satellites in gamma-spectra of nuclei of the multicharged ions and the resonant NEET (NEEC) effects in heavy nuclei of MCI). The theory is based on the relativistic energy approach (S-matrix formalism of Gell-Mann and Low) and relativistic many-body perturbation theory [5-9]. Within the energy approach, decay and excitation probability (of the electron shell shake-up process or etc) is linked with the imaginary part of energy of the excited state for the "electron shell-nucleus-photon" system. We firstly present new data about intensities of the electron satellites in gamma-spectra of nuclei in the neutral (low lying transitions) and O-and F-like MCI for isotopes Fe,Cs,Yb ${}^{57}_{26}Fe$, ${}^{133}_{55}Cs$, ${}^{171}_{70}Yb$, which demonstrate an existence of an new effect of the giant increasing (up 3 orders) electron satellites intensities (electron shell shake-up probabilities) at transition from the neutral atoms to the corresponding MCI. We develop an advanced energy approach to the NEET (NEEC) process in the heavy MCI and list values of NEET probabilities in the nuclei of Os,Ir,U, Mt,Au ${}^{189}_{76}Os$, ${}^{193}_{77}Ir$, ${}^{235}_{92}U$, ${}^{268}_{109}Mt$, ${}^{197}_{79}Au$ of the O-and F-like MCI. The data listed demonstrate an effect of the significant changing the corresponding NEET probabilities under transition from the neutral atomic/nuclear systems to the corresponding MCI.

References

[1] Ivanov L N and Letokhov V S 1987 *JETP*. **93** 396
[2] Glushkov A V, Khetselius O, Malinovskaya S 2008 *Europ.Phys.J.* **T160** 195
[3] Tkalya E V 2007 *Phys.Rev.A.* **75** 022509
[4] Palffy A, Harman Z and Scheid W 2006 *Phys. Rev.A* **73** 012715
[5] Khetselius O Yu 2013 *Progress in Theoretical Chemistry and Physics* (Springer) **26** 217-230
[6] Glushkov A V 2012 *Progress in Theoretical Chemistry and Physics* (Springer) **26** 231-252
[7] Khetselius O Yu 2009 *Phys. Scr.* **T13**5 014023
[8] Khetselius O Yu 2009 *Int. J. Quant.Chem*. **109** 3330
[9] Khetselius O Yu 2015 *Progress in Theoretical Chemistry and Physics* (Springer) **29** 54-76